Title

ELECTRICAL PROPERTIES OF ORGANIC SOLIDS I. KINETICS AMD MECHANISM OF PHOTO-CONDUCTIVITY OF METAL-FREE PHTHALOCYANINE II. EFFECTS OF ADDED ELECTRON ACCEPTORS AND DONORS

Author

Kearns, David R.

Publication Date

1960-03-25

UCRL 9120

UNIVERSITY OF CALIFORNIA

Ernest O. Lawrence

Radiation Laboratory

ELECTRICAL PROPERTIES OF ORGANIC SOLIDS
I. KINETICS AND MECHANISM OF PHOTOCONDUCTIVITY OF METAL-FREE PHTHALOCYANINE
II. EFFECTS OF ADDED ELECTRON ACCEPTORS AND DONORS

DISCLAIMER

UCRL-9120
UC-4 Chemistry
TID-4500 (15th Ed)

UNIVERSITY OF CALIFORNIA
Lawrence Radiation Laboratory
Berkeley, California

Contract No. W-7405-eng-48

ELECTRICAL PROPERTIES OF ORGANIC SOLIDS
I. KINETICS AND MECHANISM OF PHOTOCONDUCTIVITY OF METAL-FREE PHTHALOCYANINE
II. EFFECTS OF ADDED ELECTRON ACCEPTORS AND DONORS

David R. Kearns
(Thesis)

March 25, 1960

Printed in USA. Price $2.50. Available from the
Office of Technical Services
U. S. Department of Commerce
Washington 25, D.C.

ELECTRICAL PROPERTIES OF ORGANIC SOLIDS
I. KINETICS AND MECHANISM OF PHOTOCONDUCTIVITY OF METAL-FREE PHTHALOCYANINE

II. EFFECTS OF ADDED ELECTRON ACCEPTORS AND DONORS

ELECTRICAL PROPERTIES OF ORGANIC SOLIDS
I. KINETICS AND MECHANISM OF PHOTOCONDUCTIVITY OF METAL-FREE PHTHALOCYANINE
II. EFFECTS OF ADDED ELECTRON ACCEPTORS AND DONORS

David R. Kearns
(Thesis)

Lawrence Radiation Laboratory
University of California
Berkeley, California

March 25, 1960

ABSTRACT

Techniques involving the use of high-intensity, short-duration light pulses have been applied to the study of the kinetics of photoconductivity in films of metal-free phthalocyanine. These experiments, in conjunction with measurements of steady-state photoconductivity indicate that the principal route for the formation of charge carriers is via the first excited singlet state of phthalocyanine, although the lowest triplet state can to some extent contribute to charge-carrier production. Consistent with a variety of steady-state and kinetic conductivity measurements, a mechanism is proposed for the ionization of the excited states of phthalocyanine to form charge carriers. This mechanism is strongly supported by the studies of the effects of electron acceptors and donors on the electrical properties of phthalocyanine.

A method has been developed to measure the diffusivity and mobility of the majority charge carrier. Such measurements lead to a room-temperature value of $\sim 10^{-3}$ $cm^2/v\text{-}sec$ for the mobility of positive-charge carriers (holes) in phthalocyanine. Interpretation of the kinetics of flash-photoconductivity decay suggests that the mobility of charge carriers is concentration-dependent, being lower at high carrier concentration. The decay of the photocurrent is the result of a diffusion-limited bimolecular recombination of electrons and holes, with a recombination radius of approximately one molecular diameter.

The addition of ortho-chloranil to the surface of films of metal-free phthalocyanine has been found (a) to increase the dark conductivity of such films by as much as 10^7, (b) to increase the steady-state photoconductivity by as much as 10^5, and (c) to result in the formation of unpaired electrons whose concentration decreases reversibly as a result of illumination. These systems exhibit a light-induced polarization, the phthalocyanine layer becoming more positive with respect to the ortho-chloranil layer. Kinetic studies demonstrate that, upon illumination, a single process (time constant = 60 sec) results in the increase in conductivity, the decrease in unpaired spins, and the increase in polarization. The results are consistent with the following scheme. An electron transfer from phthalocyanine to ortho-chloranil occurs in the dark at room temperature, producing an ortho-chloranil negative-ion radicals (ESR signal) and holes in the phthalocyanine layer (high conductivity). Illumination results in the transfer of an electron from an excited phthalocyanine molecule to the ortho-chloranil negative ion, producing further phthalocyanine holes and ortho-chloranil double-negative ions (increase in conductivity, increase in polarization, decrease in ESR signal). By equating spin concentration with charge-carrier concentration (phthalocyanine holes), it is possible to calculate a mobility of 10^{-4} cm^2/v-sec for holes in the phthalocyanine layer. By use of this value, a quantum yield of $\sim$0.25 is calculated for the production of charge carriers in doped phthalocyanine. A value of $\approx 10^{-5}$ cm^2/v-sec was calculated for the mobility of electrons in the ortho-chloranil layer.

Additional experiments were carried out with other aromatic organic compounds (tetracene and pentacene) and other electron acceptors (ortho-bromanil, chloranil, and phenanthrene quinone) and the results were qualitatively the same as those obtained with the ortho-chloranil phthalocyanine system.

The over-all results of adding strong electron acceptors to films of organic semiconductors are to (a) produce charge carriers in the dark, (b) increase the quantum yield from production of charge carrier by light, and (c) increase charge-carrier lifetime.

I. KINETICS AND MECHANISM OF PHOTOCONDUCTIVITY OF METAL-FREE PHTHALOCYANINE

1.0 INTRODUCTION

Investigation of the photoconducting properties of organic compounds dates back as far as 1906 to the studies of Pocchettino[1] on the photoconductivity of solid anthracene and subsequent work by Volmer[2] and Koenigsberger and Schilling.[3] Little work appears to have taken place following these initial experiments, and interest in this field remained dormant until fairly recently. Then, in 1941, Szent-Györgyi proposed that transfer of π electrons from molecule to molecule played an important role in the fundamental physics of processes of living organisms.[4] The problem, as he saw it, was how energy liberated in biological systems by one molecule can be communicated to a great many similar molecules. For the answer, he proposed that these molecules might be functioning in a manner analogous to a semiconductor such as ZnS. Here, for instance, an electron from one part of the ZnS crystal may be excited and migrate to some other part of the ZnS crystal and there loose its energy. In 1946, Szent-Györgyi observed photoconductivity in certain dyed proteins and cited this in support of his theory.[5]

The ideas propounded by Szent-Gyorgyi seem to provide the needed stimulus for other workers, and there very shortly followed a number of papers on the electrical properties of a large number of aromatic organic compounds.

Eley[6,7] and, particularly, Inokuchi[8,9] were responsible for a large share of this work. From their work and the work of others, it appears that all organic materials containing closed rings of alternating double and single bonds exhibit semiconduction (i.e., conductivity σ which varies with temperature according to $\sigma = \sigma_o e^{-\Delta E/2kT}$) and photoconduction. It was by virtue of such properties that these compounds have been termed organic semiconductors.

Along with the experimental work, papers began to appear on the role of semiconduction in various biological processes. Katz[10] and Bradly and Calvin[11] proposed theories of photosynthesis based on "semiconduction" in organic materials (in that light energy absorbed by chlorophyll in one part of a plant cell is used to produce chemical oxidizing and reducing power at other parts of the cell).

The general properties of organic semiconductors have been recently reviewed by Garrett,[12] and from this review it is clear that there is presently no adequate theory of electronic conduction in these systems. This is due partly to an inability to write down satisfactory wave functions for even the simpler organic crystals and largely due to the lack of a detailed experimental description of the processes of charge-carrier formation and migration in organic semiconductors.

Eley was one of the first to propound an explanation for the thermal- or photo-activation energy necessary for conduction in organic semiconductors based on an extension of the band theory of semiconductors.[6,7,13] Briefly, it is as follows. In Fig. 1, three benzene molecules are shown side by side schematically. The molecules are represented by potential wells, the six π electrons filling up the lowest three of six molecular orbitals common to the entire molecule as shown for molecule A. Eley proposed that the conduction processes may be separated into two steps:

(a) An electron is excited either thermally or by light from the highest filled $(n/2)$th level to the lowest unfilled $(n/2 + 1)$th level. The energy required for this transition indicated by the full arrow is $\Delta\epsilon$.

(b) The excited electron may then tunnel at the $(n/2 + 1)$th level to the next molecule with a negligible energy requirement (dotted arrow, Fig. 1a). It may also be possible for an electron to tunnel at the $n/2$th level from the left-hand molecule to fill the empty space in the center molecule, and this is equivalent to a "positive hole" passing in the opposite direction as shown in Fig. 1b, the final state after electron transfer.

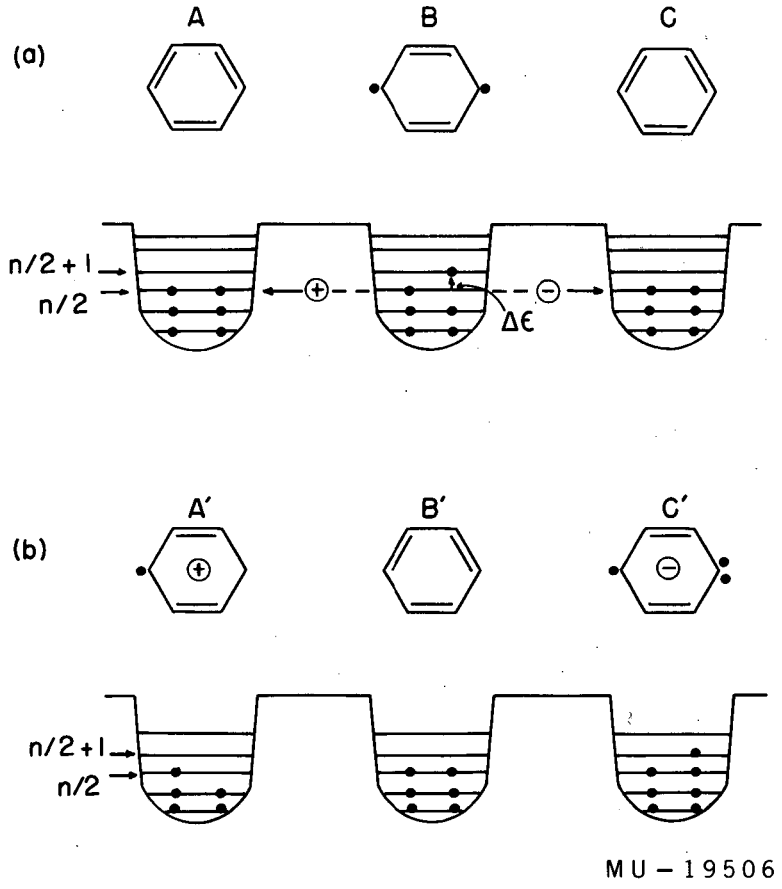

Fig. 1. Eley's model for semiconduction and photoconduction in organic polycyclic aromatic compounds. Benzene is used for illustrative purposes.

The crucial step in Eley's picture of conduction is step (b), the transfer of either an excited electron to a neighboring neutral molecule or the transfer of an electron from a molecule in the ground state to a neighboring excited molecule. In order to determine whether or not either of these steps will take place with a negligible energy requirement, consider the following reaction cycle put forth by Lyons:[14]

Step	Work required
(a) Withdraw two molecules (M) from lattice: $2M_{crystal} \rightarrow 2M_{gas}$	2 X
(b) Ionize one molecule: $M \rightarrow M^+ + e^-$	I
(c) Form M negative ion: $M + e^- \rightarrow M^-$	-A
(d) Replace M^+ in lattice: $M^+_{gas} \rightarrow M^+_{crystal}$	~ - X
(e) Replace M^- in lattice at some distance from M: $M^-_{gas} \rightarrow M^-_{crystal}$	~ - X
(f) Polarize crystal around two ions:	-2W
Net reaction: $2M_{crystal} \rightarrow M^+_{crystal} + M^-_{crystal}$	
$\Delta E_{total} = I-A-2W$	= net work required.

Here I is gaseous ionization potential of M, X is heat of sublimation, A is electron affinity of M, and W is polarization energy arising from a singly charged ion in the crystal.

In order for Eley's postulates to be valid, one requires that $\Delta E_{total} \approx \Delta\epsilon$. By Eley's definition, $\Delta\epsilon$ corresponds to $^1E_1$, the energy of the lowest singlet-singlet transition of the molecule. For the case of anthracene $^1E_1$ is 3.3 ev, A has been calculated to be +0.5 ev,[15,16] and I has been found to be 7.5 ev.[17] The polarization energy arising from the presence of a singly charged ion in anthracene has been estimated by Lyons to be around 1.0 ev,[14] and we would therefore

find $\Delta E_{total} \cong 5.0$ ev. Accroding to this calculation, approximately 1.7 ev more would be required to produce separated positive and negative charges in anthracene after an anthracene molecule had been excited to its first excited state. From this example it is clear that whether or not excitation energy corresponding to lowest singlet-singlet transition will be sufficient to produce charge carriers will depend upon the relative values of I, A, and W. It is also clear, therefore, that no direct correspondence between ΔE_{total} and $\Delta\epsilon$, as Eley proposes,[6,7] should be expected, since ΔE is not directly related to $\Delta\epsilon$ except indirectly through I and A.

Eley's mechanism may be objected to on other grounds. Davydov has shown that excitation of a molecule in a crystal to its first excited state produces an exciton, which is a nonconducting excited state of the crystal.[18]

Failure of inorganic semiconductor theory to satisfactorily describe organic semiconductor properties is not unexpected when one considers the great differences in crystal binding energies. Typical inorganic crystal binding energies may run from 1 to 3 ev, whereas organic intermolecular binding energies are usually 100 times smaller.

The cycle proposed by Lyons is useful in that it suggests a relation between ΔE_{total} and other molecular properties. Unfortunately, it tells us nothing about the actual fundamental processes of formation of charge carriers and their migration. Because most of the experimental work in the field of organic semiconductors has been concerned primarily with steady-state electrical properties, very little is known experimentally about these fundamental processes. Nelson has conducted a series of experiments on the kinetics of photoconductivity in the solid cationic dyes rhodamine B, crystal violet, and basic fuchsin.[19-21] These ionic systems, however, show memory effects as well as exceedingly long photocurrent rise and decay times (hrs), and appear to behave differently from the nonionic aromatic compounds. This is about as far as the study of kinetics of photoconductivity in organic systems has been carried.

In order to obtain a clearer picture of the processes of charge carrier formation and migration in organic semiconductors, the kinetics of photoconductivity in metal-free phthalocyanine (see Fig. 2) along with the steady-state electrical properties of this compound were investigated in detail. Metal-free phthalocyanine was chosen for this study because (a) a number of electrical measurements have been performed on it,[22-24,6,7] (b) its properties appear to be typical of the organic semiconductors, (c) its structure corresponds to the porphyrins, of which class chlorophyll is a member, and (d) it is quite stable over a wide range of temperature.

2.0 EXPERIMENTAL

2.1 Purification of Metal-Free Phthalocyanine

DuPont metal-free phthalocyanine was purified by vacuum sublimation at ~10 μHg and ~400°C in a muffle furnace (see Fig. 3). This yielded crystalline material with an average crystal length of ~0.4 cm. An analysis of the metal-free phthalocyanine purified in this manner is given in Table I.

2.2 Experimental Techniques and Apparatus

A. Surface Cell

The surface cell which was used for most of the conductivity measurements is diagrammed in Fig. 4. It was constructed by first applying a coat of Alkadag (graphite suspended in alcohol) to a glass microscope slide. When the Alkadag was dry, a scalpel was used to remove parallel strips to produce a series of narrow bands of graphite separated by a ~0.01-cm gap of insulating glass. The graphite strips were then connected at each end in such a manner as to form two meshing comb-like electrodes. The phthalocyanine samples were then applied to this electrode system by a second sublimation of the crystalline phthalocyanine in the apparatus shown in Fig. 5. A variety of residual gases (air, O_2, natural gas) were used during the sublimations, but the results appeared to be independent of the

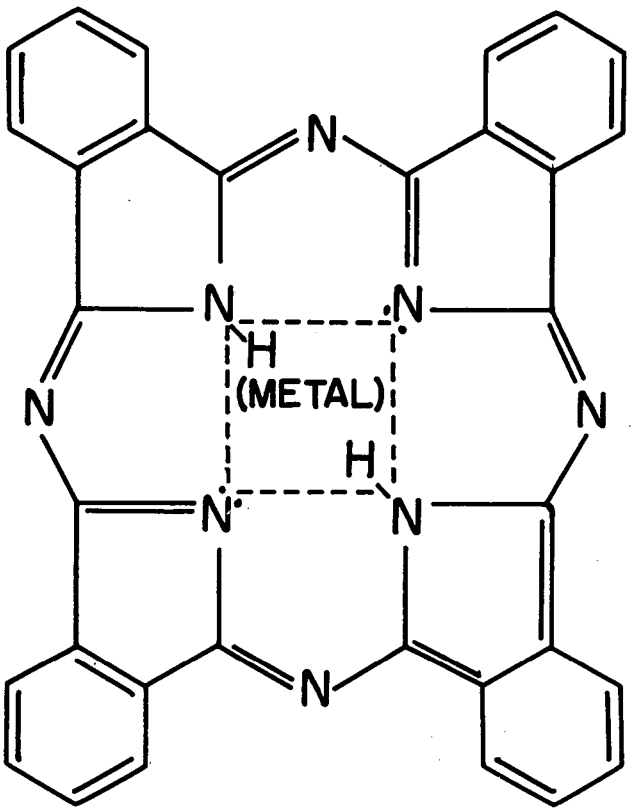

PHTHALOCYANINE

MU – 19405

Fig. 2. Structure of metal-free or metal phthalocyanine.

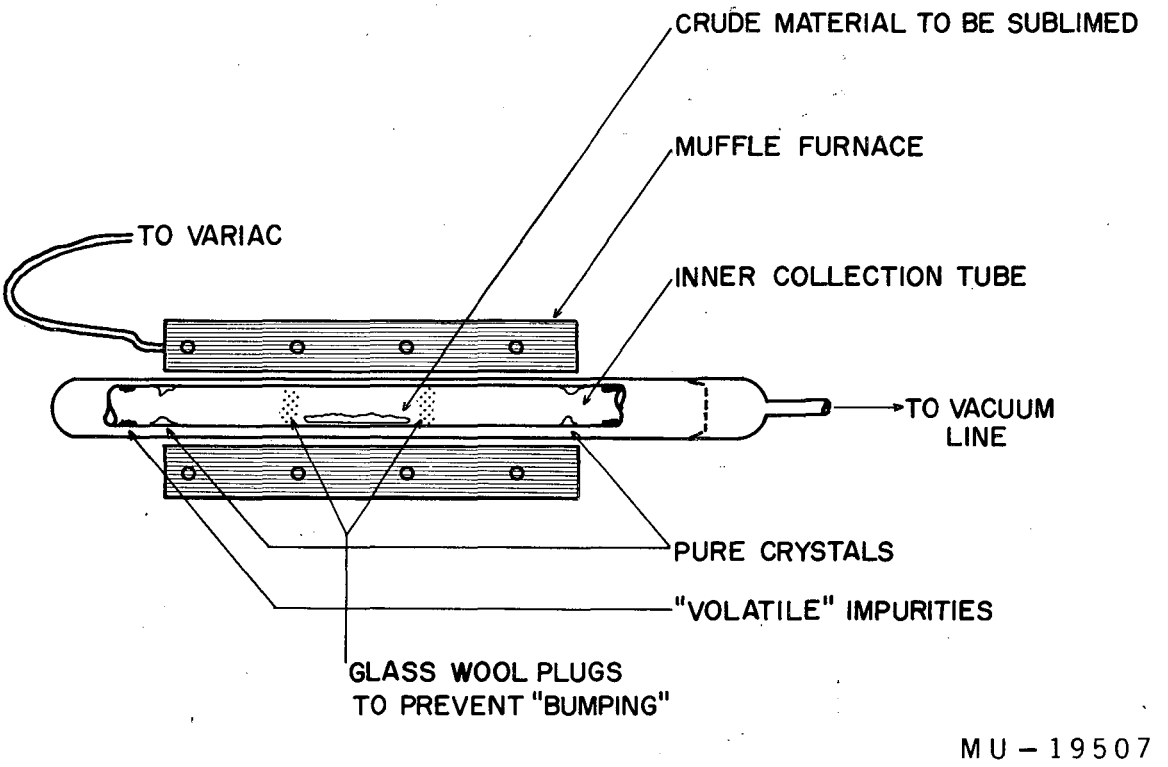

Fig. 3. Vacuum sublimation apparatus used to purify compounds.

Table I

Comparison of a spectroscopic analyses of metal-free phthalocyanine with analyses given by Eley[6, 7, 13] and by Fielding and Gutman.[23]

	Fe	Cu	Mn	Mg	Si	Co	Ni	Al	Pb	Sn	Ti	Cr
Eley	---	0.1-0.01	1-0.1	1-0.1	1-0.1	---	---	---	0.01-0.001	0.1-0.01	---	---
F and G	<0.01	<0.02	0.002	<0.002	<0.002	0.002	0.0007	<0.0004	---	---	---	---
Kerns	0.05	0.05	<0.0001	0.0005	0.001	0.0005	<0.0001	<0.0001	---	---	<0.0001	<0.0001

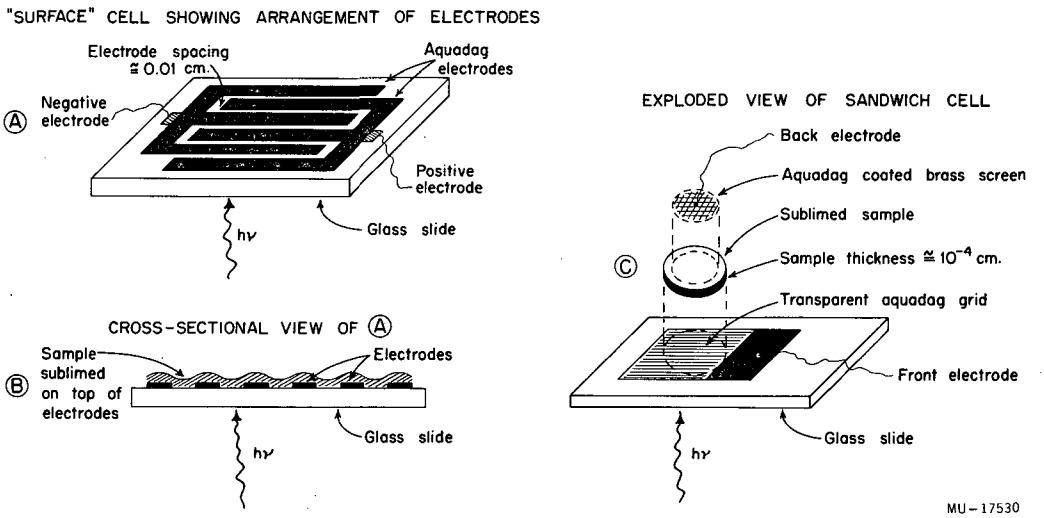

Fig. 4. Diagram of surface cell and sandwich cell.

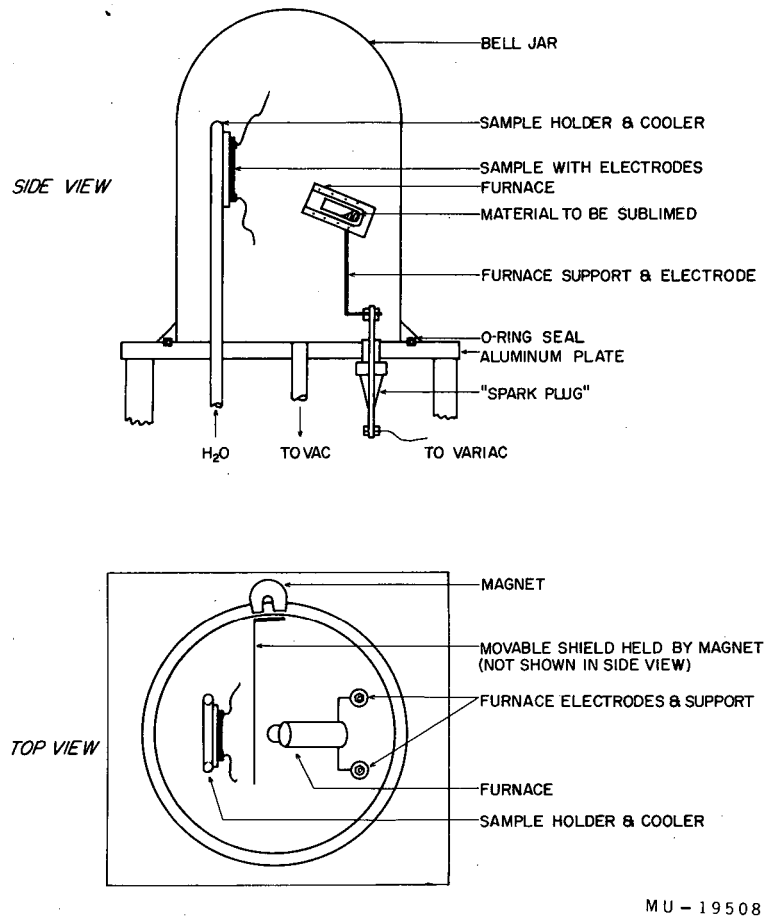

Fig. 5. Vacuum sublimation apparatus used to prepare conductivity samples.

gas used. X-ray diffraction studies indicated that the sublimed phthalocyanine films were essentially amorphous. These films could be made microcrystalline, however, by annealing the entire cell at 270°C for several days under reduced natural-gas pressure. The crystals formed in this manner were about 1 μ in diameter and 10 μ long. Figure 6 is a photograph of a thin film crystallized in this manner.

B. Sandwich Cell

The sandwich cell was a second type of sample holder used, and this is also diagrammed in Fig. 4. It was prepared essentially in the same manner as the surface cell, except that the semi-transparent graphite layer on the glass slide served only as one electrode. The second electrode was an alkadag coated brass screen that was applied to the exposed back surface of the phthalocyanine film after it was sublimed onto the slide.

Subsequent to application of electrodes, a cell could be coated with a clear acrylic resin. This coating served merely as a protective coating and was found to produce no changes in any of the measured properties of the phthalocyanine.

C. Light Sources

For the kinetic studies of the photoconductivity, the samples were illuminated by a light pulse from a G.E. FT-230 flash tube operated at 1500 v with a load capacitance of 2 mf. The shape of the light pulse produced under these conditions is shown in Fig. 7a. The calculated output of this lamp is about 10^{24} quanta per flash of light in the visible region, 10% of which may impinge on the sample. A standard triggering system was used to "fire" the flash.

Some additional experiments were performed using a GE FT-503 flash tube operated at 2500 v with a load capacitance of 256 mf to give a calculated output of 10^{26} quanta per flash of visible light. The shape of the light pulse from this lamp is shown in Fig. 7b.

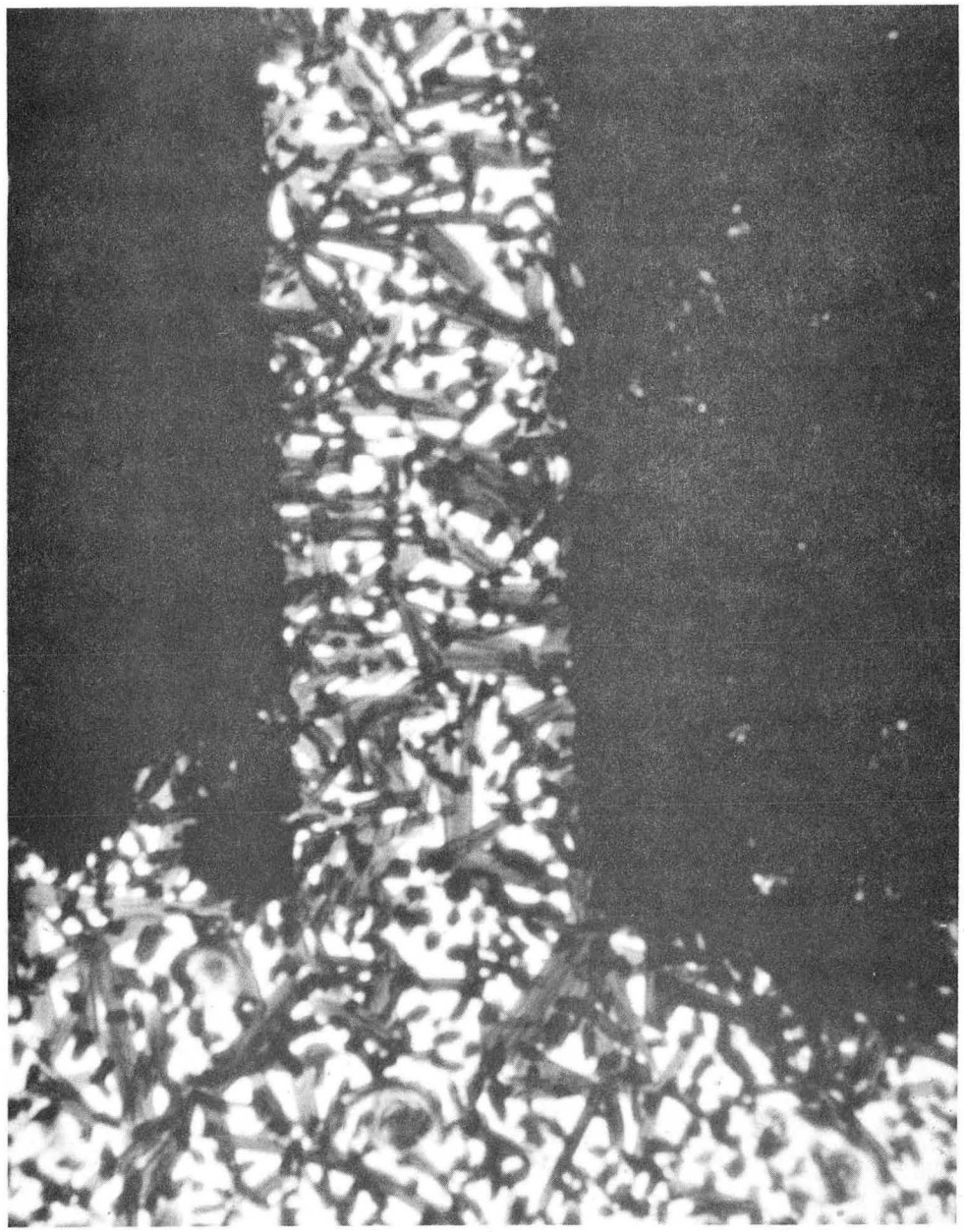

ZN-2377

Fig. 6. Photograph of an annealed surface cell of phthalocyanine. The two black rectangular areas are graphite electrodes and the distance between them is 10μ.

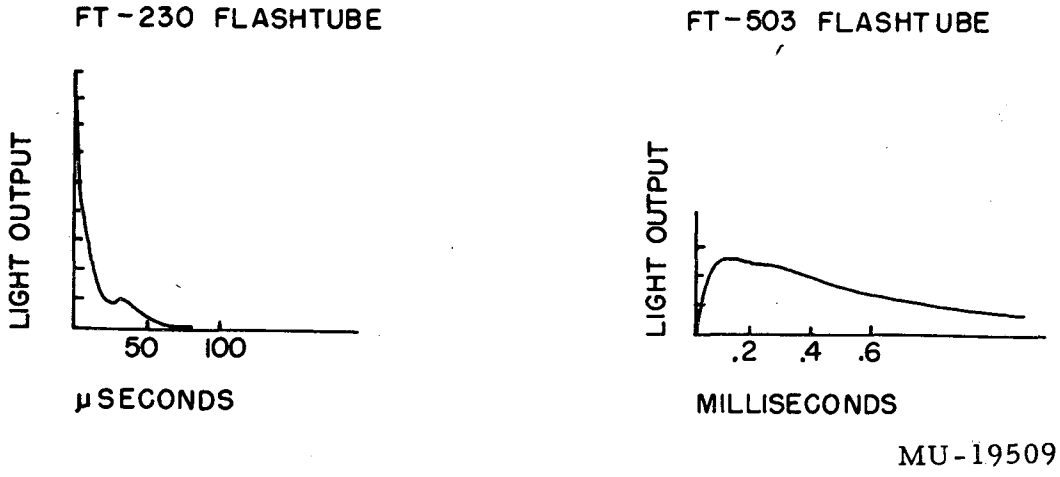

Fig. 7. Rise and decay characteristics of light pulse from GE flash tubes.

For the steady-state photoconductivity measurements, a Hanovia type-507c 800-w xenon-filled arc lamp or a 500-watt tungsten projection bulb was used to illuminate the sample. Photoconductivity spectral response measurements were made by using the above light sources in conjunction with a Bausch and Lomb 500-mm grating monochromator or a series of 1000 A band-pass filters. Other filters were used with the monochromator to remove second-order components, and a mechanically driven iris was used to maintain constant energy output at all wave lengths.

D. Conductivity Apparatus.

Conductivity measurements with the above sample cells were carried out with the cell mounted on the top end of a copper bar that was enclosed in an inverted and capped glass dewar. The bottom of the copper rod extended through the dewar cap and could be heated or cooled to vary the sample temperature. The dewar was completely covered with aluminum foil, except for a light window, so that the sample was electrically shielded and thermally insulated. Sample temperatures were measured by a thermocouple placed in good thermal contact with the sample. Dry nitrogen was admitted into the dewar during low-temperature runs to prevent condensation of moisture. A field strength of about 5×10^3 v per cm was used for most of the measurements.

Figure 8 is a block diagram of the measuring circuit used. Photocurrent generated in the sample by a light flash was passed through a calibrated resistance R with values ranging from 10^3 to 10^6 ohms. The value of R was always chosen to be at least several orders of magnitude smaller than that of the sample during the time of the measurement. The voltage developed across R was fed either through a cathode follower (gain = 0.95) and a Tektronix model-112 amplifier (gain $\sim \times 2,500$) to a Tektronix 514 oscilloscope (maximum sensitivity = 30 mv/cm), or directly to a Sanborn stabilized dc preamplifier and Model 151 recorder and to a Leeds and Northrup Speedomax Type-G recorder. Thus, with this apparatus it was possible to

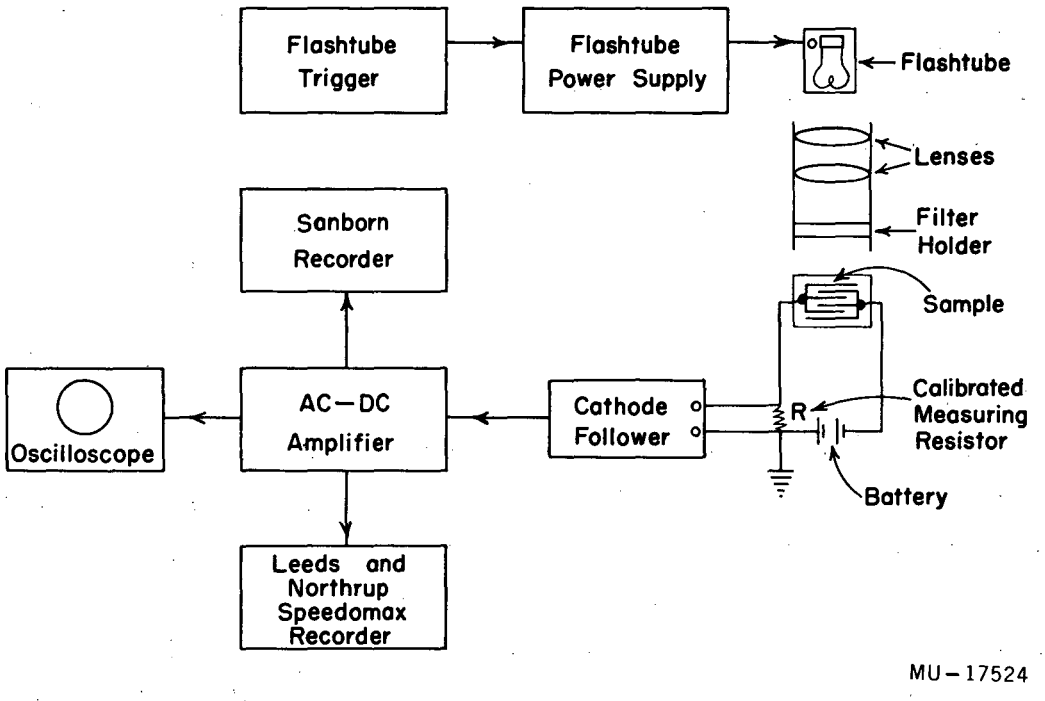

Fig. 8. Block diagram of conductivity apparatus.

follow the decay of the flash photocurrent from 1 μsec after flashing to about 100 sec. The photosignal itself was used to trigger the oscilloscope sweep, and thus it was possible to observe the rise of the photocurrent as well. A permanent record of the oscilloscope data was obtained by photographing the scope trace with a Polaroid 2620 camera.

E. Compressed-Pellet Conductivity Apparatus.

A third type of sample cell used to measure the temperature dependence of the dark conductivity of compressed powders is diagrammed in Fig. 9 along with the associated measuring circuit. With this apparatus, a sample could be heated to 300°C or cooled to -40°C while a constant electrode pressure of 150 k gm/cm^2 was maintained.

3.0 RESULTS AND DISCUSSION

3.1 Kinetics of Photocurrent Decay.

Typical photocurrent decay-curve data are shown in Fig. 10. These were obtained with unannealed metal-free phthalocyanine in the "surface" cell shown in Fig. 4. Unless otherwise stated, all the following results apply to samples of this type. The rise time of the photocurrent in the flash experiments is never less than 1μsec even if a neutral density filter of 1% transmission is placed between the flash light and sample. This indicates that the rise time of the photocurrent is limited by the rise time of the light flash, which is 1 μsec.

In Fig. 11, log photocurrent (I) is plotted vs log time, t, for data obtained at 23 and -35°C.

For the purpose of discussion, the room temperature curve may be divided into three regions, as indicated in Fig. 11. Interpretation of this curve is easier if region I is considered first. In this region (~1 to ~100 sec) the current obeys the relation

$$I \propto (t)^{-1} . \qquad (1)$$

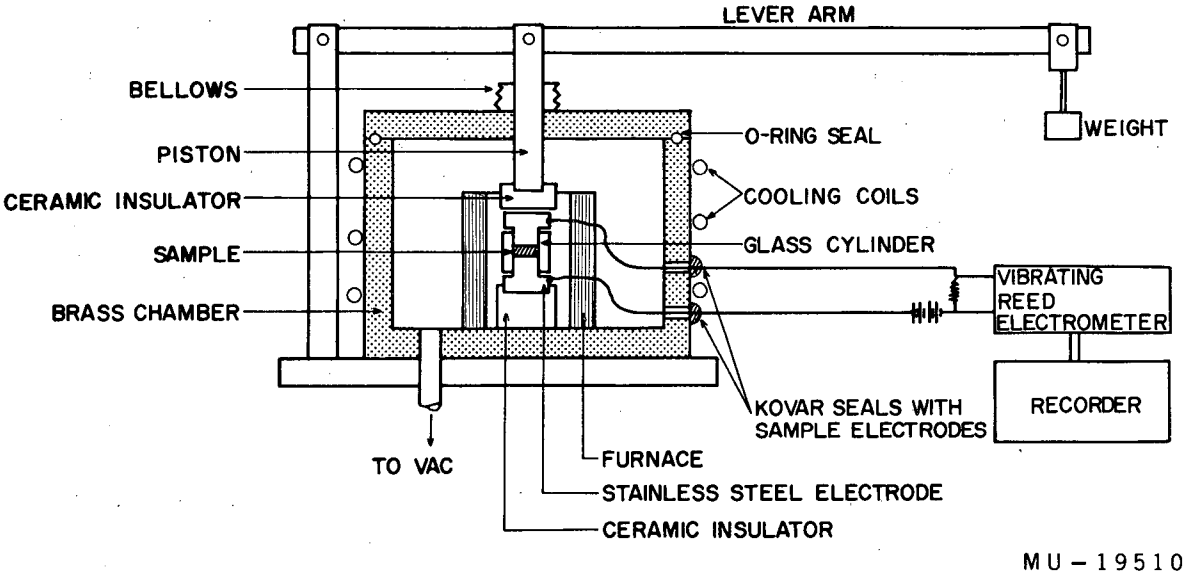

Fig. 9. Pellet conductivity apparatus.

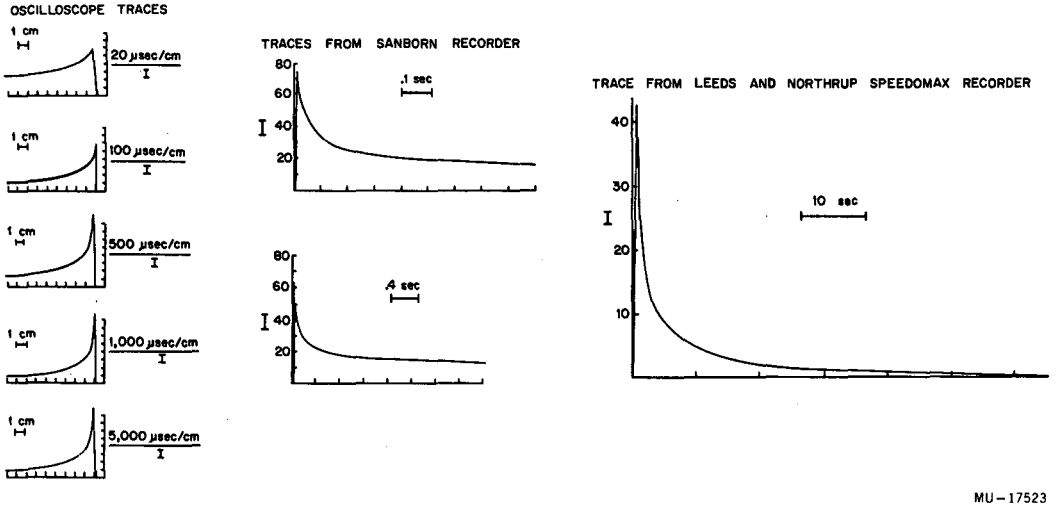

Fig. 10. Typical flash photoconductivity decay curves for metal-free phthalocyanine at room temperature.

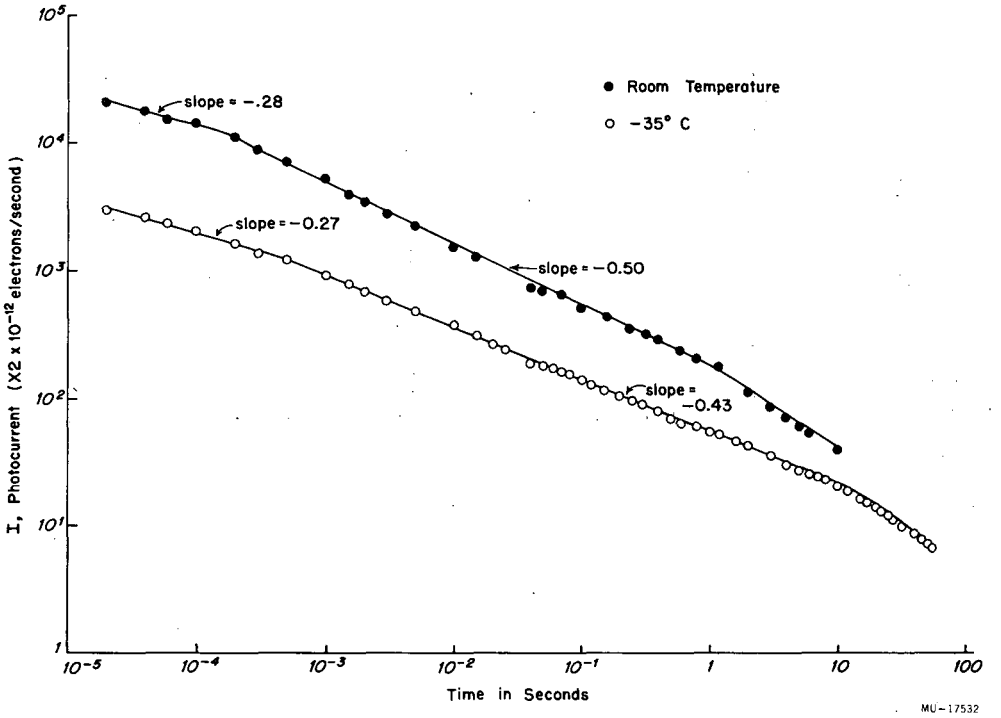

Fig. 11. Log flash-photocurrent versus log time for a metal-free phthalocyanine surface cell at room temperature and - 35°C. Region I is from ~1 sec to ~100 sec, Region II ~100 μsec to ~1 sec, and Region III ~10 μsec to ~100 μsec.

This decay law is precisely what one would expect for a process involving the recombination of oppositely charged carriers. In this case, we may write

$$dn/dt = -Kn^2, \tag{2}$$

where n is the concentration of positively or negatively charged carrier and K is the molecular rate constant (in units of cm^3/sec-carrier). We obtain upon integration of Eq. (2)

$$1/n = kt + \text{constant}, \tag{3}$$

and for large t the constant is negligible. If we assume that the photocurrent is proportional to the concentration of photoproduced carriers, we may arrive at Eq. (1).

Proceeding to shorter times after flashing, we see that in region II (~100 μsec to ~1 sec) the photocurrent decay is slower than in region I, in spite of the fact that the currents, and therefore carrier concentrations, are higher. This may be accounted for by assuming that charge-carrier mobility is dependent upon the concentration of charge carriers. In some ways this is analogous to what is observed for ion mobilities in solutions of high ionic strength.[25]

If one makes the above assumption, the picture of a bimolecular decay process may be retained. An empirical relation between the photocurrent, I, and carrier concentration, n, which will lead to a satisfactory description of the experimental results is

$$I = (\mu_o/(n + c)^{1-1/x}).\ nAE, \tag{4}$$

where n is the total carrier concentration, E is the field strength, A is the cross-sectional area of conducting material, $\bar{\mu} = \mu_o/(n + c)^{1-1/x}$ is the apparent average carrier mobility at a particular value of n, and c and x are constant for a given sample and temperature. Here c represents a critical concentration of carriers below which the mobility is concentration-independent.

Assuming a bimolecular rate law (2), one can derive the following equations:

For $n \ll c$:

For this value of n, we can write:

$$I = (\mu_o/(c)^{1-1/x}).\ nAE \tag{5}$$

Solving for n in terms of I and substituting in Eq. (2) yields

$$dI/dt = -(Kc^{1-1/x}/\mu_o AE).\ I^2 \tag{6}$$

or, upon integration,

$$1/I = (Kc^{1-1/x}/\mu_o AE)\ .\ t\ + \text{constant}. \tag{7}$$

If the photo-current decay is actually due to recombination of the positive and negative charges, diffusion of the charges to neighboring sites in the crystal should be the only limiting step. The mathematics of diffusion-limited reactions have been treated by Waite.[26] For a bimolecular diffusion-limited process, Waite derives, for the rate law at low reactant concentrations, the expression

$$dn/dt = -\ 4\pi\ r_0 D\ n^2 = -K\ n^2, \tag{8}$$

where r_0, the capture radius, is the distance of separation of reactants within which reaction is rapid but outside of which there is essentially no interaction, D is the average diffusivity (in units of cm^2/sec-carrier), K is the bimolecular rate constant as previously defined in Eq. (2), and n is the concentration of holes or the concentration of electrons. Therefore, we have

$$K = 4\pi\ r_0\ D. \tag{9}$$

From the Einstein equation,[27]

$$D = \frac{\mu KT}{e}, \tag{10}$$

where μ is the apparent average carrier mobility at low carrier concentration, we obtain:

$$K = \left(4\pi\ r_0\ \frac{\mu_0}{c^{1-1/x}}\right).\ \frac{kT}{e}\ . \tag{11}$$

From Eq. (7), the slope of a log of 1/I vs as low I is equal to

$$\frac{Kc^{1-1/x}}{\mu_o AE} = B. \tag{12}$$

Upon substitution of Eq. (11) into Eq. (12), one obtains

$$\frac{4\pi r_0}{AE} \cdot \frac{kT}{e} = B, \tag{13}$$

or, rearranging,

$$r_0 = \frac{BAE}{4\pi} \cdot \frac{e}{kT}. \tag{14}$$

Thus, Eq. (14) permits the calculation of r_0 from experimental data. Figure 12 is a 1/I vs t plot, and from this data r_0 is calculated to be approximately 25 Å (about one molecular diameter), and about 200 Å at -35°C. At temperatures up to 50°C, r_0 remained at about the room-temperature value, within experimental error.

The fact that one can obtain reasonable values for r_0 suggests that the assumption that recombination is diffusion-limited is moderately accurate. The observed increase in r_0 at low temperatures may be due to a decrease in thermal scattering.

For $n \gg c$:

For this value of n, we can write:

$$I = \mu_o n^{1/x} AE. \tag{15}$$

Upon substition in Eq. (3) and after solving for n, one obtains

$$I = (\mu_o AE/K^{1/x}) \cdot t^{-1/x}. \tag{16}$$

Thus the current, I, should decay at low carrier concentrations (Region I) according to Eq. (14) and at high carrier concentrations (Region II) according to Eq. (16), in agreement with the results illustrated in Fig. 11. For all the samples studied, x varied from 1.6 to 2.5. For the cases illustrated in Fig. 11, x was 2.0 at room temperature and 2.33 at -35°C.

Some question may be raised regarding the possible effect of the time constant ($RC = K\epsilon_o p \approx 10^{-3}$ sec) of the sample on the measurement of the kinetic behavior of the phthalocyanine photoconductivity. However, the measurements were carried out using a calibrated

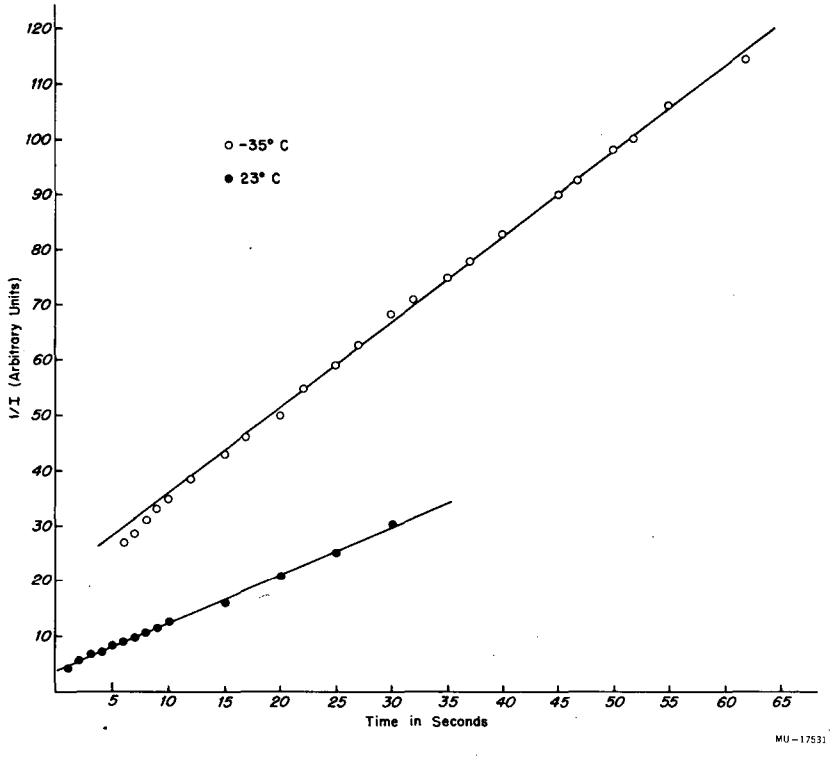

Fig. 12. 1/I versus t plot for metal-free phthalocyanine at room temperature and - 35°C. The unit on the ordinate is 2×10^6 amp^{-1}.

measuring resistor (see Fig. 4) that was many orders of magnitude smaller than the sample resistance. Thus, unless there were barriers at the electrodes, the voltage across the sample remained constant, in spite of changes in sample resistivity. Consequently, the RC of the sample should not effect the photokinetic measurements. The possibility of unsuspected electrode barriers that had to be charged or discharged can be eliminated by the observations that:

(a) The decay of the flash photoconductivity is not exponential or a sum of exponential decays, as would be expected for discharge of a condenser or several condensers;

(b) The resistivity of the sample may be changed by a factor of 10^7 (see part II) without effect on the kinetics of the initial flash-photoconductivity decay. Such a change in resistance would produce a large change in the RC of the sample.

3.2 Intensity Dependence of Flash Photocurrent Decay

The only region of the decay curve yet to be discussed is region III (~10 μsec to ~100 μsec). In this region the photocurrent decays even more slowly than would be predicted by the proposed mechanism. A study of flash intensity dependence of the photocurrent decay curve demonstrated that the functional relation between the measured photocurrent and carrier concentration in regions I and II (see Eq. 4) did not change with flash intensity. The decay rate in region III, however, decreased markedly with a decrease in flash intensity. This effect is shown in Fig. 13 and suggests that there exists a photoproduced, long-lived (10^{-4} sec), high-energy intermediate which leads to production of charge carriers for 10^{-4} sec after a sample is flashed. One possibility for such an intermediate is the lowest triplet state. This hypothesis would be consistent with the low-intensity flash behavior of the current decay, where the triplet lifetime would be longer under low-intensity illumination because of a decreased probability of self-quenching.[28] A lifetime of about 10^{-4} sec is also reasonable for the triplet state.

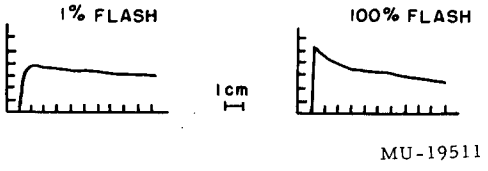

Fig. 13. Intensity dependence of the initial flash photoconductivity for a typical metal-free phthalocyanine sample. The flash intensity was varied with neutral density filters. Sweep rates are 20 μsec/cm. The 1% curve has been multiplied by 100.

The initial 10 μsec of flash photocurrent decay are complicated by the decay of the light pulse, and therefore no further consideration will be given to this portion of the decay curve.

3.3 Temperature Dependence of Flash Photocurrent Decay

A change in temperature over the range from 60 to -35°C does not affect the kinetics of the major portion of the decay curve (20 μsec to 100 sec) within experimental error. In particular, the photocurrent decay remains bimolecular at low currents, indicating that there are no majority carrier trapping centers with depths greater than about 0.05 ev.

A decrease in temperature was found to cause a slight decrease in the 1/x value. For example, 1/x is 0.50 at 23°C and 0.43 at -35°C, as shown in Fig. 11. Inasmuch as one would expect a decrease in mobility at lower temperatures, these results suggest that there is an inverse relationship between mobility and the concentration dependence of mobility. This is further demonstrated by the fact that the concentration-dependent portion of the decay curve extends to longer times at the lower temperature (see Fig. 11).

3.4 Flash-Photoconductivity Rise

The decay of the flash photoconductivity has now been described, and the final region of interest in the kinetic experiments is the rise of the photoconductivity. The current was found to have a rise time of 1 μsec, even when the flashlight intensity was reduced two orders of magnitude with neutral-density filters. The rise time of the flashlight pulse was also ~1 μsec, and it must be concluded that the rise of the photocurrent was limited by the rise of the light pulse, and is probably somewhat faster than 10^{-6} sec. The spectral response of the peak flash photoconductivity for front-face illumination of a relatively thick sample is shown in Fig. 14 along with the phthalocyanine absorption spectrum. From this we concluded that the first action of the light is to produce phthalocyanine molecules in the excited singlet

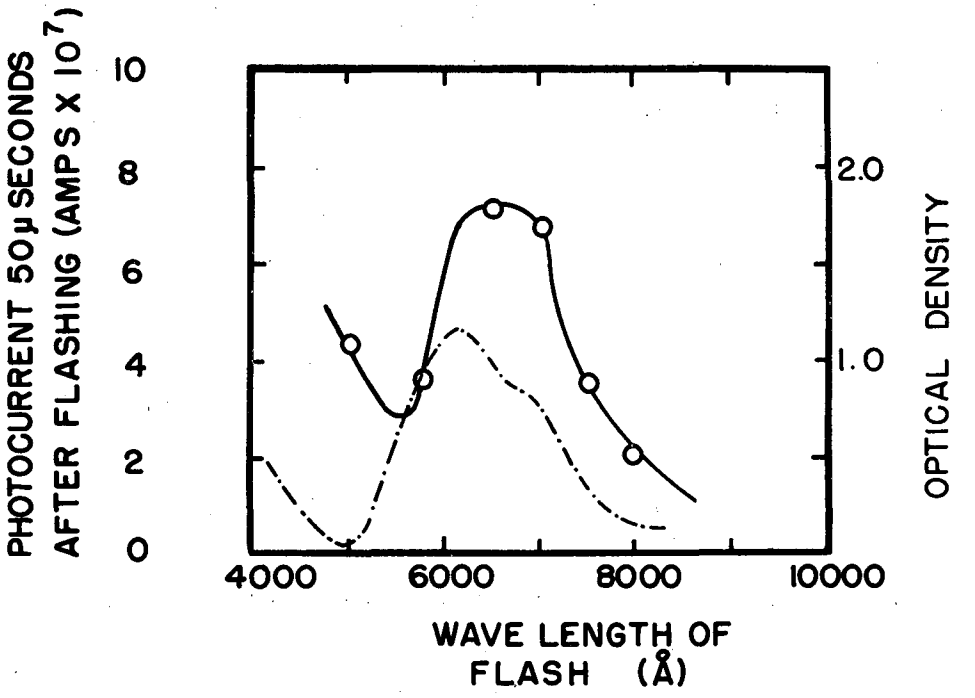

Fig. 14. Spectral response of the photocurrent 50 μsec after flash illumination of a typical metal-free phthalocyanine sample. The solid-state absorption spectrum of metal-free phthalocyanine is indicated by the dashed line.

state, and that these are ionized in a time shorter than 10^{-6} sec to form the majority of charge carriers. The question of the mechanism of ionization of excited singlet states will be deferred until Part II.

3.5 Results with Sandwich Cells and Annealed Samples

Room-temperature photoconductivity decay curves were also measured for sandwich-type cells of metal-free phthalocyanine. These gave essentially the same kinetics as did the "surface" cells. In general, the sandwich cells were more difficult to prepare and had a signal-to-noise ratio only about 1/100 as good as the "surface" cells.

A common method used to indicate the sign of the majority charge carrier in a sandwich cell is to measure the magnitude of the photocurrent as a function of the polarity of the illuminated electrode. When this was done for a sandwich cell of metal-free phthalocyanine, higher currents (about double) were obtained when the illuminated electrode was positive than when it was negative. This indicates that holes are the more mobile carriers, in agreement with investigations of other organic compounds.[29,30,31]

Microcrystalline (annealed) "surface" cells exhibit the same photocurrent kinetic behavior as do the unannealed samples. However, the annealed samples exhibit a smaller concentration dependence of carrier mobility. It is to be expected that more ordered samples would contain fewer scattering centers and therefore possess higher carrier mobilities. This is consistent with the fact that higher photocurrents were obtained with annealed samples than with unannealed samples under identical conditions. Again, it would appear that larger carrier-mobility concentration dependences are associated with lower carrier-mobilities.

This completes most of the analysis of the kinetics of photoconductivity, and now some of the steady-state electrical properties will be considered in more detail.

3.6 Temperature Dependence of the Dark Conductivity

The temperature dependence of the dark conductivity of a pellet of crystalline phthalocyanine was measure in the apparatus shown in Fig. 9. During the measurements, the chamber pressure was reduced to 5×10^{-6} mm Hg, and the temperature was varied from -30 to +160°C. A plot of log resistence versus (temperature)$^{-1}$ is given in Fig. 15 where it can be seen that the conductivity obeys the following relation:[32]

$$\sigma_{dark} = \sigma_o e^{-\Delta E/2kT}. \qquad (17)$$

From these measurements the activation energy, ΔE, was calculated to be 1.73 ev. No hysteresis effects were observed upon heating and cooling, and no change in activation energy was detected. These results are in excellent agreement with those of Fielding and Gutman who, using single crystals of phthalocyanine, calculated an activation energy of 1.71 ev and likewise found no hysteresis effects or change in the activation energy.[23] These results disagree with those of Eley using polycrystalline metal-free phthalocyanine.[6,7] He finds an activation energy of 1.5 ev, hysteresis effects, and changes in the activation energy with temperature. Fielding and Gutman suggest that the discrepancies between their measurements and Eley's are caused by the fact that Eley worked with polycrystalline material, while they worked with single crystals. Our experiments show this is not the reason, since our measurements on polycrystalline material of high purity gave results identical to those performed on high-purity single crystals. A spectroscopic analysis of our material is given with that of Eley's and Fielding and Gutman's in Table I. The results show that Eley's phthalocyanine is a great deal more impure by comparison, and we conclude that the discrepancies between this work and ours are due to impurities. This is an important fact, since it indicates that the activation energy for dark conductivity, while independent of the number of grain boundaries in a sample, is quite sensitive to certain impurities. The effects of impurities in the host lattice will be discussed in Part II.

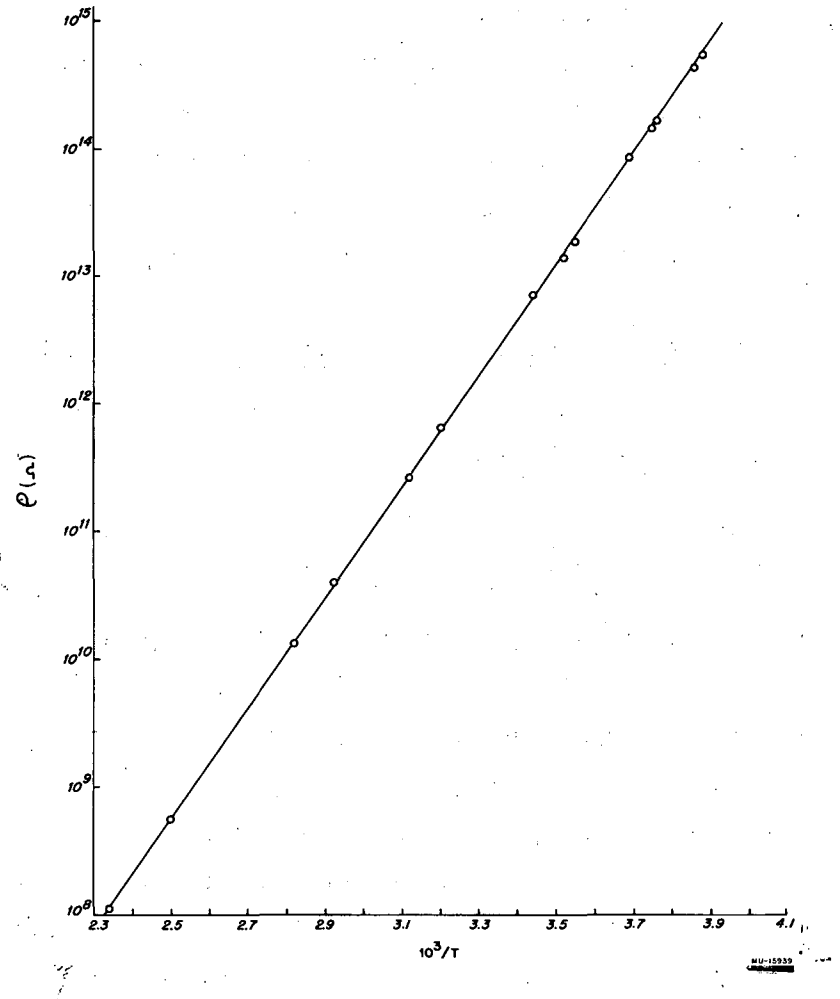

Fig. 15. Log resistance versus (temperature)$^{-1}_2$ for a pellet of metal-free phthalocyanine 1 cm^2 in area and 0.1 cm thick.

Fielding and Gutman found a σ_o value of 37 Ω^{-1} cm^{-1} while we find a $\sigma_o = 0.3\ \Omega^{-1} cm^{-1}$ in our compressed-pellet measurements. This difference is to be expected, since an increase in the number of grain boundaries would decrease the intermolecular interaction and thus increase the resistance to intermolecular electron transfer.

The temperature dependence of the surface-cell dark current was more difficult to measure because of temperature fluctuations, but it wal slso found to have an exponential temperature dependence, with an activation energy somewhere in the range 1 to 2 ev.

3.7 Temperature Dependence of the Steady-State Photocurrent

The steady-state photocurrent of a surface cell was found to have the following temperature dependence:[33]

$$I = I_o e^{-\Delta\epsilon/kT}, \tag{18}$$

where $\Delta\epsilon = 0.2$ ev, in agreement with other reported values.[22]

Kommandeur et al. have suggested that the small magnitude of the activation energy for photoconductivity indicates that the effect of temperature is not to be associated with the optical generation of carriers, but rather with the transport process.[33] They postulate that this activation energy, $\Delta\epsilon$, could arise from the existence of shallow traps or small potential-energy barriers possibly caused by a polarization of lattice molecules by the charge carriers. In support of this notion, they find that the magnitude of $\Delta\epsilon$ increases with the polarizability of the aromatic molecule. These ideas will be discussed more fully in connection with the results of Part II.

3.8 Voltage Dependence of the Steady-State Photocurrent and Dark Current.

As can be seen from Fig. 16, which is a plot of log current, I, vs log applied voltage, V, both the steady-state photocurrent and the dark current vary with the three-halves power of V. Such a current-voltage relation has also been observed with films of β-carotene.[34] The departure of both the dark conductivity and the photoconductivity from Ohm's law suggests that the applied electric field may affect the probability of charge carrier formation.

The slope B, of a plot of 1/I vs time, t, where I is the flash photocurrent seconds after flashing, is [recalling Eq. (12)]

$$\frac{KC^{1-1/x}}{\mu_o AE}.$$

From the above data, however, it is clear this B should be rewritten as

$$B = \frac{K'C^{1-1/x}}{\mu_o AE^{3/2}} = \frac{K''}{E^{3/2}}, \qquad (19)$$

where K'' is a constant. Accordingly, for a given sample and temperature, $(BE^{3/2})$ should remain approximately constant. The product $(BE^{3/2})$ was measured over a range of voltages and found to remain constant within 30% in going from 45 to 180 v, in fair agreement with predicted behavior.

The kinetics (the functional relation between current and time) were independent of the applied field.

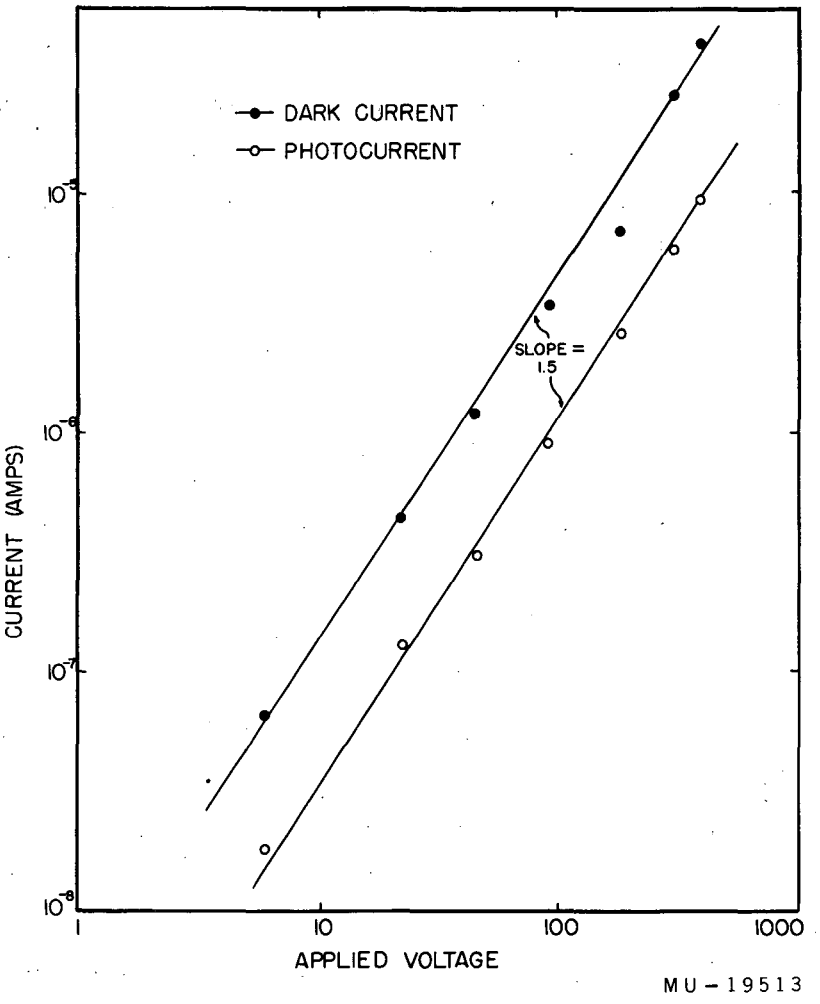

Fig. 16. Voltage dependence of the steady-state photoconductivity and dark conductivity.

3.9 Spectral Response of Steady-State Photoconductivity

The spectral response of the photoconductivity for front-face illumination (illumination through the electrode face) of both thick and thin samples is shown in Fig. 17, along with the absorption spectrum of a thin film of metal-free phthalocyanine. It is apparent that it is light absorbed by phthalocyanine which is effective in producing photoconductivity. Furthermore, from the fact that illumination of the back of thick samples (also shown in Fig. 17) yields a spectral response that is the inverse of the absorption spectrum, it can be concluded that light absorbed close to the electrodes is more effective in causing photoconductivity than is light that is absorbed on the back of the sample.

3.10 Intensity Dependence of the Steady-State Photoconductivity

The assumptions required to successfully describe the kinetic behavior of the photoconductivity put certain limitations on the behavior of the steady-state photoconductivity. If a sample is illuminated with a constant light source at steady-state Eq. (2) becomes

$$\frac{dn}{dt} = 0 = -Kn^2 + qL, \tag{20}$$

where L is the light intensity in quanta per second and q is related to the quantum yield for production of charge carriers.

At low light intensities, Eq. (5) applies and, upon substitution into Eq. (20), one obtains

$$I_{\substack{\text{steady-state} \\ \text{(low-light)}}} = \frac{\mu_o AE}{c^{1-1/x} K^{1/2}} \cdot L^{1/2}. \tag{21}$$

At high light intensity, Eq. (15) applies, and one obtains, upon substitution in Eq. (20),

$$I_{\substack{\text{steady-state} \\ \text{(high light)}}} = \frac{\mu_o AE}{K^{1/2x}} \cdot L^{1/2x}. \tag{22}$$

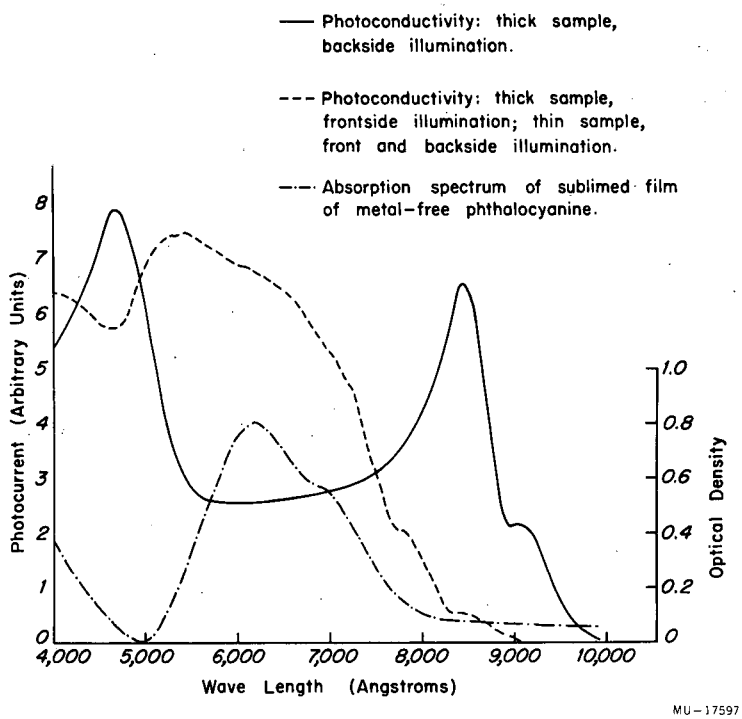

Fig. 17. Spectral response of the steady-state photoconductivity and the absorption spectrum of metal-free phthalocyanine films (50 Å band width).

Equation (21) predicts that at low light intensities the steady-state photocurrent should vary as the square root of the light intensity. That this is approximately so is shown in Fig. 18, which is a log-log plot of photocurrent as a function of light intensity.

From the room-temperature curve of Fig. 11, it is apparent that x is 2 under these conditions. Thus, for this sample the steady-state photocurrent should vary as the fourth root of the light intensity at very high light intensities, if the mechanism proposed above is correct. That this is also approximately the case is demonstrated by Fig. 18. These data were obtained by focusing the unfiltered light from the 800-watt xenon-arc lamp through a water bath onto the front-face sample.

While these data tend to support the mechanism proposed to describe the decay of the flash photoconductivity, there is a complicating factor that must be considered. This is the effect of generation of carriers by strongly absorbed, high-intensity radiation, and their diffusion away from the surface where they were created. Assuming these conditions, Moss has derived the following expression for the intensity dependence of surface photoconductivity:[35]

$$I \propto (L)^{1/3}. \tag{25}$$

The data presented in Fig. 18 were obtained with a nearly transparent sample and therefore the complications due to nonuniform production of charge and their diffusion away from the region of generation should not be a factor. We may conclude that the intensity dependence data do support the proposed decay mechanism.

Some interesting conclusions can be drawn from a consideration of the intensity dependence of the photoconductivity of samples of varying thicknesses. In these experiments, either the front (surface with electrodes) or back (surface opposite to one with electrodes) face of a sample was illuminated with strongly absorbed 6000 to 7000 Å light. The results are given in Fig. 19, where log photocurrent is plotted as a function of log light intensity.

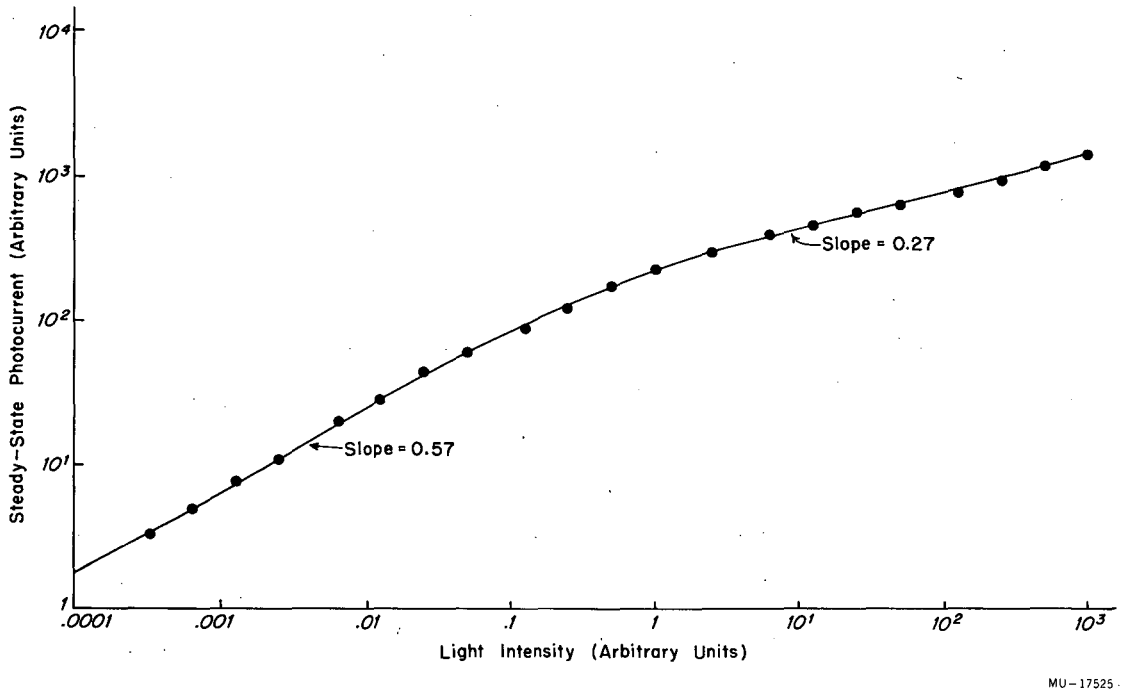

Fig. 18. Intensity dependence of the steady-state photoconductivity of metal-free phthalocyanine. The unit on the ordinate is 10^{-8} amps.

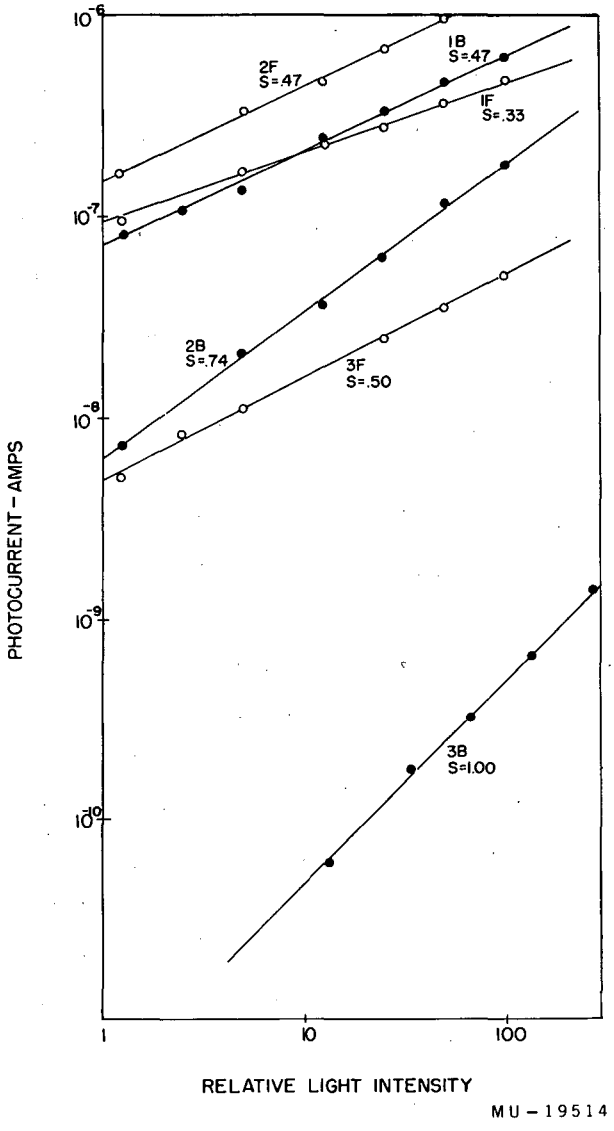

Fig. 19. Intensity dependence of steady-state photoconductivity for front or back face illumination of phthalocyanine surface cells of varying thickness. Light used was 6000 to 7000 Å.

1 F = front-face illumination of 10^{-5}-cm-thick cell
1 B = back-face illumination of 10^{-5}-cm-thick cell
2 F = front-face illumination of 10^{-4}-cm-thick cell
2 B = back-face illumination of 10^{-4}-cm-thick cell
3 F = front-face illumination of 8×10^{-4}-cm-thick cell
3 B = back-face illumination of 8×10^{-4}-cm-thick cell.

In order to account for these data, it is necessary to assume that phthalocyanine does possess bulk conductivity, but charge carriers in the region near the phthalocyanine-glass interface have a higher mobility. The observed photoconductivity thus is primarily due to charge carriers in this region of higher conductivity. According to this assumption it is possible to have contributions to the photocurrent from carriers generated in two different regions of the sample:

(a) current, i_a, from carriers generated in the highly conducting region near the phthalocyanine-glass interface

(b) current, i_b, from carriers generated some distance from the highly conducting region but which diffuse into the conducting region.

Lyons has formulated a theory of photoconductivity based upon the assumption that excitons migrate to the surface of the solid before they can generate carriers.[36] This process will be governed by the diffusion of the excitons, and Lyons predicted that the photocurrent will vary linearly with light intensity. This theory has been modified by Compton to include the case where carriers may be formed in the bulk of the solid, but must diffuse to the electrode surface of the solid before they can conduct.[31] Again a linear relationship between photocurrent and ligh intensity is predicted.

Therefore, the contribution, i_b, to the photoconductivity due to diffusion of charge carriers into the higher conductivity region will vary linearly with the light intensity. As stated before, at high light intensities the photocurrent, i_a, due to carriers generated near the surface will vary as the fourth root of L. The relative contribution of i_a and i_b to the photoconductivity will then determine the over-all observed steady-state intensity dependence. For front-face illumination, the photoconductivity varies with L^Z where Z goes from 1/3 to a maximum value of 1/2 as sample thickness is increased (see Fig. 19, curves 1F, 2F, 3F). Thus even for front-face illumination there appears to be a significant contribution of i_b to the photocurrent. Over the same range of light intensities, the photoconductivity produced by back-face illumination varied as L^Z, where Z goes

from 1/2 to 1 as sample thickness is increased (see Fig. 19, curves 1B, 2B, and 3B). Obviously, in this case, as the sample thickness is increased, the i_a contribution to the photoconductivity becomes insignificant.

The above explanation of the intensity dependence of the steady-state photoconductivity is further supported by the results of the following experiment. Figure 20 shows the rise and decay of 6000 to 7000 Å photocurrent for both front-and back-face illumination of a thick surface cell. The front-face photocurrent initially rised very rapidly due to the production of charge carriers in the conducting region. A short time later, carriers produced in the "nonconducting" region began to diffuse into the "conducting region." The diffusivity of carriers is presumed to be low, and hence carriers produced some distance from the conducting region will not contribute to conduction immediately.

When the back-face of the thick sample is illuminated, almost all of the photocurrent is due to diffusion of carriers produced at the back surface into the conducting region near the front surface. As can be seen from Fig. 20, the main contribution to the photocurrent comes from a process with a long time constant (i.e., a diffusional process).

3.11 Measurement of the Carrier-Diffusivity and Mobility

The conclusions reached with regard to the discussion of intensity dependence of the steady-state photoconductivity suggest a method by which the diffusivity and hence the mobility of charge carriers in phthalocyanine can be measured. If a thick sample (thick with respect to the region of high conductivity) receives a short pulse of strongly absorbed light on the back surface, there should be a time lapse between the light pulse and the arrival of carriers in the region of high conductivity. Although the concentration of excited phthalocyanine molecules may be initially well localized near the back surface, exciton migration would extend the region of excitation in greater than 10^{-5} cm from the surface.[37] Thus in

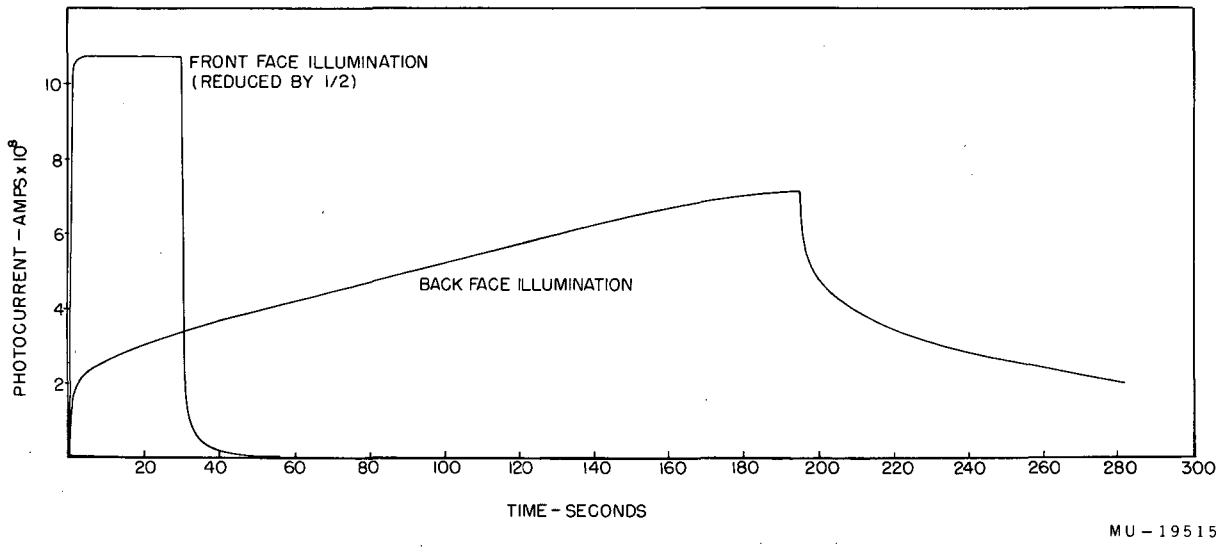

Fig. 20. Rise and decay of steady-state photocurrent for front- and back-face illumination of a 5×10^{-4}-cm-thick phthalocyanine-surface cell.

practice a few carriers arrive almost immediately in the conducting region. The arrival peak of the photocurrent, however, should have a rather large time lag between it and the peak of the flash provided a thick enough sample is used. As will be shown later, this time delay can be related to the diffusivity of the charge carriers and the distance between their site of production and the region of "high conductivity."

In the following experiments, samples of different thicknesses were illuminated by the light pulse from the FT503 flash tube operated at 2200v with a load capacitance of 256 μf. In each case either the back or front face of a sample was illuminated and a 6000 to 7000 Å band-pass filter was interposed between the flash tube and the sample.

Illumination of a semi-transparent sample in this maner produced a photocurrent pulse whose maximum corresponded with the maximum of the light pulse regardless of whether the front or back face was illuminated. In Fig. 21b the flash photocurrent produced by front-face illumination of a sample 4×10^{-4} cm thick is compared with the shape of the light pulse (Fig. 21a). Again, as expected, the peak of the photocurrent coincides with the peak of the light pulse. When the back surface of this sample is flashed with the 6000 to 7000 Å light (Fig. 21c) there is a 300 μsec delay between the peak of the light pulse and the current pulse, and this delay increases to over 500 μsec when the sample thickness is increased to 8×10^{-4} cm. This is shown in Fig. 21d.

To calculate the diffusivity, we use the following model. Consider a semi-infinite solid bounded by the planes $x = 0$ and $x = \ell$. Assume that we now introduce at time $t = 0$ a quantity of charge carriers into the region $0 < x < h$ such that the concentration of charge carriers, C, at $t = 0$, is

$$C = C_o \text{ if } 0 < x < h$$
$$C = 0 \text{ if } x > h.$$

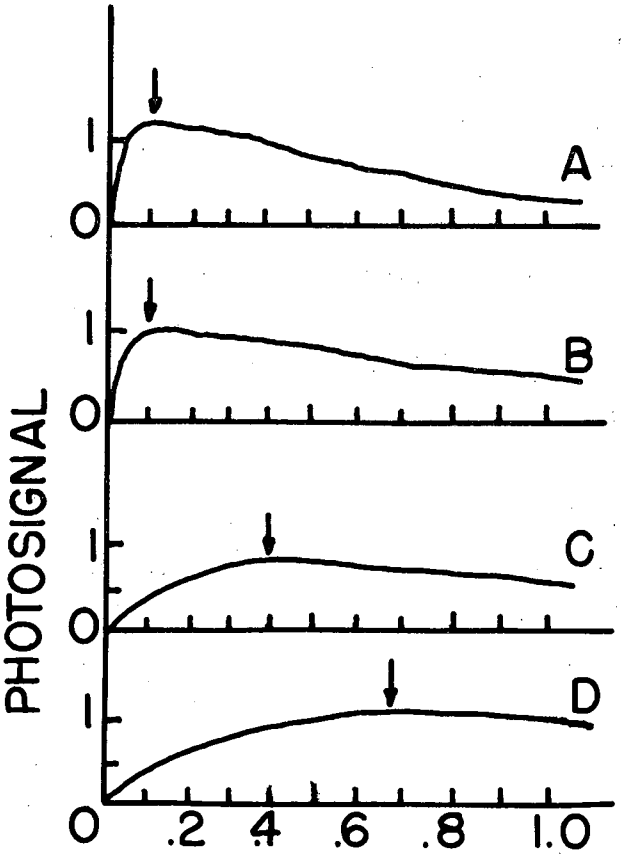

Fig. 21. Carrier diffusion experiment. Curve A - Rise and decay characteristics of FT-503 light pulse with a 6000 to 7000 Å band-pass filter. This light pulse was used to obtain curves B, C, and D. Curve B - Photocurrent pulse for front-face illumination of 4×10^{-4}-cm-thick surface cell. Curve C- Photocurrent pulse for back-face illumination of 4×10^{-4}-cm-thick surface cell. Curve D - Photocurrent pulse for back-face illumination of 8×10^{-4}-cm-thick surface cell.

Because of the concentration gradient, carriers will diffuse out of the region $0 < x < h$ toward the region of high conductivity, δx, located at $x = \ell$. The time dependence of the carrier concentration C at $x = \ell$ for such a system can be expressed by[38]

$$C = C_o \left\{ \frac{h}{\ell} + \frac{2}{\pi} \sum_{n=1}^{n=\infty} \left[\frac{1}{n} e^{-\left(\frac{n\pi}{\ell}\right)^2 Dt} \cdot \cos\left(\frac{n\pi x}{\ell}\right) \cdot \sin \frac{n\pi x}{\ell} \right] \right\}, \quad (24)$$

where D is the diffusivity of the charge carriers. Since strongly absorbed light was used in these experiments, the charge carriers will be initially 90% contained in the region within 10^{-5} cm of the illuminated surface. Therefore, $h = 10^{-5}$ cm should be used in Eq. (24), and if we assume various values for ℓ and D the curves shown in Fig. 22 can be obtained. Because charge-carrier recombination has been neglected so far these theoretical curves approach a limiting value of $C_o\, h/\ell$ rather than going through a maximum. Reference to Fig. 21b demonstrates that the rise of the flash photocurrent is quite a bit more rapid than the decay. It is therefore reasonable to assume that the peak of the photocurrent occurs at a time when the rate of diffusion of carriers into the region of high conductivity is beginning to decrease. From the theoretical curves, we might expect this to occur at approximately 0.8 $(C_o \frac{h}{\ell})$. For the 4×10^{-5}-cm-thick sample, one would estimate a diffusivity of 10^{-4} cm^2/sec from the data given in Fig. 21b and the theoretical curves of Fig. 22. For the 8×10^{-4}-cm-thick sample, the data again yield a diffusivity of approximately 10^{-4} cm^2/sec. This is an upper limit on the diffusivity for the following reasons:

(a) The effect of recombination may have been underestimated, and consequently the peak photocurrents may be occuring at less than 80% theoretical maximum.

(b) The region of high conductivity (δx) may not be completely negligible, and this would result in a smaller value for ℓ than that used in the calculations. Again, this would lead to a high value for the diffusivity.

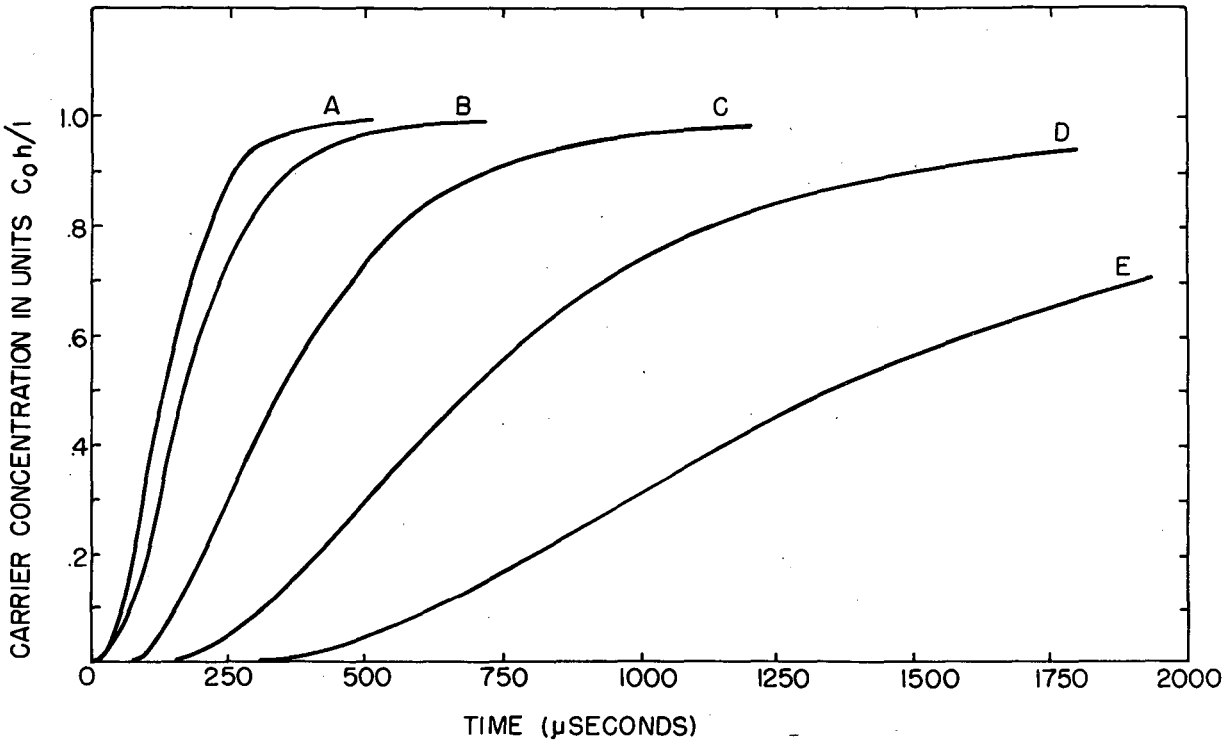

Fig. 22. Theoretical photocurrent rise curves.
$h = 10^{-5}$ for all curves.
A: $D = 10^{-5}$ cm^2/sec, $\ell = 10^{-4}$ cm
B: $D = 10^{-4}$ cm^2/sec, $\ell = 3.5 \times 10^{-4}$cm
C: $D = 4 \times 10^{-4}$ cm^2/sec, $\ell = 10^{-3}$cm
or $D = 5 \times 10^{-5}$ cm^2/sec, $\ell = 3.5 \times 10^{-4}$cm
D: $D = 5 \times 10^{-5}$ cm^2/sec, $\ell = 5 \times 10^{-4}$cm
or $D = 10^{-4}$ cm^2/sec, $\ell = 7 \times 10^{-4}$ cm
or $D = 2 \times 10^{-4}$ cm^2/sec, $\ell = 10^{-3}$ cm
E: $D = 10^{-4}$ cm^2/sec, $\ell = 10^{-3}$ cm.

Since the mobility, μ is $\frac{e}{kT} \times D$, a value of $\mu \cong 4 \times 10^{-3}$ cm^2/sec-volt may be calculated from the room-temperature value of the diffusivity.

The effect on the current pulse of the application of an electric field perpendicular to the plane of the sample was investigated. Two plates of conducting glass were positioned on opposite faces of, but insulated from, a surface cell. When the back surface plate was maintained at + 1200 v with respect to the front plate, the conductivity pulse arrived 70 μsec earlier than when 1200 v was applied to the back plate. This is shown in Fig. 23A. These results are in keeping with the conclusion reached earlier that positive holes carry the bulk of the current.

When the temperature of a sample is lowered from 25 to -35°C, the delay between the flash and photocurrent maxima increased from 470 μsec to 600 μsec. This is shown in Fig. 23b. Because of the broadness of the conductivity pulse, it was difficult to accurately locate the peak of the photocurrent. It is clear, however, that the mobility of the carriers decreases with a decrease in temperature.

With the above value for the bulk mobility and the data from Section 3.6, it is possible to estimate the concentration of charge carriers, N, present at room temperature by using the equation

$$\sigma = \sigma_o e^{-\Delta E/2kT} = N \cdot \mu \cdot \frac{1}{6 \times 10^{18}} . \qquad (25)$$

Experimentally, we have $\sigma_o = 0.3\ \Omega^{-1}\ cm^{-1}$, $\Delta E = 1.73$ ev, $\mu = 10^{-3}\ cm^2$/volt-sec, and $T = 300°K$. Thus we obtain $N \cong 2 \times 10^7$ carriers/cm^3. Photocurrents are approximately the same order of magnitude as dark currents so N is approximately the number of photocarriers produced during illumination of a sample under ordinary conditions. This rather low value for charge-carrier concentration explains why it has been impossible to observe photo-induced unpaired-electron spin in such samples with a spectrometer capable of detecting a minimum of 10^{13} spins.

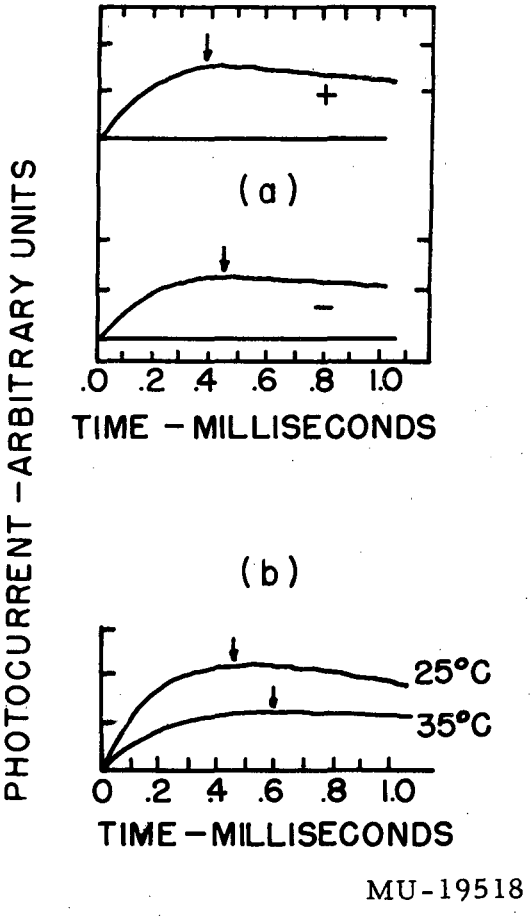

Fig. 23. (a) Field effect on the photocurrent pulse. The ± signs indicate the polarity of back face with respect to the front face. These results were obtained with back-face illumination of the 4×10^{-4}-cm-thick surface cell.

(b) Temperature effect on the photocurrent pulse of the 4×10^{-4}-cm-thick surface cell.

3.12 Negative Photoconductivity

Under certain conditions, when a sample was subjected to very-high-intensity illumination of the proper wavelength, the conductivity is reduced below the steady-state dark conductivity value. This effect is shown in Fig. 24a for steady-state photoconductivity produced by high-intensity illumination with 4000 to 5000 Å light. With the onset of illumination, the conductivity initially increases, but rapidly decreases exponentially to a value below the dark value (time constant = 17 sec). When illumination ceases, the conductivity increases slowly to the original dark value. The same effect is observed in flash photoconductivity measurements where the conductivity initially rises upon flashing, but rapidly decrease to a value lower than the original dark conductivity. This effect is shown in Fig. 24b.

Both the flash and steady-state negative photocurrents appear to have the same spectral response in that the effect is localized in the region between 3500 to 4500 Å.

The maximum decrease in the conductivity below the dark value as a result of flash illumination with 4000 Å light was measured at various flash intensities by using neutral density filters and found to vary almost linearly with the light intensity. The steady-state negative photoconductivity appeared also to have a strong intensity dependence. At low 4000 Å light intensities, negative photocurrents were not observed in either flash or steady-state photocurrents.

If a sample is illuminated with low intensity of ambient light and simultaneously flashed or illuminated with high intensity 4000 Å light, the negative photoconductivity is enhanced. This effect is shown in Fig. 25 for a 4000 Å flash illumination. The intensity of the flash was low enough that negative photoconductivity was not observed until the sample was also illuminated with ambient light. The magnitude of the ambient-light photocurrent appears to be the important factor rather than the wavelength of the ambient light.

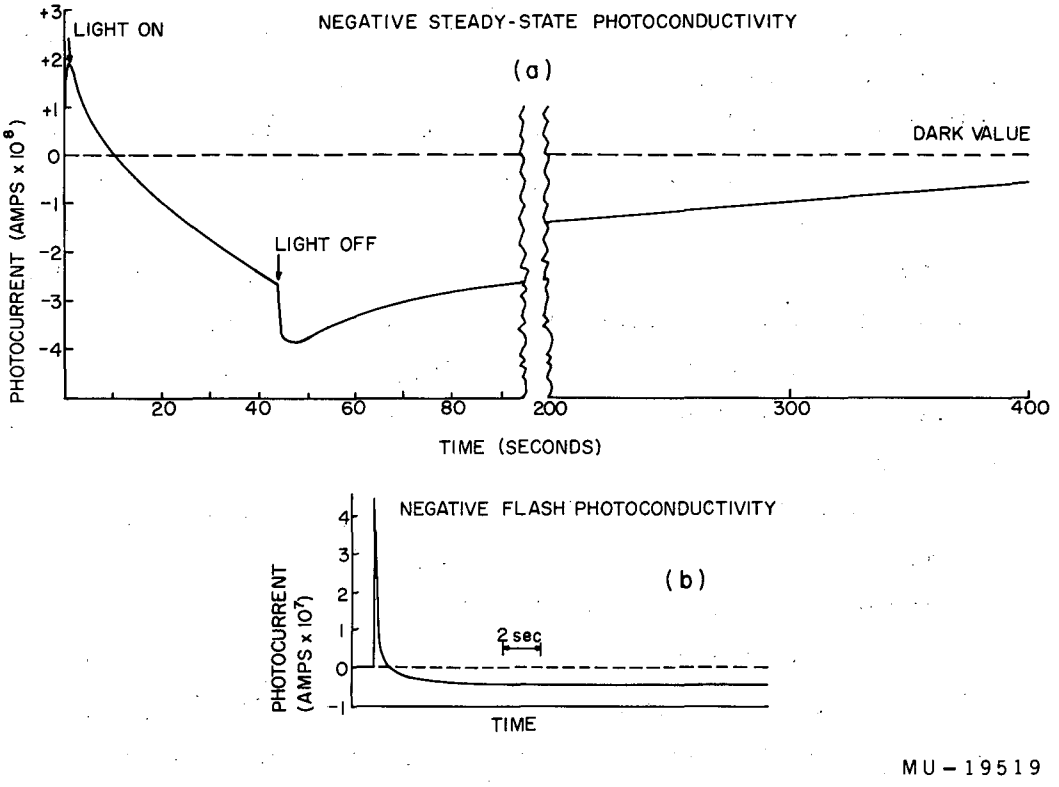

Fig. 24. (a) Negative steady-state photoconductivity. (b) Negative flash photoconductivity.

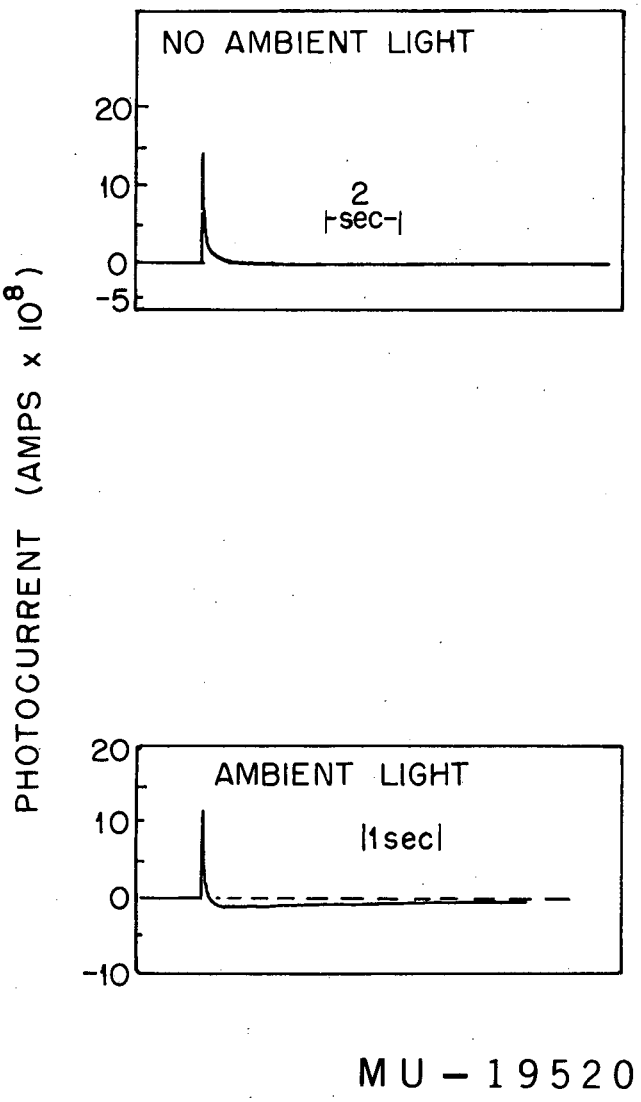

Fig. 25. Ambient-light effect on negative flash photoconductivity.

The magnitude of the steady-state negative photoconductivity was quite sensitive to the voltage applied to the sample, disappearing when the field strength dropped below 5×10^3 volts/cm.

When the sample was cooled, both the steady-state and flash negative photoconductivity disappeared. This is shown in Fig. 26 for the flash photoconductivity.

These results may be explained by the following model. Assume that there exist "impurities" in the phthalocyanine lattice (possibly oxidized phthalocyanine) which may acquire an extra electron from neighboring phthalocyanine molecules, with a certain expenditure of energy. Further, assume the negative ion of the "impurity" has an excited electronic level which lies higher relative to the ground state of a phthalocyanine negative ion. (This is shown in Fig. 27.)

Thermal excitation (process 1) or photo-excitation (process 2) of neutral phthalocyanine molecules results in transfer of an electron to an acceptor impurity, A, to form A^- and Ph^+. According to this diagram, we sould associate the energy change of process 1 with the thermal activation energy of dark conductivity (see Section 3.6). If the A^- ion is now excited by light ($\approx$4000 Å, process 4) to its first excited state, it may loose an electron to a neutral phthalocyanine molecule to form $A^o + Ph^-$. If the extra electron on the Ph^- is free to migrate, it will initially increase the conductivity but will rapidly combine with Ph^+ to give a net decrease in the number of charge carriers and conductivity. At room temperature, thermal excitation of Ph (process 1) will rapidly reform A^- and Ph^+ so that a net decrease in Ph^+ will be observed only when the rate of process 4 transitions is large, i.e., only with a very-high-intensity illumination. This explains the intensity dependence of the effect and why negative photocurrents are observed only with very-high-intensity light.

When the temperature is lowered, the concentration of Ph^+ in the dark decreases, and recombination with Ph^- produced by processes 4 and 5 is reduced. The rate of formation of Ph^+ by process 1 will be correspondingly reduced so that at first we might expect to see

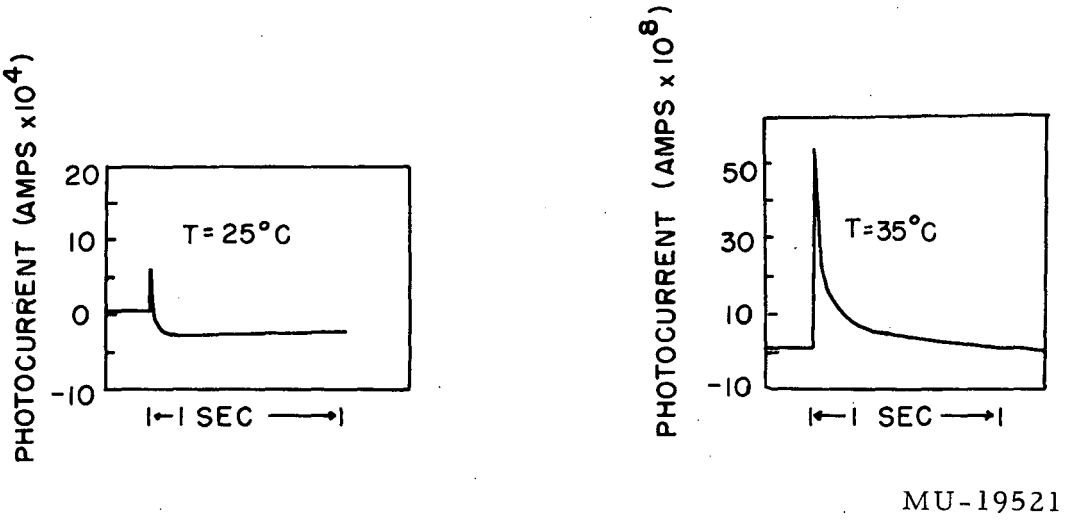

Fig. 26. Effect of temperature on negative flash photoconductivity.

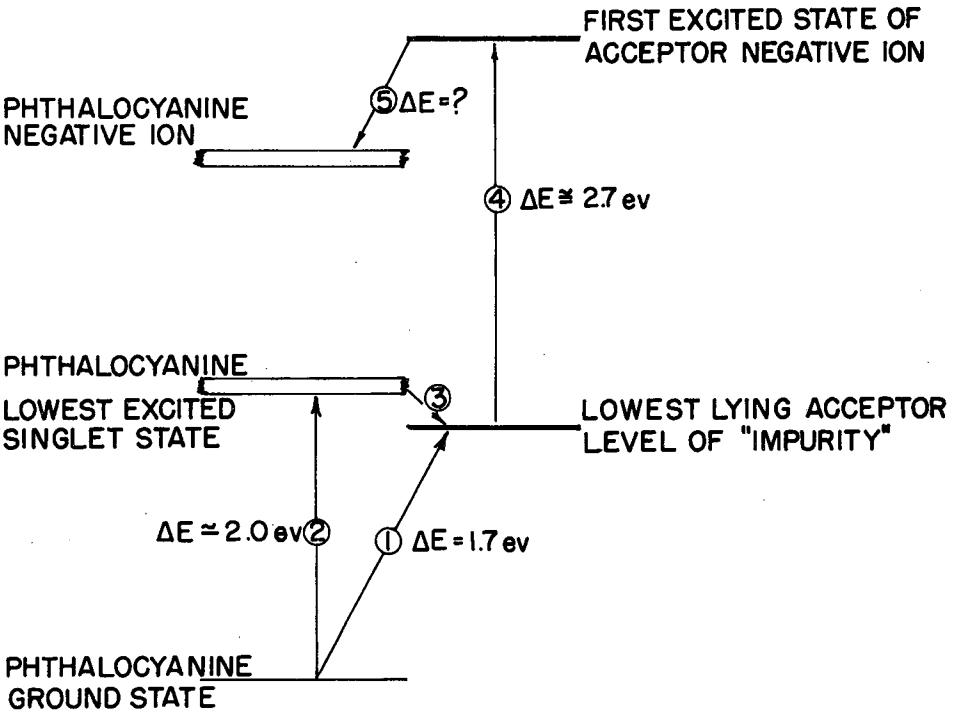

Fig. 27. Model showing the relation between energy levels of phthalocyanine and impurity.

no change in the negative photoconductivity effect with temperature. As temperature is decreased, however, the mobility (see Section 3.11) and hence the carrier recombination rate constant (see Eqs. 8 and 9) also decreases. The decrease with temperature in the rate of recombination of Ph^+ and Ph^- due to hole migration is apparently great enough that at low temperatures the total concentration of carriers, $Ph^+ + Ph^-$, is greater during illumination with 4000 Å light than the Ph^+ concentation in the dark.

Ambient light which ordinarily produces positive photoconductivity accentuates the negative photoconductivity since it produces a higher concentration of Ph^+ through processes 2 and 3, allowing Ph^- formed by 4000 Å light to recombine more rapidly with the Ph^+. Thus it is the magnitude of the photocurrent produced by the ambient light rather than the wavelength which is important.

Application of high field strengths may increase the steady-state concentration of Ph^+ as well as increase the probability of process 5. In either case, the negative photocurrent effect would be enhanced.

The model also explains why holes are the principal carriers. Transfer of electrons from A^- to A is impossible if A is present, as it should be, in low concentrations, and transfer of an electron from A^- to Ph is possible only if A^- is excited. Therefore the negative charges are essentially localized at the sites of A molecules, while the positive charges are mobile.

3.13 Effect of Ambient Illumination on Photoconductivity

If a sample is illuminated with a steady light source and simultaneously subjected to flash illumination, the photocurrent due to the flash decays more rapidly than it would in the absence of the ambient light (see Fig. 28). The effect is greater with greater intensity of the ambient light. At highest ambient-light intensity, the flash-photocurrent decay becomes approximately unimolecular after about 0.01 sec. This effect may be interpreted simply as a concentration effect in which the ambient-light-produced carriers are present in concentrations greater than flash-produced carriers at the longer times. This causes the flash current to decay pseudo-unimolecularly. This hypothesis is supported by the spectral response curves of the long-time decay when the wave length of the ambient light was varied. In these experiments, the sample was flash-illuminated from one side and illuminated with ambient light from the other side. It was found that the ambient light had its greatest effect on the decay curve at wave lengths that corresponded to the inverse of the phthalocyanine absorption spectrum, indicating a direct interaction between flash-produced carriers and ambient-light-produced carriers (see Fig. 29). Wave lengths in the infrared region of the spectrum had no effect on the decay, again indicating the absence of trapping of positive holes. According to the discussion of Section 3.12, the electrons are localized at "impurity" sites in the solid.

In these samples, the room-temperature dark current was approximately twice as great as the photocurrent produced by the highest-intensity ambient light. In addition, as indicated in Section 3.2, neither an increase nor a decrease in this dark current over several orders of magnitude produced any change in the kinetics of decay of the flash photocurrent. This might suggest that the measured dark current was not an intrinsic property of the phthalocyanine, but rather an artifact of the sample cell. This possibility was eliminated by the observation that the photocurrent produced by a standard light was

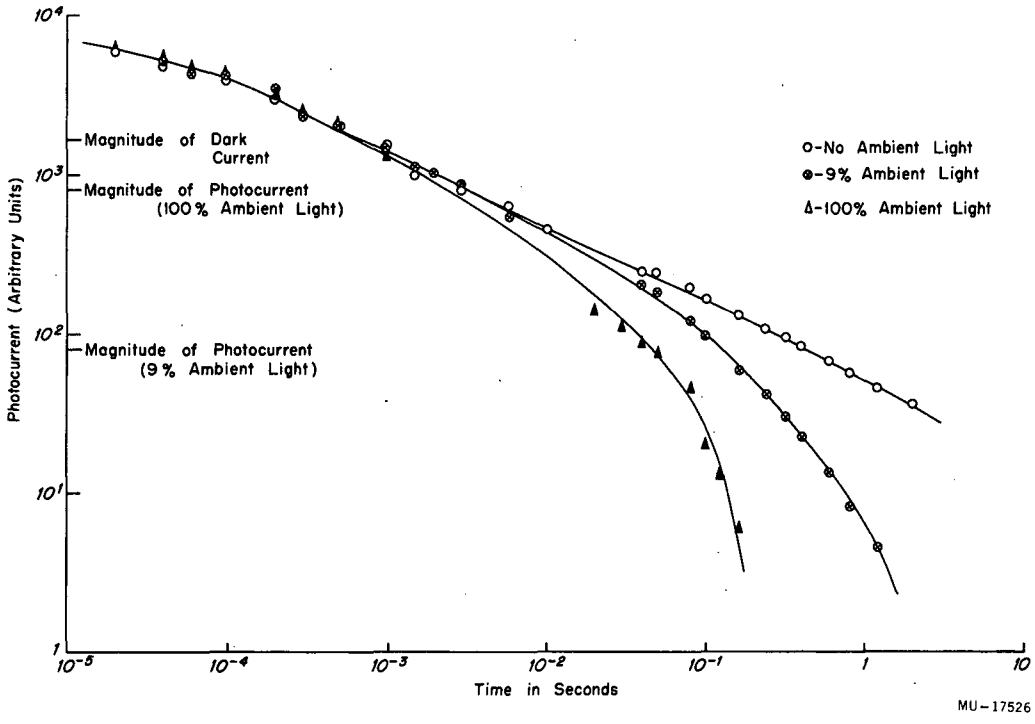

Fig. 28. Ambient-light effect on flash photoconductivity decay. The unit on the ordinate is 10^{-8} amps.

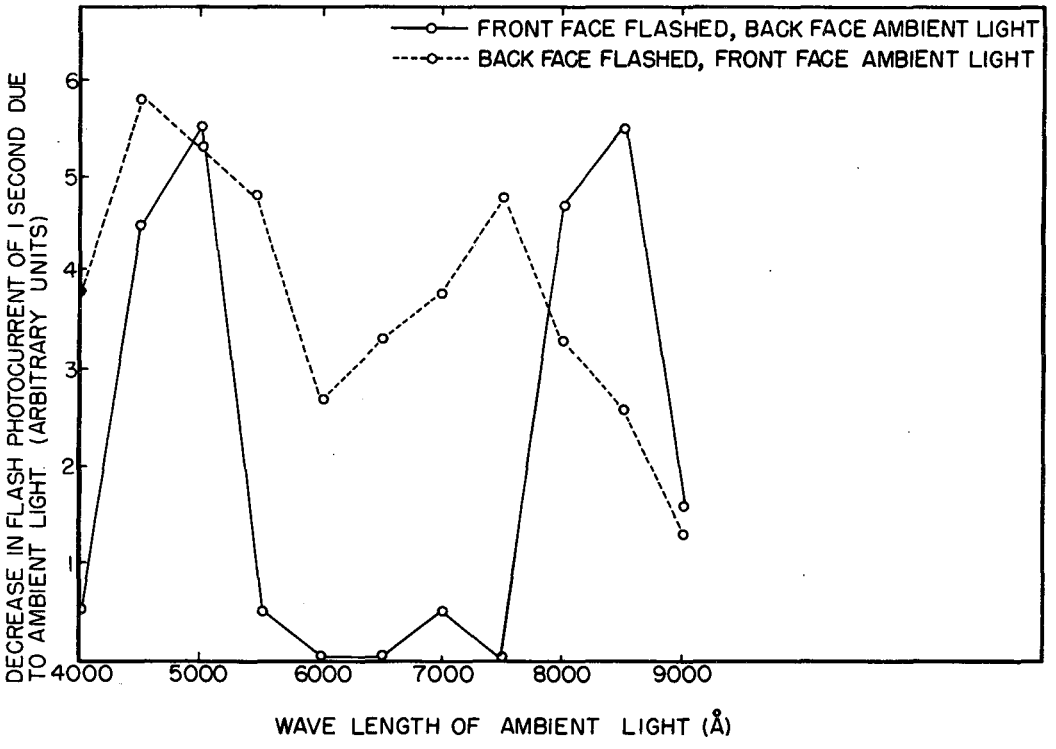

Fig. 29. Spectral response of the ambient-light effect on flash-photoconductivity decay.

was essentially proportional to the measured dark current for a series of seven different samples. These results and the ambient-light experiments suggest that the dark current is somehow different from the photocurrent. It is not possible to explain this difference at present.

4.0 CONCLUSIONS

The experimental results presented in the preceding sections suggest the following mechanism for photoconduction and dark conduction in metal-free phthalocyanine.

From the correspondence between the phthalocyanine absorption spectrum and the spectral response of photoconduction in nearly transparent surface cells, it is concluded that the first action of light is to raise phthalocyanine molecules into their first excited singlet state. This excitation energy may certainly migrate through the crystal in the form of an exciton[18] and may travel over 10^{-5} cm. At the same time, some of the excited singlets will be converted into triplet states which are certainly much less mobile.[39] Evidence that phthalocyanine molecules in the triplet state can lead to production of charge carriers comes from consideration of the initial decay of the flash photoconductivity and the flash-intensity dependence of the decay. While triplet-state excitons are not mobile, excited singlet states could be formed by thermal excitation of triplets. In any case, when the excitation energy, triplet or singlet, is transferred to a phthalocyanine molecule located next to an electron-accepting impurity, an electron is transferred from that phthalocyanine molecule to the acceptor, A, to form Ph^- and A^-. It is not clear at this point whether phthalocyanine in the triplet state can transfer an electron to the acceptor without additional energy. Quite possibly it can. In any case, it appears that the triplet state can be an intermediate in the photoproduction of charge carriers.

The evidence for the existence of an electron-accepting impurity in the phthalocyanine matrix comes from two sources:

(a) Consider the following argument. Suppose phthalocyanine negative ions were actually formed by photo excitation of the solid. The extra electron on the Ph^- is in an excited π molecular orbital which would be larger than the lower-lying orbitals in which the electrons move for positive charge migration. Certainly overlap of molecular orbitals between neighboring molecules is necessary for electron transfer between molecules, and we conclude that electron transfer should proceed more easily when the higher-lying, larger molecular orbitals are involved than when the more localized molecular orbitals used in positive-charge migration are involved. This very crude argument requires that the negative charge be more mobile than the positive charge (holes). The polarity photocurrent measurements demonstrate, however, that holes are the more mobile carriers. This is accounted for if we assume that Ph^- ions are not formed in significant concentration during the usual measurements but rather A^- are formed with the result that the negative charges are essentially immobile.

(b) The most direct evidence for the existence of electron accepting impurities in the phthalocyanine lattice comes from the results of the negative photoconductivity experiments.

Analysis of the photocurrent decay data indicates that the positive and negative charges may move independently of each other once they are separated onte to two molecular diameters. Electron transfer from Ph^* (phthalocyanine in its first excited state) to A separates the charges about one molecular diameter and apparently with little added energy the positive charges may migrate away from A^-. It is also possible that energy is gained in transfer of an electron from a phthalocyanine molecule in its first excited singlet state to A, and this energy may be sufficient to allow for complete charge separation. The greater-than-linear increases of the photoconductivity with increase in applied field suggests that application of a strong electric field aids the charge-separation step.

The measurement of the diffusivity of holes ($< 10^{-4} cm^2/sec$) and the mobility calculated from this value ($< 4 \times 10^{-3} cm^2/volt\text{-}sec$) indicate hole migration is more of a hopping process than migration in a "conduction band" similar to those found in inorganic semiconductor crystals.

When the exciting light is removed, the photocurrent decays due to recombination of the mobile holes and the localized negative charges. As noted before, this recombination takes place when the charges are within one to two molecular diameters apart. It is also possible to obtain stimulated recombination. Photo- or thermal excitation of A^- will permit an electron to be transferred to a neutral phthalocyanine molecule. As discussed above, extra electrons on phthalocyanine molecules should be even more mobile than the hole, and recombination should occur more rapidly.

Dark conductivity is achieved simply by thermal excitation of phthalocyanine causing direct electron transfer of an electron to acceptor impurities without going through the excited singlet state.

It is now possible, using the data presented in previous sections, to test to some degree the plausibility of the mechanism presented above by calculating the minimum number of A molecules required. The relation between the specific conductivity, σ, and the number of charge carriers, $N = A^- = Ph^+$, is given in Eq. 25.

From section 3.6, we have $\Delta E = 1.73$ and $\sigma_o = 0.3\ \Omega^{-1} cm^{-1}$, and from section 3.11, $\mu = 10^{-3} cm^2/volt\text{-}sec$. If we choose the highest temperature at which conductivity measurements have been made with high-purity phthalocyanine (400^oC) to make the calculations for A^-, we will have a lower limit on the number of A molecules required to explain the conductivity data.

In section 3.11 it was found that the carrier mobility increases with increasing temperature. This substantiates to some degree the notion discussed in section 3.7 that there is an activation energy, $\Delta t = 0.2$ ev, associated with carrier migration. On this basis, the carrier mobility at 400^o will be increased by a factor of 70 over

the room temperature value. Using this value, we calculate

$$[A^-]_{400} = 7 \times 10^{12} \text{ ions/cm}^3$$

from the above data. The number of phthalocyanine molecules in 1 cm^3 is 10^{21}; therefore, the concentration of A molecules must be greater than one part in 10^8. This is of course well within the realm of possibility and in fact an organic-impurity concentration of 1 part in 10^4 would certainly not be unreasonable. If the impurity concentration were actually two parts in 10^7, a temperature of approximately 625°C would be required to convert all A's and A^-'s. At this temperature it should then be possible to begin to produce Ph^- ions and the conductivity should increase, but with a higher activation energy. In addition, the current should change from positive-hole majority carriers to negative-charge majority carriers.

We conclude that the proposed mechanism for photo- and dark conduction is easily capable of accounting for the electrical behavior of metal-free phthalocyanine. This mechanism will be further supported by the results discussed in Part Two.

REFERENCES

1. A. Pochettino, Acad. Lincei Rendiconti 15, 355 (1906).
2. M. Volmer, Ann. Physik 40, 775 (1913).
3. J. Koenigsberger and K. Schilling, Ann. Physik 32, 179 (1910).
4. A. Szent-Gyorgyi, Science 93, 609 (1941).
5. A. Szent-Gyorgyi, Nature 157, 875 (1946).
6. D.D. Eley, G.D. Parfitt, M.J. Perry, and D.H. Taysum, Trans. Faraday Soc. 49, 79 (1953).
7. D.D. Eley and G.D. Parfitt, Trans. Faraday Soc. 51, 1529 (1955).
8. H. Inokuchi, Bull. Chem. Soc. Japan, 24, 222 (1951).
9. H. Inokuchi, Bull. Chem. Soc. Japan, 27, 22 (1954).
10. E. Katz, in Photosynthesis in Plants, J. Franck and W.E. Loomis, Eds. (Iowa State College Press, Ames, Iowa, 1949), p. 291.
11. D. F. Bradley and M. Calvin, Proc. Nat. Acad. Sci. U.S. 41, 563 (1953).
12. C. G. B. Garrett, in Semiconductors N. B. Hannay, Ed. (Reinhold Publishing Corporation, New York, 1959), p. 634.
13. D. D. Eley, Research Applied in Industry XII, 293 (1959).
14. L. E. Lyons, J. Chem Soc., 5001 (1957).
15. R. M. Hedges and F. A. Matsen, J. Chem. Phys. 28, 95 (1958).
16. J. Blackledge and N. S. Hush, quoted by N. S. Hush and J. A. Pople, Trans. Farad. Soc. 51, 600 (1955).
17. M. E. Wacks and V. H. Dibeler, J. Chem. Phys. 31, 1557 (1959).
18. A. S. Davydov, J. Exptl. Theoret. Phys. (U.S.S.R.) 18, 210 (1948).
19. R. C. Nelson, J. Chem. Phys., 22, 885 (1954).
20. R. C. Nelson, J. Chem. Phys., 22, 880 (1954).
21. R. C. Nelson, J. Chem. Phys. 22, 892 (1954).
22. A. T. Vartanyan and I.A. Karpovich, Doklady Adad. Nauk. (U.S.S.R.) 111, 561 (1956).
23. P. E. Fielding and F. Gutman, J. Chem. Phys. 26, 411 (1957).
24. H. Meier, Z. Elektrochem., 58, 859 (1954).
25. W. J. Moore, Physical Chemistry (Prentice-Hall, New York, 1950), p. 451.

26. T. R. Waite, Phys. Rev. 107, 463 (1957).
27. N. F. Mott and R. W. Gurney, Electronic Processes in Ionic Crystals (Clarendon Press, Oxford, 1950).
28. G. Porter and M. R. Wright, Disc. Farad. Soc. (in press, 1960).
29. H. P. Kallmann and M. Silver, Proc. of Symposium on Fluorescence and Semiconductors, Garmisch-Partenkirchen, Fall, 1956.
30. D. C. Northrup and O. Simpson, Proc. Roy. Soc. (London) 244A, 377 (1958).
31. D. M. J. Compton, W. G. Schneider, and T. C. Waddington, J. Chem. Phys., 27, 160 (1957).
32. N. F. Mott and R. W. Gurney. op. cit., pp. 156 et seq.
33. J. Kommandeur, G. J. Korinek, and W. G. Schneider, Can. J. Chem. 35, 998 (1957).
34. B. Rosenberg, J. Chem. Phys. 31, 238 (1959).
35. T. S. Moss, Optical Properties of Semiconductors (Academic Press Inc., New York, 1959), p. 251.
36. L. E. Lyons, J. Chem. Phys. 23, 220 (1955).
37. D. S. McClure, in Solid State Physics (Academic Press, New York and London, 1959), Vol. 8, p. 1.
38. R. M. Barrer, Diffusion in and through Solids (University Press, Cambridge, 1941), p. 14.
39. D. L. Dexter, J. Chem. Phys. 21, 836 (1953).

II. EFFECTS OF ADDED ELECTRON ACCEPTORS AND DONORS

1.0 INTRODUCTION

A number of studies have indicated that the conductivity of organic semiconductors may be significantly altered by the presence of impurity materials. For example, gases such as O_2, Cl_2, and NO_2 have been found to increase both the semiconductivity and photoconductivity of anthracene crystals by several orders of magnitude.[1,2] Similar effects have been observed with O_2 and metal-phthalocyanines.[3] Akamatu et al. have studied complexes between halogens and polycyclic aromatic compounds and have found 10^7-to 10^9- fold increases in dark conductivity over that of the pure hydrocarbon.[4,5] All the above effects have been tentatively interpreted by the respective authors as due to an increase in the mobility of charge carriers caused by interaction between the impurity and the host molecules.[1-3,6,7]

Matsunaga[8] has studied the magnetic susceptibility of violanthrene-iodine complex, which was found to have very high conductivity.[4] He found the complex contained unpaired electrons and suggested that this may be related to the conductivity of the complex. High conductivities have been observed in chloranil, iodanil, and bromanil complexes of dimethylaniline;[9] electron spin resonance (ESR) has been observed in molecular compounds of diamines and substituted benzoquinones.[10,11,12]

The results quoted above suggest that there may be a general effect of oxidizing agents (electron acceptors) upon the conductivity properties of certain organic substances (donors). Furthermore, it appeared that the high conductivity of certain complexes was related to the presence of unpaired-electron spin in the complex.

In an effort to further characterize the processes of charge-carrier formation and migration in organic systems, the effects of organic oxidizing and reducing agents on the electrical and magnetic properties of metal-free phthalocyanine were studied. Both steady-state and photo-kinetic measurements as well as electron

spin-resonance measurements were applied to characterize as completely as possible the nature of the conducting state of an organic solid. Further interest in this problem is generated by the fact that aggregates of porphyrin molecules (chlorophyll) and organic oxidizing agents (quinones, coenzyme Q,[13] etc.), as well as reducing agents (carotenoids[14,15]) occur together in photosynthetic materials, and their interaction may be of importance in the primary quantum-conversion process.

2.0 EXPERIMENTAL PROCEDURE

The electrical properties of "purified" metal-free phthalocyanine have already been studied in great detail, and so this compound was also used for this study. The methods of purification, sample-cell preparation, and conductivity measurements were as described in Part One. When surface cells were used, the oxidizing or reducing agents were applied by spraying a benzene solution onto the exposed area of the phthalocyanine. This produced a lamellar system in which the phthalocyanine layer separated the additive layer from the electrodes. A second type of conductivity sample was prepared by grinding the phthalocyanine with the reagent to be incorporated and then pressing the powder into a pellet. The apparatus shown in Fig. 9 of Part One was then used for the pellet conductivity measurements. The solubilities and sublimation properties of the oxidizing and reducing agents were very different from those of the phthalocyanine, so it was not possible to prepare completely homogeneous mixture.

Ortho-chloranil, a strong electron acceptor, was used for most experiments, although a few experiments were also carried out with ortho-bromanil and ortho-iodanil. These compounds were purified by recrystallization from various organic solvents.

Phenothiazine and N, N, N', N', tetra-methyl-p-phenylene diamine were the two strong electron donors used. They were purified by vacuum sublimation.

A block diagram of the spectrometer in which the electron spin-resonance measurements were carried out is shown in Fig. 30. The spectrometer was operated at a klystron frequency of about 9.6 kMc with a magnetic field modulation of 200 cps and a lock-in detection system to present the first derivative of the absorption. A balanced double-bolometer bridge was used to balance out low-frequency noise components in the klystron output. Automatic frequency stabilization of the klystron on the resonance frequency of the sample cavity was achieved by frequency modulation of the klystron at

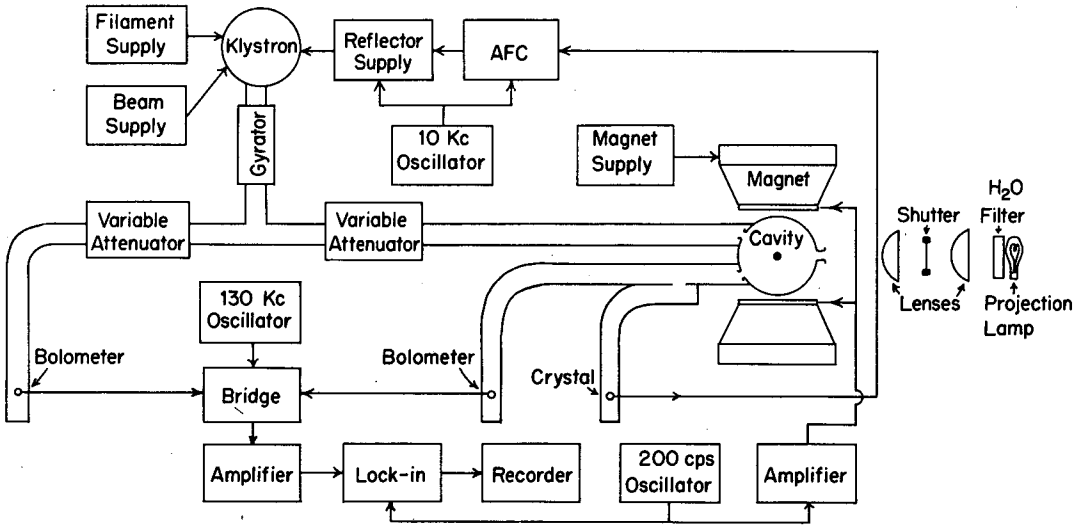

Fig. 30. Block diagram of electron-spin-resonance spectrometer.

10 kc and lock-in detection. A cylindrical transmission cavity operating in the TE_{011} mode was used.

A small 1/4-in.-diam. hole in the cavity wall allowed samples to be illuminated in the cavity during absorption measurements. A 300-watt projection lamp was used as a light source and quarts lenses were used to focus the light on the sample. A 2.5-cm-thick water filter, various Federal Engineering band-pass filters, and an IR filter were used to restrict the incident light to suitable wave lengths.

Powdered samples were simply placed in small tubes in the cavity for the spin-resonance measurements. Films sublimed on glass were mounted on the end of glass rods and could also be placed in the cavity.

3.0 RESULTS: PHTHALOCYANINE WITH ORTHO-CHLORANIL ADDED

3.1 Dark Conductivity

A. Variation with Amount of Ortho-Chloranil Added

The variation of the room-temperature dark conductivity of a phthalocyanine sample with the amount of added ortho-chloranil is shown in Fig. 31. It is apparent that the dark conductivity increases with increasing amounts of ortho-chloranil (doping) to a maximum value of about 10^7 times that of the pure phthalocyanine. This increase in the phthalocyanine conductivity occurs within seconds after the addition of the ortho-chloranil.

B. Temperature Dependence

A decrease in temperature from 25 to - 100°C resulted in a decrease in the dark conductivity of a heavily doped phthalocyanine sample by a factor of about 10^3. This corresponds to an activation energy of approximately 0.2 ev.

C. Effect of Heat Treating

A surface cell was treated with 10^{-5} moles of ortho-chloranil, then heated at 200°C for various lengths of time, and finally heated at 120°C in vacuum. The room-temperature dark conductivity was measured at various stages during this heat treatment. The results are shown in Fig. 32. A mixture containing 86% by weight phthalocyanine and 14% by weight ortho-chloranil was ground and pressed into a pellet. This pellet was heated for various lengths of time at 100°C and the dark conductivity was found to vary not more than a factor of two throughout a total heating time of 90 min. at 100°C, a result similar to that found by using the surface cell. (see Fig. 32).

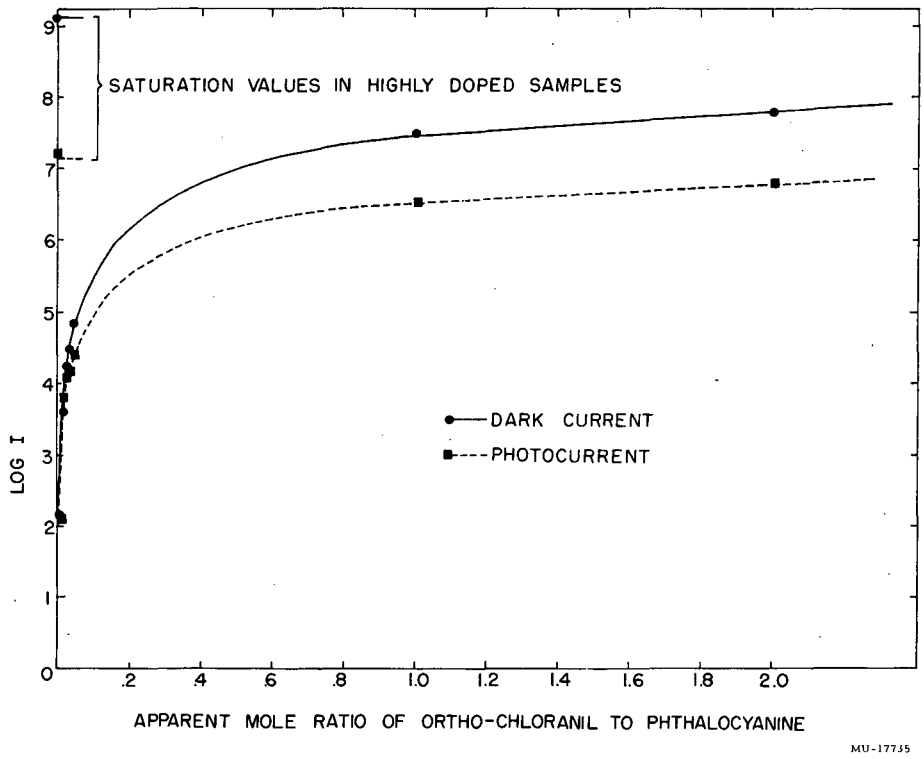

Fig. 31. Variation of the dark conductivity and photoconductivity of phthalocyanine with amount of orthochloranil added.

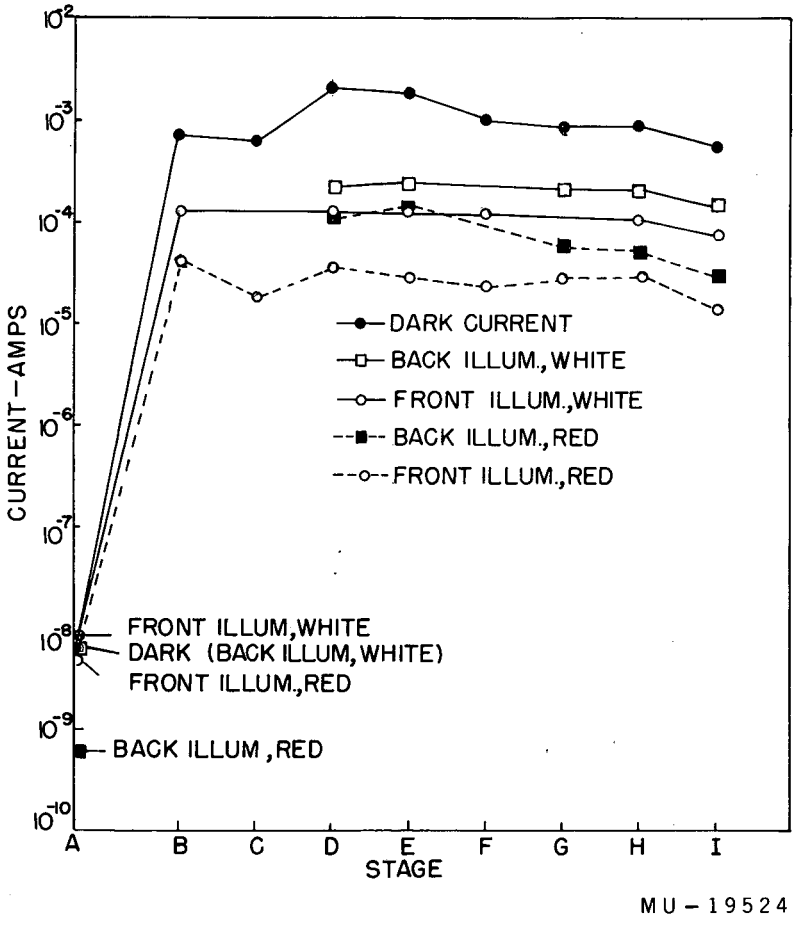

Fig. 32. Heat-treatment effect on the dark and photoconductivity of a surface cell of phthalocyanine treated with 10^{-5} moles of ortho-chloranil. The various stages were:

A - pure phthalocyanine
B - 10^{-5} moles of ortho-chloranil added
C - 20 hr later
D - + 5 min at 200°C
E - + 5 min at 200°C
F - + 15 min at 200°C
G - 24 hr at room termperature
H - 1 hr at 100°C
I - 6 hr at 120°C under reduced pressure (~10μ Hg).

D. Effect of Phthalocyanine Crystallinity

A phthalocyanine surface cell was annealed for 14 days at 275°C in a reduced natural-gas atmosphere to produce a highly crystalline sample. (See Fig. 6 of Part I). This annealed sample was then treated with 10^{-5} moles of ortho-chloranil, as was an unannealed surface cell. In Table II, the effects on the conductivity of doping the two different types of samples are compared. The dark conductivity of the amorphous sample increased a factor of 2×10^5, while that of the annealed sample increased a factor of 2×10^2 to a value about one-thirtieth that of the amorphous sample.

E. Effect of Sample Thickness

Phthalocyanine surface cells with thicknesses ranging from $\sim 10^{-4}$ cm to $\sim 10^{-3}$ were treated with 10^{-5} moles of ortho-chloranil. The dark conductivity was measured before and after doping, and virtually no difference in behavior was noted with the various samples. The thinnest and thickest sample cells had final resistances of 3×10^5 ohms while an intermediate sample had a resistance after doping of 6×10^5 ohms.

3.2 Steady-State Photoconductivity

A. Variation with Doping

The variation of the room-temperature steady-state photoconductivity of ortho-chloranil-doped phthalocyanine with ortho-chloranil concentration is also shown in Fig. 31. The maximum photocurrent obtained with a heavily doped sample was about 10^5 times that obtained with undoped material. As with the dark current, the photoconductivity increase occurs within seconds of the doping.

B. Temperature Dependence

A decrease in temperature from 25 to - 100°C resulted in a decrease by a factor of about 4×10^2 in the photoconductivity of a heavily doped phthalocyanine sample. This again corresponds to approximately a 0.2-ev activation energy. Because of the experimental

Table II

Comparison of the effect of doping a crystalline and an amorphous surface cell. This table gives the currents after doping with 10^{-5} moles of ortho-chloranil.

Type of surface cell	Dark current (amps)	Photocurrent (amps)			
		Front-face illumination		Back-face illumination	
		Red light	White light	Red light	White light
Crystalline	5×10^{-5}	6×10^{-6}	2×10^{-5}	6×10^{-6}	2.5×10^{-5}
Amorphous	1.5×10^{-3}	4×10^{-5}	10^{-4}	1.2×10^{-4}	2.6×10^{-4}

difficulties involved in measuring the temperature dependence of dark conductivity in cells of the type used in these experiments (see Part I, Section 3.6), it is not certain that the slightly larger decrease in dark conductivity upon cooling is significant.

A summary of the above results is given in Table III.

C. Spectral Response

The spectral response of photoconductivity in a lightly doped sample follows the absorption spectrum of pure phthalocyanine. As the amount of doping increases, however, a photo-induced decrease in conductivity can be observed at certain wave lengths. The magnitude of this effect increases with increasing doping but is never more than a few percent of the photo-induced increase in conductivity produced by phthalocyanine absorption. The spectral response of this effect is shown in Fig. 33. The significance of this action spectrum is not unambiguous inasmuch as it represents the resultant of two opposing processes. Cooling the sample causes this effect to disappear, with the result that wave lengths that produced a decrease in conductivity at room temperature produce an increase in conductivity at the low temperatures. It is also possible to observe the replacement of the decrease at room temperature by an increase in photoconductivity if the illumination at that wave length is prolonged.

D. Kinetics

The rise and decay curves for photoconductivity induced in ortho-chloranil-doped phthalocyanine by light in the phthalocyanine absorption bands consist of two components. One of thses is quite rapid and has time constants essentially the same as those of the undoped material. The other component is very much slower and is unimolecular for both rise and decay, with a time constant of about 60 sec. This is shown for the photoconductivity decay in Fig. 34. The fact that rise time equals decay time requires that the process be determined by the balance of the rate of input of quanta and the intrinsic decay rate, $dx/dt = (\text{const}) I_0 - \lambda X$, where I_0 is the rate of

Table III

Comparison of the maximum values of the conductivity of ortho-chloranil-doped metal-free phthalocyanine with the conductivity of pure metal-free phthalocyanine. The room-temperature specific resistivity of pure metal-free phthalocyanine was approximately 10^9 ohm cm, and that for the doped material was approximately 10^2 ohm cm. The units in the table are relative to the value for pure phthalocyanine at -100°C.

Temperature	Undoped		Doped		Doped/Undoped	
	Dark cond.	Steady-state photo-conductivity	Dark cond.	Steady-state photo-conductivity	Dark cond.	Steady-state photo-conductivity
25°C	10^3	10^3	10^{10}	10^8	10^7	10^5
-100° C	10^{-7}	1	10^7	2.5×10^5	10^{14}	2.5×10^5
25°C/-100°C	10^{10}	10^3	10^3	4×10^2	--	--

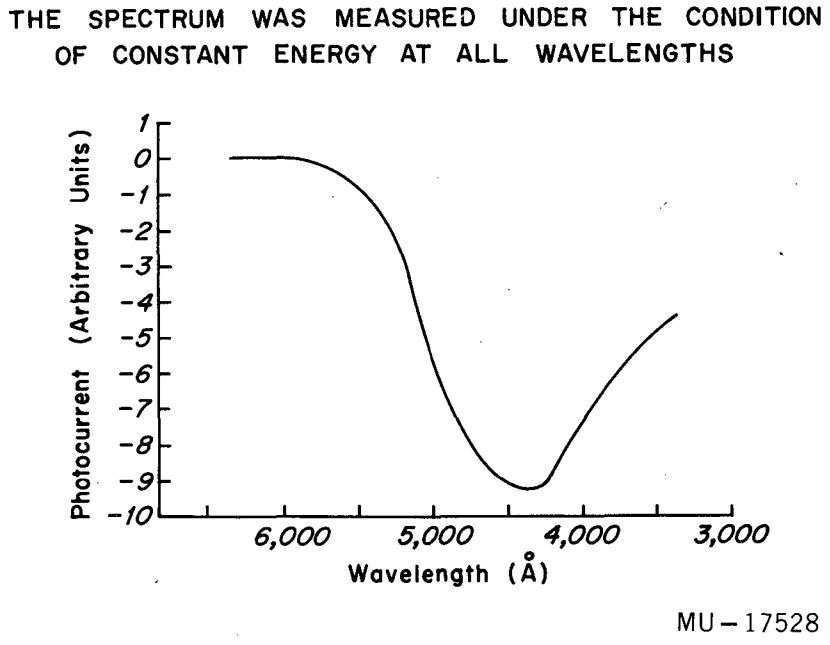

Fig. 33. Spectral response of negative photoconductivity in a heavily doped phthalocyanine sample. (100 Å bandwidth). The spectrum was measured under the condition of constant energy at all wave lengths, and a scanning rate of approximately 100 Å/3sec.

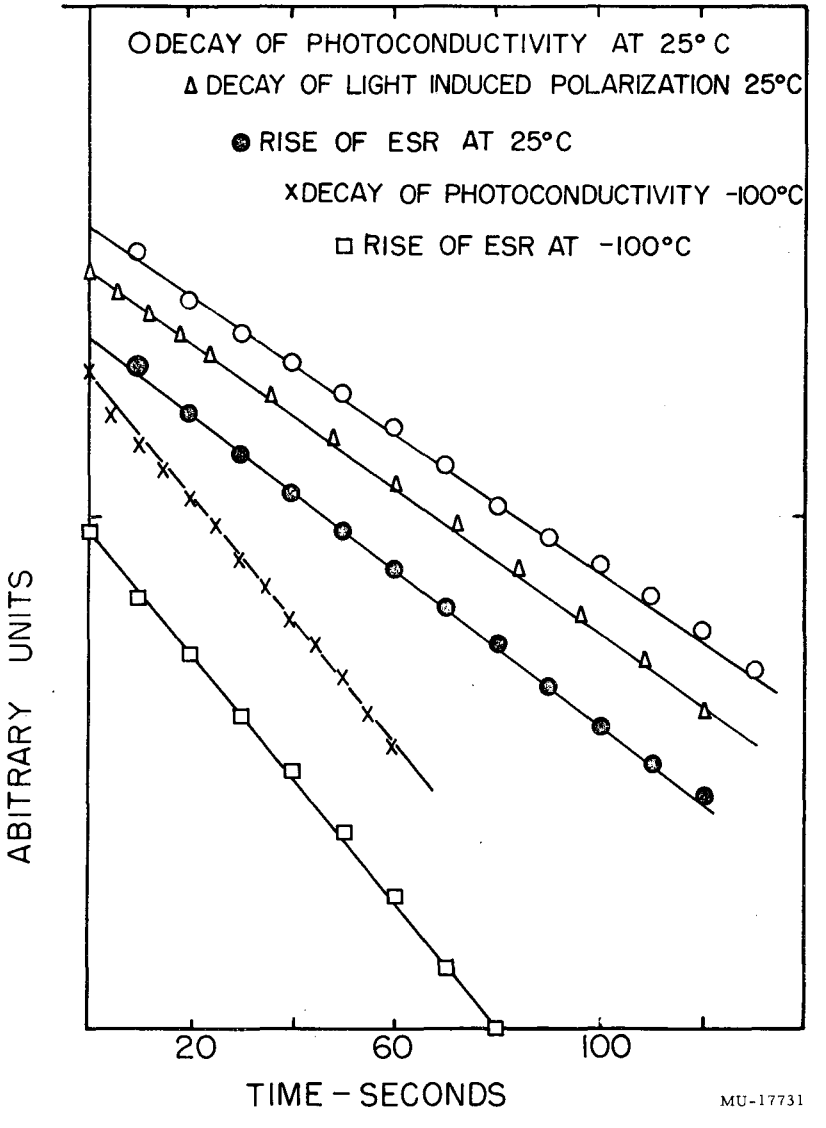

Fig. 34. Semi-log plots of the time dependence of photoconductivity light-induced electron spin resonance, and light-induced polarization in ortho-chloranil-doped phthalocyanine. The relative positions of the curves are not comparable.

input of quanta, and λ is the unimolecular decay constant. The ratio of slow to fast components increases with increasing doping. In the most heavily doped samples, the photoconductivity rise and decay can be attributed almost entirely to the process with the 60-sec time constant. At low temperatures, the time constant decreases and is about 36 sec at - 100°C.

E. Intensity Dependence of the Steady-State Photoconductivity

The intensity dependence of the steady-state photoconductivity for front-face illumination was measured for a thick sample with various amounts of ortho-chloranil. These results are shown in Fig. 35, which is a log-log plot of photocurrent as a function of 6000-to-7000-Å light intensity. It can be seen that, for front-face illumination, the photocurrent I is $(L)^Z$, where Z increases from 0.47 for undoped samples to 0.80 for a moderately doped sample and is 1.0 for a heavily doped sample. These results were obtained by focusing the filtered light from a 500-watt tungsten bulb through a water bath with IR filter onto the sample.

F. Heat Treatment

A phthalocyanine surface cell doped with 10^{-5} moles of ortho-chloranil was heat-treated as described in Section 3.1C. Measurements of the photoconductivity were made for both front- and back-face illumination with both white light and 6000- to - 7000- Å light. These results also appear in Fig.32, along with the dark-conductivity measurements. The photoconductivity due to illumination of the front surface (surface with the electrodes) with 6000-to 7000-Å light increased a factor of 5×10^3 with doping. The photoconductivity due to illumination of the back surface with the same light increased a factor of 2×10^5, or 40 times more than did the front-face-illumination photoconductivity.

G. Effect of Phthalocyanine Crystallinity

The photoconductivity of an annealed sample (see section 3.1D) was measured before and after it was doped with 10^{-5} moles of ortho-chloranil. A summary of these results is given in Table II, along with

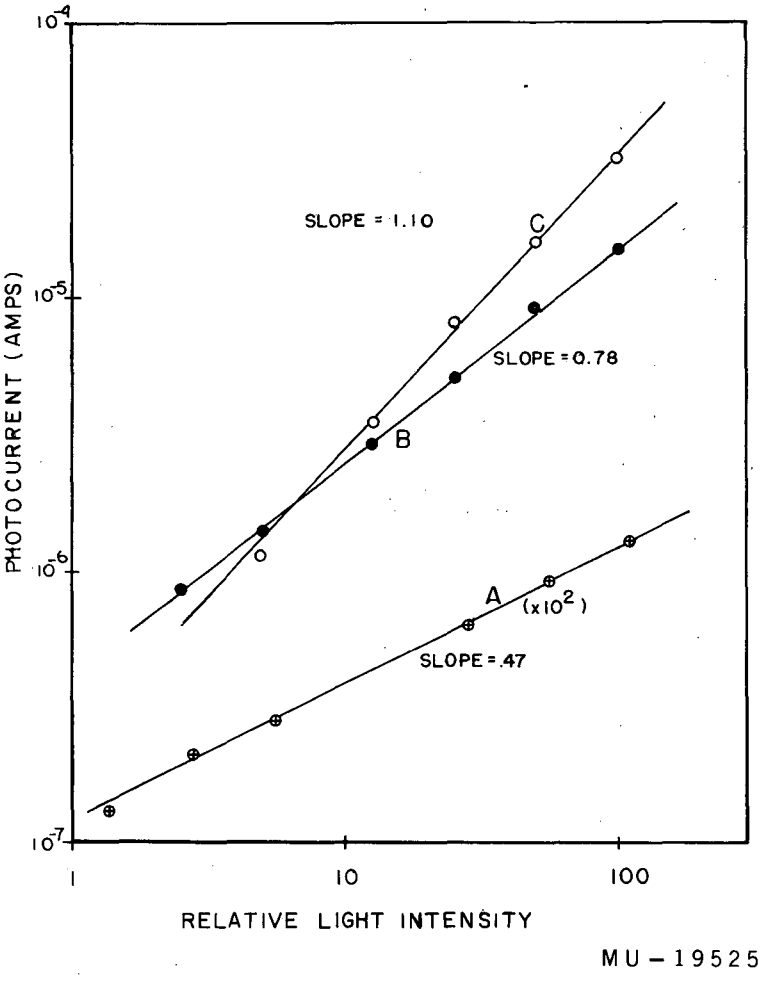

Fig. 35. Intensity dependence of the steady-state photoconductivity of phthalocyanine with various amounts of ortho-chloranil.
A - pure phthalocyanine. This curve has been multiplied by 100.
B - phthalocyanine + 10^{-5} moles of ortho-chloranil.
C - phthalocyanine + 5 x 10^{-5} moles of ortho-chloranil.

similar results for the amorphous surface cell described under section 3.2C. While the amorphous cell did exhibit slightly higher photocurrents under equivalent conditions than did the annealed sample, these differences never exceeded a factor of ten. This is significant, for if diffusion of the ortho-chloranil toward the electrode surface were a prerequisite for increased conductivity, much smaller currents would be expected with ortho-chloranil-treated annealed phthalocyanine than with the amorphous sample.

H. Effect of Sample Thickness

The photoconductivity due to front-or back-face illumination with white light or 6000- to 7000-Å light was measured for phthlocyanine samples varying in thickness from $\sim 10^{-4}$ cm to $\sim 10^{-3}$ cm before and after doping with 10^{-5} moles of ortho-chloranil. The increase in photoconductivity was very nearly the same for all the samples, with almost no difference between the final photocurrents observed with the thickest and thinnest sample.

I. Ferric Phthalocyanine

The conductivity of ferric phthalocyanine, both pure and with ortho-chloranil, was studied. Very similar to the results obtained with metal-free phthalocyanine, the dark conductivity and the photoconductivity of the metal phthalocyanine increased with increasing amounts of added ortho-chloranil. An important difference, however, between the metal and the metal-free systems was found in the decay of the photoconductivity. As noted in section 3.2, (see Fig. 34), the decay of the photocurrent in an ortho-chloranil-doped, metal-free phthalocyanine was exponential with a time constant of ~60 sec.

Figure 36 is a semi-log plot of the photocurrent decay for metal-free phthalocyanine and ferric phthalocyanine, both doped with 10^{-5} moles of ortho-chloranil. The time constant decreases from 65 sec to 50 sec in going from metal-free to ferric phthalocyanine.

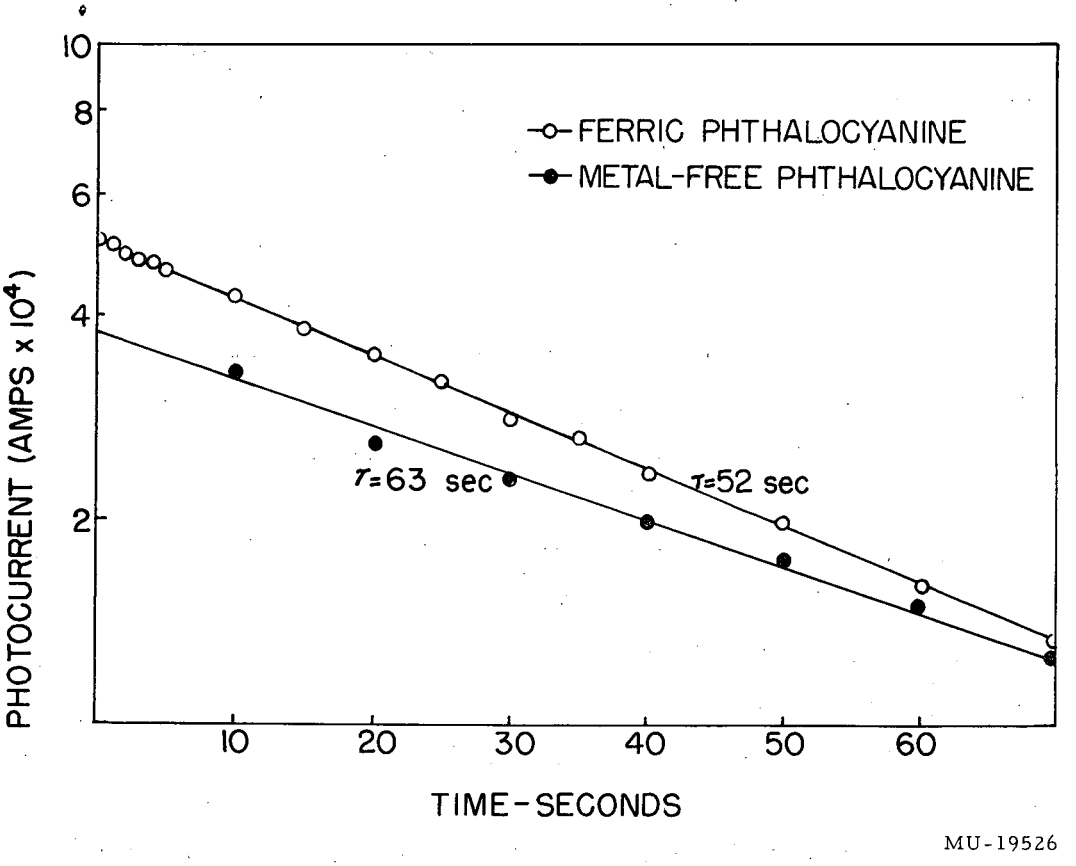

Fig. 36. Semi-log plot of the time dependence of the photoconductivity decays of ortho-chloranil doped ferric and metal-free phthalocyanine.

3.3 Electron Spin Resonance

A. Variation with Doping

It was observed that when ortho-chloranil was added to a sample of phthalocyanine in the manner described above, a large ESR absorption could be detected, corresponding to the presence of unpaired electron spins in the sample (see Fig. 37). The greater the extent of doping, the greater the ESR signal.

As it was not possible to achieve uniform mixing of phthalocyanine and ortho-chloranil, it was therefore not possible to measure the ratio of unpaired spins to the number of ortho-chloranil molecules in actual contact with phthalocyanine molecules. The number (by comparison with α, α- diphenyl β-picryl hydrazyl) of unpaired spins per total number of ortho-chloranil molecules added is 0.01. It is of interest to note that even in those cases for which stoichiometric compounds between the electron donor (reductant) and the electron acceptor (oxidant) have been measured, the number of unpaired electron spins is always much smaller than that expected for simple, complete, electron-transfer complexes ($[\dot{D}]^+$, $[\dot{A}]^-$).[12,16,17]

B. Temperature Dependence

When the sample was cooled to about 100°C in the spectrometer cavity, no change in spin concentration or line shape could be observed.

C. Effect of Heat Treatment

Electron spin-resonance (ESR) measurements were made on a portion of the 86% by weight phthalocyanine and 14% ortho-chloranil sample used for the pellet-conductivity study (see section 3.1C). The spin-resonance sample was subjected to the same heat treatment as the conductivity pellet and the spin concentration varied less than 20%, paralleling the conductivity changes.

D. Photosensitivity of Unpaired-Electron Spin Concentration. Spectral Response and Kinetics

When a heavily doped sample was illuminated in the ESR spectrometer, a decrease in unpaired spins could be observed (Fig. 38). The magnitude of this effect corresponded to a decrease of approximately 5

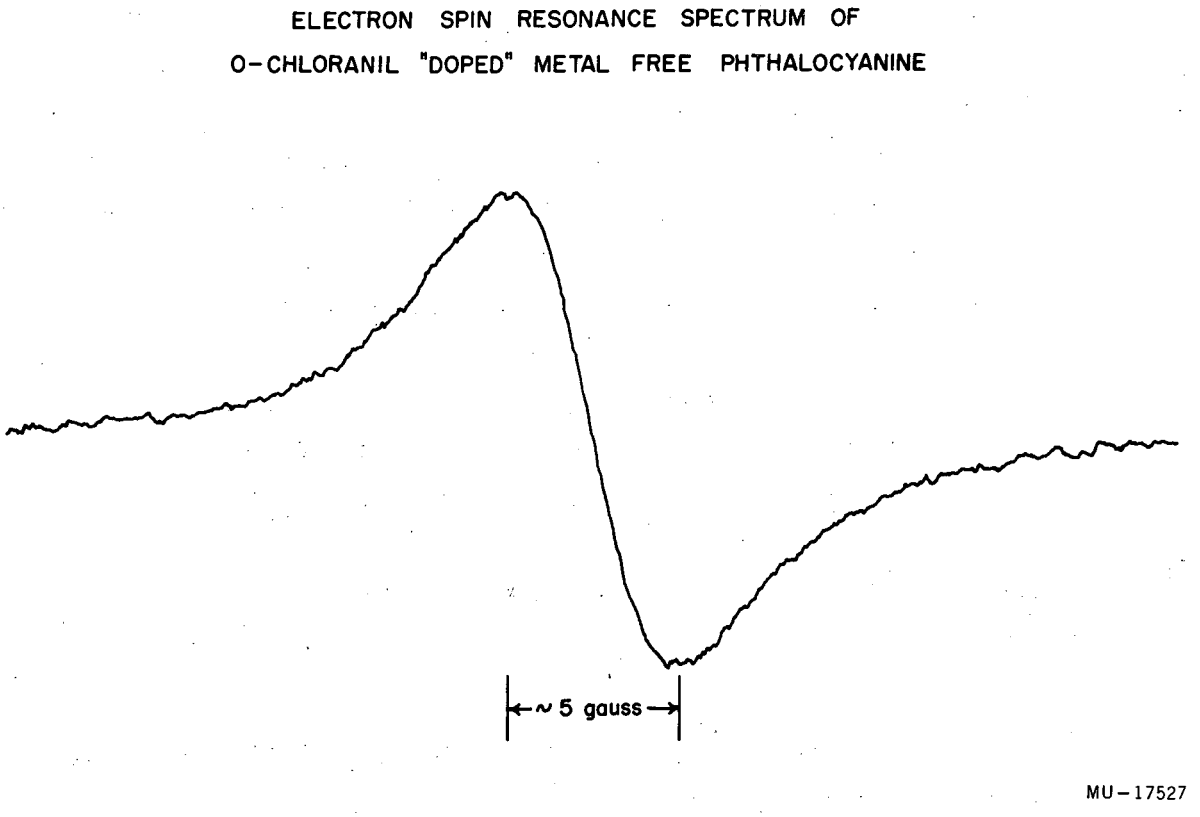

Fig. 37. Electron-spin-resonance spectrum of ortho-chloranil-doped phthalocyanine. The curve represents the first derivative of the absorption.

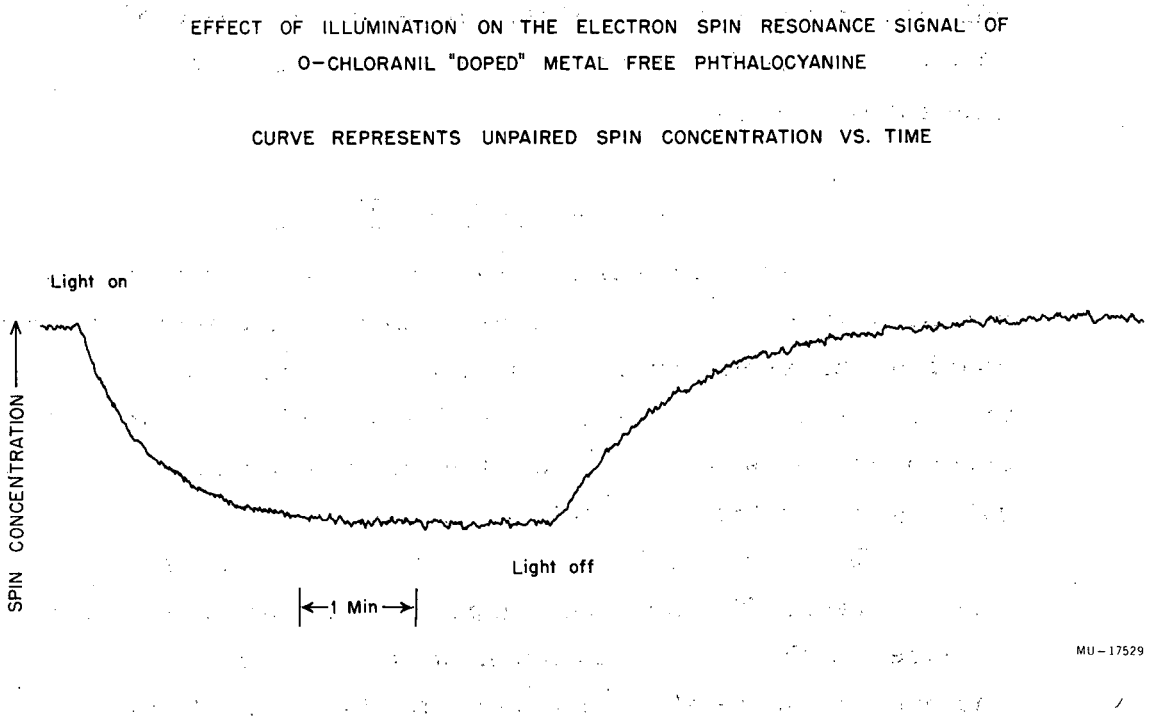

Fig. 38. Effect of illumination with white light on the electron-spin-resonance signal in ortho-chloranil-doped phthalocyanine. Curve represents unpaired spin concentration vs time.

to 20% in the spin concentration, depending upon the sample used, and was independent of the temperature. The spectral response of the photodecrease in spin concentration followed the phthalocyanine absorption spectrum. The photoinduced decrease in ESR and the subsequent rise in spin concentration, when the light was turned off, followed unimolecular kinetics, with a time constant of approximately 60 sec. At - 100°C, the time constant decreased to about 36 sec. These data are given in Fig. 34.

3.4 Light-Induced Polarization

When an ortho-chloranil-doped phthalocyanine film was placed between the plates of a condenser, a charging of the condenser could be observed by using a vibrating-reed electrometer to measure the voltage developed (Fig. 39). The sign of the induced charge on the condenser plates indicated that the phthalocyanine layer was positive with respect to the ortho-chloranil.

When such a cell was illuminated, an increase in polarization was observed. The spectral response of the photoinduced charge produced on the plates corresponded to phthalocyanine absorption. The polarity of the effect demonstrated that upon illumination the phthalocyanine layer became more positive with respect to the ortho-chloranil layer.

The rise and decay of the photoinduced charge on the condenser plates followed unimolecular kinetics with a room-temperature time constant of about 60 sec (Fig. 34). The experimental arrangement did not permit cooling of the sample.

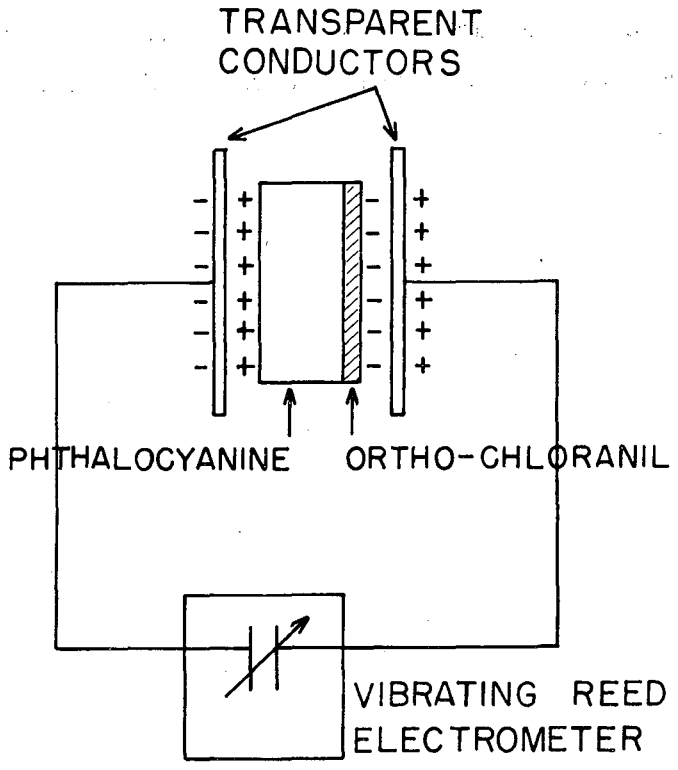

Fig. 39. Schematic diagram of polarization apparatus. The plates of the condenser were approximately 10^{-2} cm apart. The maximum voltage obtainable in this system upon illumination was about 100 mv.

3.5 Flash-Induced Photoconductivity

A moderately doped sample of phthalocyanine was examined by the flashing-ligh method described previously (See Part One, section 3.1). The decay of the photoconductivity produced by light in the phthalocyanine absorption region is shown in Fig. 40, together with a decay curve for undoped material with and without ambient illumination.

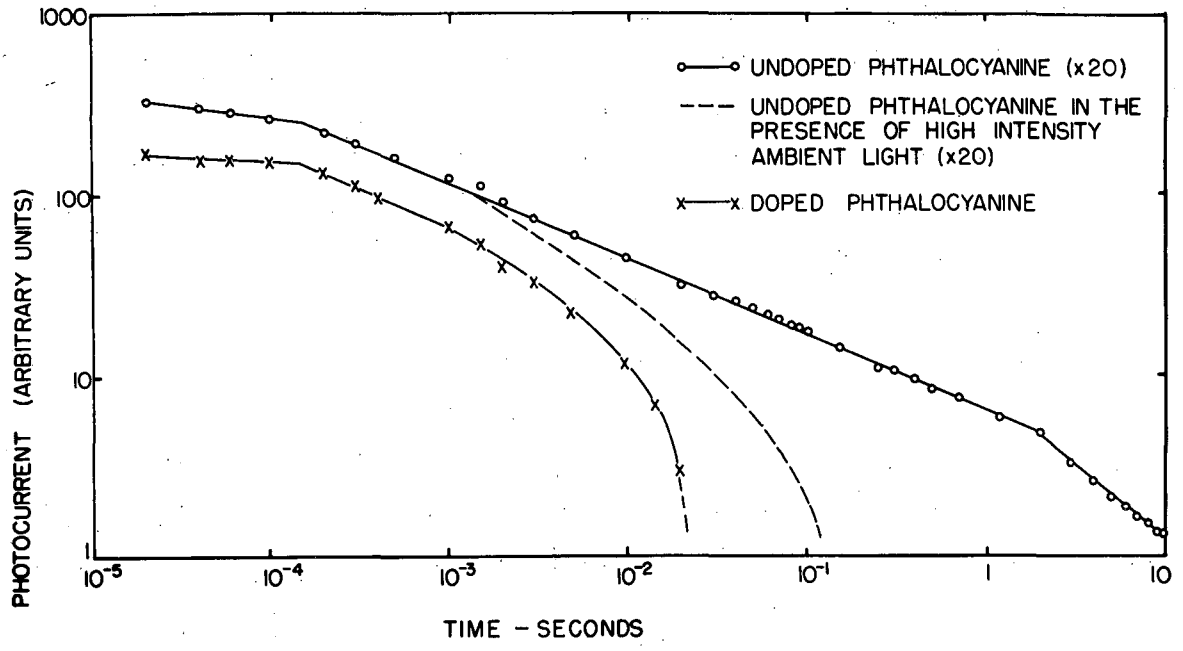

MU - 17732

Fig. 40. Flash-induced photoconductivity in doped phthalocyanine compared with that in undoped phthalocyanine with and without ambient illumination.

4.0 RESULTS: ORTHO-CHLORANIL WITH PHTHALOCYANINE ADDED

In the following series of experiments, the roles of phthalocyanine and ortho-chloranil were reversed in that small amounts of phthalocyanine were added to ortho-chloranil. Doping was achieved either by covering the exposed surface of an ortho-chloranil surface cell with powdered phthalocyanine and heating to the ortho-chloranil melting point or by grinding a mixture of phthalocyanine and ortho-chloranil for several minutes in a dental amalgamator. Surface cells were made from the ground mixtured by simply heating this material on a sample holder. Sandwich cells were constructed by compressing the mixture between two stainless steel pistons contained in a glass sleeve.

4.1 Dark Conductivity

The specific resistivity of pure ortho-chloranil, as measured in the conductivity apparatus described in Part One, Section 2.2E, was found to be 10^{15} ohms-cm. The temperature dependence of the conductivity, also measured in the above apparatus, was found to obey the relation $\sigma = \sigma_o e^{-\Delta E/2kT}$, with $\Delta E \approx 3.0$ ev.

When 10% by weight of phthalocyanine was admixed with ortho-chloranil and formed into a sandwich cell as described above, the specific resistivity of the ortho-chloranil decreased from 10^{15} ohms-cm to 5×10^{6} ohms-cm. A surface cell of ortho-chloranil, doped on the back face with powdered phthalocyanine, was heated to the melting point of ortho-chloranil to form a continuous film. When the temperature of this sample was lowered from 25 to - 50°C, the dark current decreased by a factor of eleven. If we assume exponential temperature dependence of $\sigma = \sigma_o e^{-\Delta E/kT}$, a $\Delta E \approx 0.20$ ev may be calculated.

4.2 Photoconductivity

A. Variation with Doping

The photoconductivity of a surface cell of pure ortho-chloranil was found to be too small to obtain a spectral response curve. When the sample was illuminated (front face) with 10^{17} quanta/sec of 6000- to 7000-Å light, a photocurrent of 6.6×10^{-11} amp was observed with 90 v applied to the sample. Under these same conditions, the surface cell of ortho-chloranil doped with phthalocyanine produced a photocurrent of 3.3×10^{-5} amps, representing an increase of 5×10^{5} in photoconductivity due to doping with phthalocyanine.

B. Temperature Dependence

When the temperature of this sample was lowered from 25 to - 50°C, the photocurrent also decreased a factor of eleven, indicating an activation energy for photoconduction of ≈ 0.2 ev.

C. Spectral Response

The spectral response of the photoconductivity for the above surface cell is shown in Fig. 41 for back-face illumination. The phthalocyanine was fairly well localized to the back surface and the spectral response of the photocurrent resulting from illumination of this face is the same as the phthalocyanine absorption spectrum.

D. Kinetics of Decay

The decay of the 6000- to 7000- Å photocurrent at 25 to - 50°C in a surface cell is shown in Fig. 42, where the logarithm of the photocurrent is plotted as a function of the time after cessation of illumination. The photocurrent decay at both temperatures is exponential with a time constant of 84 sec at 25°C and 59 sec at - 50°C.

E. Steady-State Intensity Dependence

The intensity dependence of the steady-state photocurrent resulting from front-face illumination with 6000 to 7000 Å of the surface cell described above is shown in Fig. 43 for 25 to - 50°C.

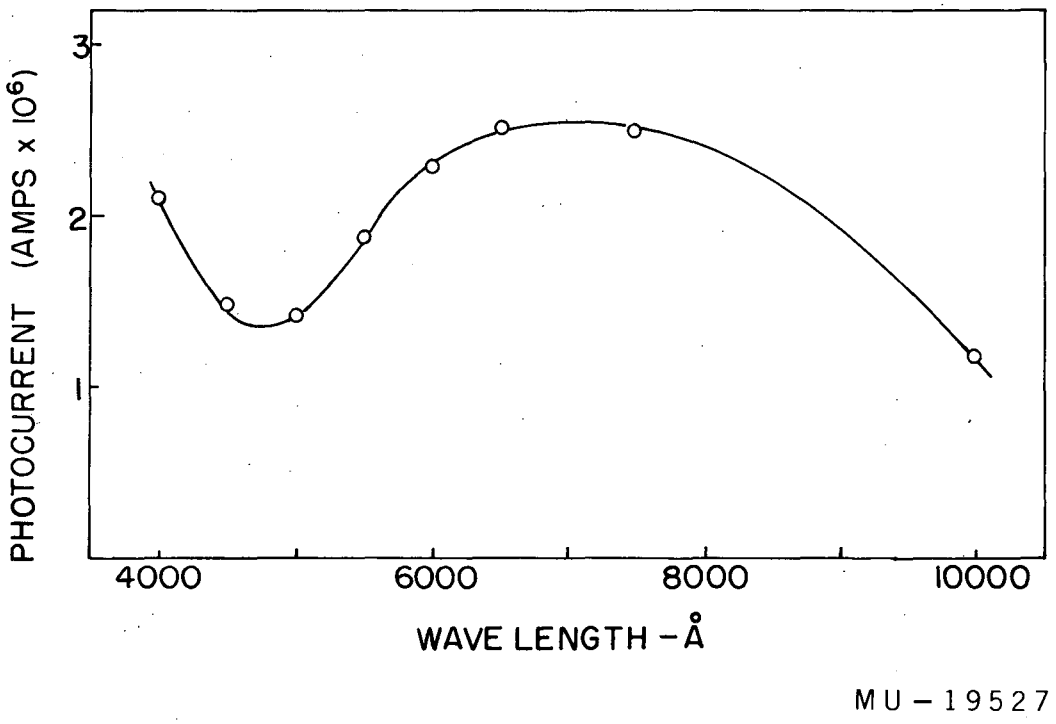

Fig. 41. Spectral response of steady state of photoconductivity of ortho-chloranil with 10% by weight of phthalocyanine.

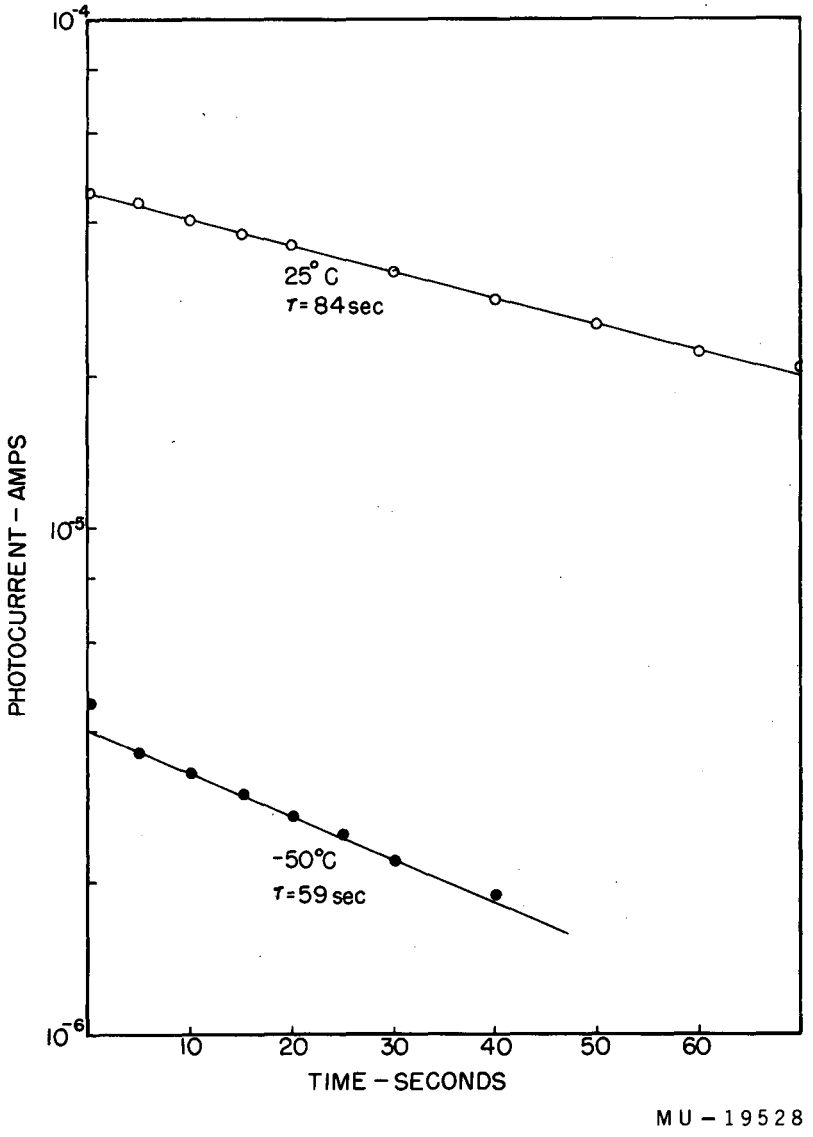

Fig. 42. Semi-log plot of the time dependence of photocurrent decay of ortho-chloranil with 10% by weight of phthalocyanine.

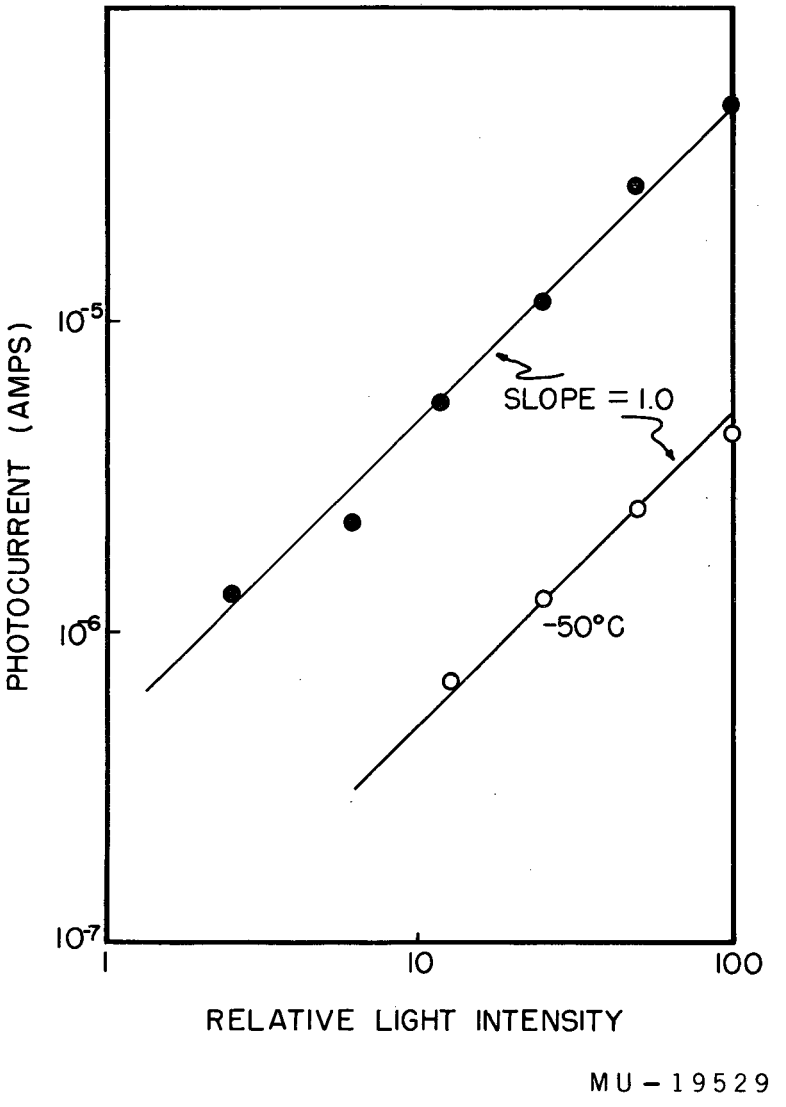

Fig. 43. Intensity dependence of steady-state photoconductivity of ortho-chloranil with 10% by weight of phthalocyanine.

From this log-log plot of current as a function of light intensity, it is clear that for red light, the photocurrent I is directly proportional to the light intensity at room temperature and at - 50°C.

4.3 Electron Spin Resonance

Pure ortho-chloranil had no observable unpaired-electron spin concentration ($< 10^{13}$ spins/gm). However, phthalocyanine doped ortho-chloranil had a high spin concentration. The shape of the spin-resonance absorption was identical to that observed in the ortho-chloranil doped phthalocyanine samples (see Fig. 37). Spin resonance measured indicated a spin concentration of 3×10^{17} spins/gm in the sample used previously in the sandwich-cell conductivity measurements described in section 4.1. There were 2×10^{-4} moles of phthalocyanine per gram of this sample, and thus 3×10^{17} spins/gm corresponds to 1 unpaired spin per 400 phthalocyanine molecules.

5.0 RESULTS WITH OTHER SYSTEMS

5.1 Results with Ortho-Bromanil-Doped Phthalocyanine

A surface cell of phthalocyanine was doped with approximately 10^{-4} moles of ortho-bromanil, another strong electron acceptor. Similar to the results obtained with ortho-chloranil, the addition of the ortho-bromanil increased the dark conductivity by a factor of 10^4 and increased the photoconductivity by a factor of 10^3.

5.2 Results with Phthalocyanine Doped with Strong Electron Donors

When a surface cell of phthalocyanine was treated with the strong electron donor N, N, N', N'' - tetra-methyl-p-phenylene diamine (crystalline powder was allowed to melt on the exposed surface of the phthalocyanine), both the dark conductivity and the photoconductivity immediately decreased by a factor of six.

A surface cell of phthalocyanine was doped with 10^{-4} moles of phenothiazine. On the basis of calculations of Karreman[18], this compound is expected to be a very good electron donor. When it was added, both the dark and photoconductivity of phthalocyanine decreased by a factor of 25.

5.3 Results with Tetracene and Pentacene

Some very preliminary experiments have been carried out using tetracene and pentacene as the semiconductor in "surface" cells. Again, large increases (x 10^3 to x 10^4) in both photoconductivity and dark conductivity were observed when the samples were treated with ortho-chloranil, para-chloranil, or phenanthrene quinone. Unpaired electron spins were also detected in these two-component systems. A photoinduced increase in unpaired-electron-spin concentration was observed with the tetracene-ortho-chloranil system, but in general the results with these systems appeared similar to those of the phthalocyanine-ortho-chloranil system.

In other experiments the tetracene and pentacene surface cells were doped with N, N, N', N'' - tetramethyl-p-phenylene diamine (TMϕD). When the TMϕD was added to the pentacene, both the dark conductivity and the photoconductivity decreased by a factor of $10^{\approx 3}$. The addition of TMϕD to tetracene decreased the dark conductivity only by a factor of three but reduced the photoconductivity by a factor of 10^3.

6.0 DISCUSSION AND CONCLUSIONS

Ortho-chloranil is a very strong oxidizing agent and phthalocyanine, because of its rather large ring system, would be expected to have a low ionization potential. Therefore, before actually considering the results of the experiments presented in this paper, a brief consideration of the general nature of the interaction between these types of molecules will be given.

The theory of charge transfer complexes in solution concerns itself with a description of the interaction of electron-donating molecules, D, (molecules with a relatively low ionization potential) and with electron-withdrawing molecules, A, (molecules with a relatively high electron affinity).[19,20] When such molecules are brought together, a donor-acceptor complex may be formed, and the ground-state wave function may be approximately written as

$$\psi_N (D, A) = a\, \psi_O(DA) + b\, \psi_1(D^+A^-) + c\, \psi_2(D^-A^+). \qquad (1)$$

ψ_0, the no-bond wavefunction, is the wavefunction for the complex where the interaction between D and A is a result of classical intermolecular forces such as dipole-dipole and dipole-induced dipole interactions. If D is a relatively strong electron donor and A a strong electron acceptor, then the structure corresponding to ψ_2 may be entirely neglected. The dative-bond wavefunction ψ_1, corresponds to a structure in which an electron has been transferred from D to A. In addition to the binding forces listed above, there is ion-ion attraction and weak chemical bonding between the odd electrons situated on the two components of the complex. If D and A are quite strong donors and acceptors, ψ_1 may contribute much more to ψ_N than ψ_O and the complex will be primarily ionic in the ground state. If both D and A are molecules with completely filled electron shells, the free ions, D^+ and A^-, each have one unpaired electron and are both in a doublet state. In the complex, the interaction between the unpaired electrons will depend upon the difference in the redox potentials of the two components and the overlap of the charge clouds

of the unpaired electrons. As Kainer has pointed out, if the overlap of the unpaired electron clouds were small, the ground state of the complex would most likely be a triplet state.[11] With no overlap, we would expect the two components of the complex to be in doublet states. So far we have considered the behavior of the D and A molecules in solution. If the D and A molecules are in the form of a solid mixture, some changes in the behavior of the complex may be expected. Wherever D and A molecules find themselves in contact, an electron will be almost completely transferred from D to A to form the $(D^+ A^-)$ complex. The D^+ component may find itself imbedded in a solid matrix of D molecules which will tend to donate electrons to the D^+. Similarly, A molecules around A^- will tend to withdraw the odd electron from A^-. In this case, charge separation by several molecular diameters may be possible. The result will be the production of the free ions, $\dot{D}^+$ and $\dot{A}^-$, both of which will be in the doublet state.

6.1 Ortho-Chloranil-Doped Phthalocyanine System

A. Mechanism of Dark Conduction

According to the above discussion, the concurrent increase in dark conductivity and ESR in phthalocyanine upon the addition of ortho-chloranil may be explained in the following manner. Ortho-chloranil is a strong oxidizing agent and therefore might be expected to remove electrons from the phthalocyanine if the two substances were placed in intimate contact. The relative case of transfer of electrons from the phthalocyanine to the ortho-chloranil would depend upon the electron affinity of ortho-chloranil and the ionization potential of phthalocyanine. If, after partial electron transfer from the phthalocyanine to the ortho-chloranil, the "odd" electrons remain paired,, it is doubtful that any change should be observed in the conductivity of the phthalocyanine layer. The variation of the dark conductivity of the metal-free phthalocyanine with amount of added ortho-chloranil suggest, however, that once a phthalocyanine molecule partially loses

an electron to an ortho-chloranil molecule, the nearly ionized phthalocyanine molecule may regain an electron from a neighboring neutral phthalocyanine molecule. It appears that the formation of the initial phthalocyanine-ortho-chloranil complex provides most, if not all, of the energy required to ionize the phthalocyanine molecule. This electron-transfer process may be represented by*

$$PH + Q \xrightarrow{dark} PH^{+} + Q^{-}, \qquad (2)$$

where the positive charge is free to migrate throughout the phthalocyanine layer and the negative charge throughout the ortho-chloranil layer. Both PH^{+} and Q^{-} should be paramagnetic, and thus reaction (2) explains the observed large increase in PH conductivity and the production of a high concentration (10^{17} spins/gm) of unpaired electron spins. The construction of the PH sample cells is such that the observed increase in conductivity with ortho-chloranil doping must be due to an increase in the PH layer conductivity and not merely due to an increase in the conductivity of the surface away from the electrodes.

The spin concentration in these systems was found to be independent of temperature, indicating that either reaction (2) is exergonic and proceeds 100% to completion wherever neutral phthalocyanine and ortho-chloranil molecules come in contact, or, the products of reaction (2), the positively and negatively charged species, are not in equilibrium with the reactants.

---

*The following abbreviations are used in the discussion:

PH = metal-free phthalocyanine

Q = ortho-chloranil

PH^{*} = first excited singlet state of phthalocyanine

PH^{+} = phthalocyanine holes

Q^{-} = ortho-chloranil negative-ion radical

$Q^{=}$ = ortho-chloranil double negative ion.

The dark polarization of the lamellar ortho-chloranil-phthalocyanine system is also consistent with reaction (2). This mechanism postulates that the increase in dark conductivity upon doping is due to the actual formation of charge carriers, rather than an increase in the mobility of charge carriers already present in the undoped material. It is supported by the following observations:

(a) The dark conductivity of purephthalocyanine has an activation energy of about 1.7 ev. This has been ascribed primarily to the process of formation and charge carriers.[21] On the other hand, the photoconductivity of pure phthalocyanine has an activation energy of only 0.2 ev, and this can be interpreted in terms of an activation energy for charge-carrier migration after their formation.[22] The fact that cooling a doped phthalocyanine sample to - 100°C does not decrease the concentration of unpaired electron spins and produce a much smaller decrease in dark conductivity than is produced in an undoped sample demonstrates that the primary process that occurs in the dark upon doping is not appreciably reversed at the low temperature. According to reaction (2) then, the concentration of charge carriers in a moderately doped sample of phthalocyanine is also independent of temperature. Doping thus eliminates the requirement of a thermal energy of formation of charge carriers in the dark, and the only temperature dependence of dark conductivity observable should be associated with the mobility of charge carriers. If it is assumed that doping affects only the process of charge-carrier formation, then the mobility of photo- or thermally-produced charge carriers should be unchanged in going from pure to doped material. This is strongly supported by the observation that the activation energy for both the dark conductivity and photoconductivity was the same as that for photoconductivity in pure phthalocyanine.

(b) When moderately doped samples are subjected to flash illumination, the decay curves for photoconductivity are essentially identical with the curves obtained with undoped samples in the presence of high-intensity ambient illumination (Fig. 11). This further indicates

that charge carriers are indeed produced by doping and that these carriers behave in the same manner as do photo-produced carriers in both the doped and the undoped samples.

Although the above results definitely indicate that the increased conductivity in doped samples is primarily the result of an increased charge-carrier concentration, it is not possible to completely eliminate a small effect upon the charge-carrier mobility.

B. Mechanism of Photoconduction

The spectral responses of the photoconductivity and of the light-induced decrease in ESR, and the time constants for the rise of photoconductivity and for the light-induced decrease in ESR, indicate that the same process gives rise to photoconductivity and results in a decrease in the concentration of unpaired spins. This may be accounted for by the following processes: The spectral response of these processes corresponds to the absorption spectrum of phthalocyanine. Hence, the first action of light must be to produce excited phthalocyanine molecules. The excited phthalocyanine molecules may then lose an electron to a negative ortho-chloranil ion. Thus we may write

$$PH + h\nu \rightarrow PH^{*} \tag{3}$$

and

$$PH^{*} + CH^{-} \rightarrow PH^{+} + CH^{=} . \tag{4}$$

It is necessary to assume here that the paramagnetic species observed in ESR measurements are CH^{-} and that PH^{+}, although paramagnetic, is not detected, perhaps because of broadening of the resonance line. The photoinduced decrease in ESR, then, is the result of the transformation of CH^{-} radicals into $CH^{=}$ ions which, owing to aromatization of the pi-electron system, would not be paramagnetic.

It is also possible to interpret the light-induced polarization phenomenon in terms of reaction (4). It is apparent from the construction of the surface cells and the method of doping, that most of the CH^{-} radicals will be in positons near one surface of the phthalocyanine layer. Therefore, the postulated electron transfer from PH^{*}

to CH^- should result in an increased polarization in which the ortho-chloranil layer becomes more negative with respect to phthalocyanine. The rise time, spectral response, and measured polarity of the photo-induced polarization are consistent with this hypothesis.

It was noted above that the decay of photoconductivity, the rise of ESR, and the polarization decay after illumination ceased were all unimolecular processes having the same time constant. This can be interpreted in terms of the following reaction as the rate-limiting step in all these processes:

$$PH^+ + CH^= \rightarrow PH + CH^-. \qquad (5)$$

The disappearance of photoproduced PH^+ and $Q^=$ ions may be expressed as

$$\frac{d\,(PH^+_{photo})}{dt} = - K \left[PH^+_{photo} + PH^+_{dark}\right]\left[Q^=_{photo}\right]. \qquad (6)$$

Inasmuch as the concentration of PH^+ is high in the dark and is not appreciably changed by illumination, Eq. (6) should result in pseudounimolecular kinetics. The 60-sec time constant observed in these experiments demonstrates that charge carriers have a considerably longer lifetime in the doped material than in the undoped material. This would result in a large increase in steady-state photoconductivity upon doping, in agreement with experiments. Since reaction (6) is relatively slow (60-sec time constant) and yet has only a negligible apparent activation energy, there must be some intrinsic improbability in it. Quite possibly this slowness is due to the change of spin. This notion is supported by a consideration of the photocurrent decay of doped ferric-phthalocyanine. The introduction of ferric ions into the phthalocyanine ring causes the time constant for Eq. (6) to decrease from 60 sec to 50 sec. As Kasha has shown in his work on singlet-triplet transitions in organic molecules, the introduction of heavy metals into molecules greatly facilitates the spin-change process.[23] Possibly the same sort of processes are operative here.

It is not possible at present to account for the decrease in the time constant with a decrease in temperature.

Examination of Fig. 32 indicates that the photoconductivity due to illumination of the back face (face opposite the side with electrodes) of a 10^{-3}-cm-thick surface cell with 6000 to 7000-Å light is increased 40 times more than the photoconductivity due to illumination of the front face of the sample when the sample was doped with ortho-chloranil. In this particular experiment, the red-light photocurrent, after doping, is four times larger when the back face is illuminated than when the front face is illuminated. This is in spite of the fact that the carriers produced by back-face illumination must diffuse at least part way toward the electrode surface before they can contribute to the photocurrent. The conclusion drawn is that the increase in photoconductivity with doping is the result of the interaction of excited phthalocyanine molecules with ortho-chloranil molecules, as postulated in Eq. (4).

The question of how much diffusion of ortho-chloranil into the phthalocyanine layer takes place and to what extent this effects the phthalocyanine conductivity can be answered by consideration of the following experimental results. The fact that the increase in dark- and photo-conductivity occurs almost instantaneously upon doping and that heat treating a doped phthalocyanine sample (see Fig. 3) did not significantly alter the dark conductivity or the photo-conductivity due to front-face illumination with 6000-to 7000-Å light suggests that diffusion of the ortho-chloranil into the bulk of the phthalocyanine layer is not necessary for increased conductivity. Rather it indicates the carriers are produced at the ortho-chloranil-phthalocyanine interface and diffuse into the phthalocyanine layer. If diffusion of the ortho-chloranil into the phthalocyanine was important, it would have been evident in the heat-treatment study.

Consideration of the results of doping a crystallized film of phthalocyanine also support the notion that it is the holes that diffuse into the phthalocyanine layer, rather than the ortho-chloranil

molecules. Here it was found (see Table II) that the photo- and dark-conductivity of a doped amorphous sample was only a factor of about 10 greater than that of a crystallized sample. Again, if diffusion of ortho-chloranil into the phthalocyanine was required for conductivity increases, much larger differences should have been observed between the amorphous and the crystalline samples.

When phthalocyanine surface cells of varying thickness were each doped with 10^{-5} moles of ortho-chloranil, the final values for photo- and dark-conductivity were essentially the same. In fact, values for the thickest and thinnest samples were almost identical seconds after doping and remained so. Clearly, diffusion of ortho-chloranil could not have been important, otherwise marked differences would have been noted.

At steady state the equation describing the concentration of PH^+ produced by light is

$$\frac{d\left[PH^+_{photo}\right]}{dt} = 0 - qL - K\left[PH^+_{photo} + PH^+_{dark}\right]\left[Q^{\dot{-}}\right], \tag{7}$$

where L is the light intensity in quanta/sec, q is proportional to the quantum yield for photoproduction of charge carriers, and K is the bimolecular rate constant in cm^3/sec-carrier. Since

$$\left[PH^+_{photo} + PH^+_{dark}\right] = PH^+_{dark}, \tag{8}$$

we find, using Eq. (7),

$$PH^+_{photo} = Q^{\dot{-}} = \left(\frac{q}{K}\right) L. \tag{9}$$

When a sample has been sufficiently doped so that the approximation $\left[PH^+_{dark} + PH^+_{photo}\right] = PH^+_{dark}$ is valid, the photocurrent should vary linearly with the light. Figure 35 shows that as the doping concentration increases, the photocurrent rapidly approaches a linear dependence on light intensity.

It was noted that doping produces a 10^5-fold increase in steady-state photocurrents, (see Fig. 11) but only a tenfold increase in flash-induced photoconductivity is observed. This may be attributed to the fact that the use of a short-duration light pulse to produce charge carriers tends to eliminate effects caused by differences in recombination times in the two systems, whereas steady-state experiments accentuate these differences.

The negative photoconductivity observed in heavily doped phthalocyanine can be explained by the same mechanism proposed in Part I to explain the negative photoconductivity in "pure" phthalocyanine. In the present case it is presumed that a measurable temperature-dependent concentration of $Q^=$ ions are formed in the dark by thermal excitation of phthalocyanine molecules. Absorption of light (4000 Å) by $Q^=$ may induce electron transfer to neighboring neutral phthalocyanine molecules, forming Q^- and PH^-. The PH^- would then rapidly combine with PH^+ to give a net decrease in carriers. When the temperature is decreased, the concentration of $Q^=$ becomes negligible and negative photoconductivity is no longer observable.

C. Charge Carrier Mobility and Quantum Yield for Photoconductivity

According to reaction (2), the number of unpaired spins produced by doping (neglecting the $CH^=$ concentration) is a measure of the number of charge carriers produced in the phthalocyanine layer. Thus, by measuring the conductivity of a surface cell of known geometry with a measured spin concentration, one can calculate a charge carrier mobility by the equation

$$I = \mu N E A , \qquad (10)$$

where I is the current in electrons per second, μ is the mobility in cm^2 per volt per second, N is the number of charge carriers per cm^3, E is the field strength (= V/d), and A is the cross-sectional area of the conductor.

In a typical experiment, we have $I = 5.8 \times 10^{15}$ e^-/sec, tN = concentration of charge carriers/cm^2 surface area = 10^{14} e^-/cm^2, A/t = length of conductor = 15 cm, and $V = 10^4$ volts/cm^2. From these data $\mu = 4 \times 10^{-4}$ cm^2/v-sec = mobility of holes in the phthalocyanine layer.

Similar experiments were carried out by using a pellet of ortho-chloranil-doped phthalocyanine. In this experiment, we have $N = 5.4 \times 10^{17}$ e^-/cm^3, $A = 3.8 \times 10^{-2}$ cm^2, and $I/V\,d = 10^{-5}$ amp/volt $\cdot$ 6.8×10^{18} e^-/sec $\times$ 0.16 cm. From Eq. (10) we would calculate a hole mobility of $\mu = 5 \times 10^{-4}$ cm^2/v-sec in good agreement with the surface-cell measurements.

From the results of pulse-light carrier-injection studies carried out in part I (see section 3.11), an upper limit of 4×10^{-3} cm^2/v-sec was set for the bulk mobility of charge carriers in pure phthalocyanine. This value is in good agreement with that measured in the doping experiments, since there is a certain amount of error involved in both measurements.

The mobility may also be calculated on the basis of a very simple hopping model, where it is assumed that the intermolecular transfer frequency is the same as an electronic vibrational frequency ($\sim 10^{12}$/sec). The diffisivity, D, would then be $D = (10^{-7}\text{cm})^2 \times 10^{12}$/sec $= 10^{-2}$ cm^2/sec for an intermolecular separation of 10^{-7} cm, or, from the Einstein relation, $\mu = 4 \times 10^{-1}$ cm^2 v-sec. This is certainly an upper limit on the mobility, particularly if a small amount of energy is required for the electron transfer. The fact that the values of carrier mobility measured by two independent methods are in reasonably good agreement and the fact that these values fall below the calculated maximum value for mobility strengthen the validity of the measurements and give strong support to the proposed mechanism of conduction in doped phthalocyanine.

It is interesting to compare the mobilities given above with those obtained in inorganic semiconductors such as germanium and silicon. These latter normally range from 1 to 1000 cm^2/v-sec at room temperature. A value of 10^{-4} cm^2/v-sec for an organic material is in keeping with the large differences between the crystal interactions in valence crystals and those in organic molecular crystals. For example, heats of sublimation are about 3 to 4 ev for valence crystals and about 10^{-2} ev for molecular crystals.

A surface cell was specially constructed for a Hall voltage experiment. A microvolt meter was used to attempt to detect the Hall voltage; however, none could be detected. This is not unexpected in view of the small value of the mobility.

If the above value for the mobility is used, it is possible to calculate a quantum yield for the photoproduction of holes in such a system in the following manner. The initial rate of rise of the photocurrent was measured when a surface cell was suddenly illuminated with a constant light source. The length of time over which the measurement was carried out was only a few seconds, so that errors due to carrier recombinations (60-sec time constant) were minimized. Under these conditions we may write:

$$\frac{dI}{dt} = \frac{dN}{dt} \cdot \mu A E = \frac{dN'}{dt} \cdot \mu \ell E , \qquad (11)$$

where dI/dt is the rate of rise of photocurrent in e^-/sec^2, dN'/dt is the rate of production of charge carriers per unit area of sample in $e^-/sec\text{-}cm^2$, ℓ is the length of the sample electrodes, and μ is the mobility = 10^{-4} cm^2/v-sec. The choice of this mobility value allows errors due to ortho-chloranil absorption and sample thickness to be compensated for.

For a heavily doped sample it was found that

$$\frac{dI}{dt} = 4 \times 10^{-4} \text{ amp/sec} \times 6.3 \times 10^{18} \text{ } e^-/\text{sec-amp} = 2.5 \times 10^{15} e^-/sec^2$$

when

$$\frac{V}{d} = \frac{90}{5\times10^{-2}} \text{ v/cm} = 1.8 \times 10^{3} \text{ v/cm} .$$

From Eq. (10) we calculate

$$\frac{dN'}{dt} = 7\times10^{15} \text{ e}^{-}/\text{sec-cm}^{2} .$$

A band-pass filter was used to restrict the light incident on the sample to the 6000- to 7000-Å region. For these measurements, the light intensity L was 2.7×10^{16} q/sec-cm^2. Under these conditions the quantum yield for the photoproduction of charge carriers was

$$\frac{\frac{dN'}{dt}}{L} = 0.26 \text{ electrons/quanta} .$$

6.2 Phthalocyanine-Treated Ortho-chloranil

A. Mechanism of Dark Conduction

The conclusions reached in the preceding section indicated that the large increase in phthalocyanine dark conductivity upon doping with ortho-chloranil was the result of transfer of electrons from phthalocyanine to ortho-chloranil molecules. The large increase in ortho-chloranil dark conductivity (2×10^{8}) upon the addition of 10% by weight of phthalocyanine can also be interpreted in terms of reaction. In this case, however, the doping agent (phthalocyanine) is acting as an electron donor, and the increase in conductivity is the result of introduction of excess electrons into the host lattice (ortho-chloranil). The activation energy for dark conduction decreased from 3.0 ev in pure ortho-chloranil to $\sim$0.2 ev in the phthalocyanine-treated material. This is agin consistent with the notion that doping

with phthalocyanine obviates the requirement of an energy of formation of charge carriers in the dark by injecting a large concentration of electrons into the ortho-chloranil lattice. The only energy requirement associated with dark conduction in this case is due to the activation energy of migration of the negative charges, and ~ 0.2 ev is a reasonable value for this.

B. Mechanism of Photoconduction

The increase in ortho-chloranil photoconductivity (5×10^5) brought about by the addition of phthalocyanine may be explained by reactions (3) and (4). In this case the increase in conductivity is due to the formation of $Q^=$ with the migration of the extra electron taking place as follows:

$$Q^= + Q^- \rightleftharpoons Q^- + Q^= . \qquad (12)$$

This mechanism is supported by the observation that the spectral response of the photoconduction is the same as the phthalocyanine absorption spectrum. As before, this indicates that increase in ortho-chloranil photoconductivity is the result first of exciting neutral phthalocyanine molecules followed by electron transfer to the ortho-chloranil matrix.

The temperature dependence of the steady-state photocurrent indicated there was a 0.2-ev activation energy associated with photoconduction. This we again interpret as an activation energy for charge-carrier migration. The agreement between this activation energy and that measured for dark conduction support this notion.

When illumination of a phthalocyanine-treated ortho-chloranil sample ceased, the decay of the photocurrent was found to be unimolecular (see Fig. 42). This is a result of recombination of $Q^=$ and PH^+ (Eq. 5) which appears to be pseudo-unimolecular because of the high concentration of PH^+ produced by the dark reaction.

Since the PH^+ will be relatively well localized in the ortho-chloranil matrix, the recombination of $Q^=$ and PH^+ will be limited by the diffusivity of $Q^=$. If the mobility of $Q^=$ in the ortho-chloranil matrix, is lower than the mobility of PH^+ in the phthalocyanine matrix, the $PH^+ - Q^=$ recombination time constant would be longer in the ortho-chloranil matrix. The fact that this time constant is 84 sec in phthalocyanine-doped ortho-chloranil as compared to 60 sec in the reverse system suggests that the mobility of $Q^=$ is lower than PH^+.

Since the decay of photoconductivity in the treated ortho-chloranil system is unimolecular, this requires that the steady-state photoconductivity vary linearly with the light intensity (see Eq. 9). That this was so is shown in Fig. 43.

C. Charge-Carrier Mobility

According to the proposed mechanism, a measurement of the unpaired-electron spin concentration in phthalocyanine-doped ortho-chloranil will also give the number of charge carriers (Q^-). For a particular sample, the concentration of unpaired-electron spins, N, was 7×10^{16} e^-/cm^3. The specific conductivity of this sample was measured, and therefore the carrier mobility could be calculated by the use of Eq. (10) and the following data:

$$A = 0.75\ cm^2,\ dE/I = 3.7\times10^5\ volt/amp,\ d = 10^{-1}\ cm$$

$$\mu = \frac{10^{-5}}{3.7}\ amp/volt \times 6.3\times10^{18}\ e^-/sec\ amp \times \frac{1}{0.75\ cm^2} \times 10^{-1}\ cm \times \frac{cm^3}{7\times10^{16}\ e^-}$$

$$= 3\times10^{-5}\ cm^2/volt\text{-}sec.$$

In view of the smaller ring size and polarizability of the ortho-chloranil compared to phthalocyanine, it is reasonable that the mobility of charge carriers be less in ortho-chloranil than in phthalocyanine.

6.3 Phthalocyanine Treated with Electron Donors

In Part I it was proposed that the dark and photoconductivity of "pure" metal-free phthalocyanine is due to a thermally or photo-induced transfer of electrons from phthalocyanine to some electron-accepting impurity. On the basis of this mechanism it is possible to explain the effect of electron donors on the conductivity of phthalocyanine. Apparently the electron affinity of a neutral phthalocyanine molecule is not great enough to remove an electron from either N, N, N', N' - tetra methyl-p-phenylene diamine (TMϕD) or pheno-thiazine when the two are placed in contact. The electron affinity of a phthalocyanine positive ion, however, should be great enough to remove an electron from the electron donor when added to a phthalocyanine surface cell. As positive charge builds up in the electron-donor layer, there is less chance that positive charges in phthalocyanine will be able to approach the electron-donor layer. In the lamellar systems, this will of course limit the magnitude of the effect. Secondly, it is quite possible that the acceptor impurities localized in the phthalocyanine layer may gain electrons from the donor layer rather than the phthalocyanine layer, decreasing the available sites for thermal or photoproduction of positive phthalocyanine molecules. Both of these effects are probably operative and hence decreases in both dark and photoconductivity are observed.

If it were possible to uniformly distribute one of the above electron donors in the phthalocyanine lattice in a concentration equal to that of the electron-accepting impurity, it should be possible to convert all of the impurities to the negative ion. In this case, the

the only electron acceptor in the lattice would be other neutral phthalocyanine molecules, and truly intrinsic "semiconductivity" should be observed with an activation energy higher than that which has been observed.

6.4 Other Systems

The preliminary results obtained using tetracene or pentacene as the semiconductor and either ortho-chloranil, para-chloranil, or phenanthrene quinone as the electron donor were qualitatively similar to those obtained with the ortho-chloranil-phthalocyanine system. This is of interest because it indicates that the concepts developed to explain the behavior of the ortho-chloranil-phthalocyanine system should be generally applicable to a discussion of the behavior of polycyclic aromatic molecules interacting with electron-accepting molecules.

The very large decreases (factor of 10^3) in the photoconductivity of both tetracene and pentacene and the dark conductivity of pentacene suggests oxidizing impurities may generally be present in the polycyclic aromatic compounds and significantly alter the electrical properties of these systems.

REFERENCES

1. W. G. Schneider and T. C. Waddington, J. Chem. Phys. 25, 358 (1956).
2. D. M. J. Compton and T. C. Waddington, J. Chem. Phys. 25, 1075 (1956).
3. A. T. Vartanyan and I. A. Karpovich, Dokl. Akad. Nauk S. S. S. R. 111, 561 (1956).
4. H. Akamatu, H. Inokuchi, and Y. Matsunaga, Bull. Chem. Soc. Japan 29, 213 (1956).
5. H. Akamatu and H. Inokuchi, in Proceedings of the Third Conference on Carbon (Pergamon Press, New York, 1959), p. 51.
6. H. Akamatu, H. Inokuchi, and Y. Matsunaga, Bull. Chem. Soc. Japan 29, 213 (1956), p. 218.
7. L. E. Lyons, A. Bree, and G. C. Morris, in Proceedings of the Third Conference on Carbon (Pergamon Press, New York, 1959), p. 87.
8. Y. Matsunaga, Bull. Chem. Soc. Japan 28, 475 (1955).
9. D. D. Eley and H. Inokuchi, in Proceedings of the Third Conference on Carbon (pergamon Press, New York, 1959), p. 91.
10. D. Bijl, H. Kainer, and A. C. Rose-Innes, J. Chem. Phys. 30, 765 (1959).
11. H. Kainer, D. Bijl, and A. C. Rose-Innes, Naturwissenschaffen 41, 303 (1954).
12. H. M. Buck, J. H. Lupinski, and L. J. Oosterhoff, Mol. Phys. 1, 196 (1958).
13. F. L. Crane, Plant Physiol. 34, 128 (1959).
14. U. Blass, J. Anderson, and M. Calvin, Plant Physiol. 34, 128 (1959).
15. D. I. Sapozhnikov, T. A. Kayasovskaya, and A. N. Maevskaya, Dokl. Akad. Nauk. S. S. S. R. 113, 74 (1957).

16. Y. Matsunaga, J. Chem. Phys. 30, 855 (1959).
17. L. J. Oosterhoff, H. M. Buck, and J. H. Lupinski, Leyden University, Netherlands, private communication, 1959.
18. G. Karreman, I. Isenberg, and A. Szent-Györgyi, Science, (in press).
19. S. P. McGlynn, Chem. Rev. 58, 1113 (1958).
20. R. S. Mulliken, J. Am. Chem. Soc. 72, 600 (1950).
21. C. G. B. Garrett, in Semiconductors, N. B. Hannay, Ed., (Reinhold, New York, 1959), Chapter 15, p. 662 ff.
22. J. Kommandeur, G. J. Korinek and W. G. Schneider, Can. J. Chem. 35, 998 (1957).
23. M. Kasha, Brookhaven Conference on Bio-Energetics, (in press).

ACKNOWLEDGMENTS

I wish to very gratefully acknowledge the consistently stimulating direction of Professor Melvin Calvin. I particulary thank him for stimulating my interests in areas of science that ranged from biophysics and chemistry to physics.

I certainly thank Drs. Gordon Tollin and Power Sogo for their aid in carrying out a number of experimental measurements and for many valuable discussions.

Many thinks are due the ORL shop personnel for their great cooperation in the construction of apparatus.

I thank my wife for seeing me through it all and for aiding in the preparation of this thesis.

This work was done under the auspices of the U. S. Atomic Energy Commission.